Title page

Non-invasive assessment of pollutant particles in the lower airway of children and adults

A thesis submitted for the degree of Doctor of Medicine,
University of Leicester

Neeta Sushrut Kulkarni MBBS, MRCP
2005

Department of Infection, Immunity and Inflammation
Division of Child Health
University of Leicester
Leicester UK

ProQuest LLC
789 East Eisenhower Parkway
P.O. Box 1346
Ann Arbor, MI 48106-1346

Abstract

Non-invasive assessment of pollutant particles in the lower airway of children and adults

Neeta S Kulkarni

Epidemiological studies in children suggest that inhalation of particulate matter (PM) adversely affects children's respiratory health. However, the relationship between markers of PM exposure and the quantity of particles entering the paediatric airway is unclear. The hypothesis was that, the carbon in alveolar macrophages (AM) reflects individual exposure of healthy children to PM. The aim was to quantify carbon in AM, in subjects exposed to biomass smoke (Ethiopia) and traffic derived primary PM in the UK. For the traffic derived PM exposure, the aim was also to establish the relationship between carbon in AM and: i) markers of PM exposures, ii) lung function and iii) markers of airway inflammation.

Healthy children were recruited and exercise parameters were recorded. AM were sampled by induced sputum. The median carbon area was determined by image analysis of digitized light microscopic images of AM. Exhaled nitric oxide, sputum neutrophil percentage and interleukin–8 were measured. AM carbon was quantified by similar technique in adults in the UK and women and children exposed to biomass smoke.

The median carbon area in AM was higher in Ethiopian women compared with UK adults, ($p = 0.0002$). Median carbon area in Ethiopian children was higher than UK children ($p = 0.0002$). In traffic derived PM exposure, a weak, but significantly positive, association was found between median carbon area and modelled primary PM_{10} ($p= 0.022$), and a stronger inverse association between median carbon area and FEV_1% predicted ($p = 0.004$), and FEF_{25-75} % predicted ($p = 0.004$). There was no significant association between median carbon area and exercise variables and markers of airway inflammation.

I conclude that analysis of carbon area in AM is a practical way of quantifying natural exposure of the lower airway cells in children and is a promising indicator of PM_{10}-associated impairment of lung function.

Index

List of Tables

List of Figures

Acknowledgments

I am indebted to Dr Jonathan Grigg for the ideas for this study and for the freedom to explore new methods and his support. He continues to inspire me for future projects. I would like to thank Nevil Pierse for summarising the PM_{10} and for help with statistical analysis. I would like to acknowledge Dr Lesley Ruston for advice and support regarding the statistical analysis. I would like to thank Professor Mike Silverman, Dr Claudia Kuehni and Dr Adrian Brooke for allowing me to recruit children from the cohort group. I would like to thank Andrew Rutman (under the supervision of Professor Chris O'Callaghan) who processed the samples for transmission electron microscopy (TEM) and imaged the alveolar macrophages by TEM. I appreciate the valuable advice given by Dr Caroline Beardsmore in interpreting the lung function data. I would like to acknowledge Catherine Mallon from The Pollution Control Group, Leicester City Council for providing the monitored and the modelled particulate matter data. Bob Harris of the Institute of Environment and Health, University of Leicester, UK provided distance from road data and the grid reference points for all children. Ananth Tellabathi (AT) performed immunostaining for MARCO and Dawn Jotham for the exhaled nitric oxide analysis. Dr Lester Kobzik (Harvard University, Boston) supplied the monoclonal antibody to MARCO. Lucy Woodman (Glenfield General Hospital, Institute for Lung Health, Leicester) analysed supernatant for IL-8. Daniela Kempkens helped me with sputum processing during the development of simplified method. Finally, I would also like to thank local education authorities; head teachers, parents and children, without their help the study would have been impossible. I would like to thank Michelle Moore for secretarial support, especially in posting the letters to schools. I am very grateful to the Health Effects Institute Boston, USA, for financial support of the project.

Declaration

The work presented in this thesis was performed at the University of Leicester over the years 2002 –2004 and at the Gondar College of Medical Sciences, Ethiopia in May and July 2003. I trained Dr Benjamin Prudon and Dr Sri Panditi at the University of Leicester, to induce sputum and process it by simplified method. They performed the sample collection and processing at the Gondar College of Medical Sciences. Dr Yekoye Abebe provided support in Gondar. Technical staff performed assays of mediators and persons (as detailed in the acknowledgements), provided the data regarding the distance from road and modelled PM.

Abbreviations

AM	Alveolar Macrophage
ATS	American Thoracic Society
BAL	Bronchoalveolar Lavage
BAM	Beta Attenuated Monitor
CI	Confidence Interval
DTT	Dithiothrietol
EELS	Electron Energy Loss Spectroscopy
eNO	Exhaled Nitric Oxide
ERS	European Respiratory Society
FEF_{25-75}	Forced Expiratory Flow between 25 and 75 % of Forced Vital Capacity
FEV_1	Forced Expiratory Volume in 1 Second
FVC	Forced Vital Capacity
GIS	Geographic Information System
H+S	Home (24 - school hours) and School (school hours) Exposures Combined
MARCO	Macrophage Receptor of Collagenous Origin
MET Score	Metabolic Activity Score (MET hr/week)
IL-8	Interleukin 8
PBS	Phosphate Buffered Saline
PM	Particulate Matter
PM_{10}	PM with Aerodynamic Diameter < 10 microns
$PM_{2.5}$	PM with Aerodynamic Diameter < 2.5 microns
ppb	Parts per billion

SEM	Standard Error of Mean
SE	Standard Error
SEM- EDX	Scanning Electron Microscopy - Energy-Dispersive X-ray Microanalysis
SD	Standard Deviation
SMHI	Swedish Meteorological and Hydrological Institute
TEM	Transmission Electron Microscopy
TEOM	Tapered Element Oscillating Microbalance
VIG hr/week	Vigorous Activity hr/wk averaged over past year for activities with > 6 METs
Z-score	Standard Deviation Score

Chapter 1: Introduction

Wood, leaves and crop residues have been used for cooking for many centuries, exposing human beings to very large amounts of particulate matter (PM). In the last century, with an advance in technology, there has been an increase in the use of fossil fuels, like diesel and petrol. No doubt there are economic and social benefits, but there are inherent health hazards of exposing the respiratory tract to these pollutants. Although the type of particulate matter has changed by moving up the energy ladder, the health hazards still exist. There is evidence of inhaled soot particles in one of the oldest mummies, Tyrolean Iceman; proving that humans have long been exposed to particulate matter (Pabst and Hofer, 1998).

1.1 Particulate matter

Airborne PM is not a single pollutant, but a mixture of many subclasses, with diverse chemical composition and size distribution. The health hazards can be influenced by the size and also chemical composition.

1.1.1 CHEMICAL COMPOSITION

The major constituents of PM are sulfate, nitrate, ammonium, chloride, elemental and organic carbon, crustal material and biological materials(Harrison and Jones, 1995;Harrison and Yin, 2000).The same major components are seen in air samples from urban areas around the world, although in different proportions.

Sulfate is derived from sulfur dioxide oxidation in the atmosphere. This process is slow and there is very small spatial variation in levels of sulfate, on a scale of tens of miles. Nitrate is formed mainly from oxidation of atmospheric nitrogen dioxide and is a more rapid process compared to sulfur oxidation; therefore the spatial patterns are not uniform.

Sea spray and road de-icing salt are major sources of chloride. Elemental carbon is mainly from combustion processes, mostly road traffic and forms the core of the particle. The core often has surface coating of semi-volatile organic compounds. Crustal materials include soil dust and wind blown minerals with bacteria, spores and pollens forming the biological materials. Trace element components represent less than 1% of total particle mass. Iron, aluminium, silica and calcium are some of the main trace elements in the particles. The metals such as lead; cadmium, mercury, nickel, chromium, zinc and manganese are used in metallurgical processes. Some occur as impurities or additives in fuels and others are used in industrial products. These and other uses cause emissions to the atmosphere, but concentrations are generally very small. The toxicity of airborne particulate matter depends on the chemical composition, trace metal content, strong acid content, sulfate content and particle size(Harrison and Yin, 2000).

1.1.2 SIZE

Depending on the 50% cut off point of sampling devices, PM can be classified as $PM_{2.5}$ (upper size limit at 2.5μm aerodynamic diameter), $PM_{10\text{-}2.5}$ and PM_{10} (upper size limit at 10μm aerodynamic diameter). PM_{10} are also called thoracic particles because of their ability to penetrate deep into the respiratory tree.

1.1.3 SOURCE AND FORMATION

A wide range of sources contributes to PM, which can be roughly divided into 3 categories. Primary particles originate from incomplete combustion in motor vehicle engines or stationary combustion plants and most of this is of local origin (in Leicester mostly traffic derived)(Leicester Air Quality Report Review and Assessment, 2000). Secondary particles consist of ammonium sulphates, ammonium nitrate and secondary organic aerosols and are formed in the atmosphere. As secondary particles are formed relatively slowly, their contribution to PM_{10} is more uniform. Coarse particles include

natural e.g. wind blown dust and anthropogenic materials like spores. The AIRVIRO gives a PM_{10} prediction for primary emitted particles by using the emission database (Leicester Air Quality Report Review and Assessment, 2000). The secondary and coarse components of PM_{10} must be added to the model results. A constant value of 5 $\mu g/m^3$ is used to represent the coarse component. Therefore:

Total PM_{10} = Primary PM (modelled) + Secondary PM (sulfate monitoring) + Coarse (constant)

1.2 Health effects of particulate matter

There is increasing evidence of epidemiological associations between traffic derived particulate air pollution (PM_{10}) and adverse health effects on adults and children. The health effects are predominantly borne by susceptible groups, such as those with pre-existing lung or cardiac conditions, elderly and children. In adults, both the acute and chronic PM exposures are implicated in observed cardiovascular morbidity and mortality effects(Dockery et al., 1993;Peters, 2005). Preterm delivery and low birth weight have been reported to be associated with prenatal exposure to air pollution(Xu et al., 1995;Bobak, 2000). Along with increased respiratory-related hospital admissions, a major concern in children is that particulate pollution impairs lung development (Schwartz, 2004). Daily fluctuations of PM_{10} levels are associated with acute respiratory hospital admissions in children, school and kindergarten absences, decreases in lung function (peak flow) in normal children and increased use of asthma medications(American Thoracic Society, 1996). Cross-sectional and longitudinal epidemiological studies suggest that inhalation of particulate matter and gases from fossil fuel combustion have a deleterious effect on the lung function of normal children (Brunekreef and Hoek, 1993;Jedrychowski et al., 1999;Horak, Jr. et al., 2002;Gauderman et al., 2004;Ward and Ayres, 2004). Two recent studies have provided insights into the short- and long-term effects of PM_{10}, and $PM_{2.5}$ on paediatric lung function. Ward and

Ayres (Ward and Ayres, 2004) showed in a systematic review of 22 panel studies in children aged between 6 and 11 years, that short-term variations in ambient PM are associated with changes in peak expiratory flow rate. Over the longer term, Gauderman *et al* (Gauderman et al., 2004) reported that children living in communities with high mean annual average $PM_{2.5}$, have decreased annual growth of forced expiratory volume in 1 sec (% predicted FEV_1), forced expiratory volume (FVC), and maximal midexpiratory flow rate (MMEF). The mechanism for these long-term effects is unclear, but may reflect a reduction in the number of alveoli, or chronic airway inflammation (Gauderman et al., 2004).

1.3 Health effects of biomass fuel derived particulate matter

For the world's poorest populations, the burning of biomass fuels such as wood, animal dung, and crop residues results in levels of exposure to carbonaceous PM that are an order of magnitude above the health-based guidelines of the developed world (Ezzati and Kammen, 2001b). This widespread exposure to PM from biomass smoke is estimated to cause two million excess deaths per year (Bruce et al., 2000), a major proportion of these in young (under 5 year old) children (Smith et al., 2000). The major concern is an increased incidence of acute respiratory infection in children exposed, leading to increase in mortality and morbidity (Ezzati and Kammen, 2001a). The other adverse effects like otitis media and an increase in pulmonary tuberculosis have been extensively reviewed by Bruce et al (Bruce et al., 2000). Chronic obstructive pulmonary disease and chronic bronchitis have been reported to be higher in women exposed to biomass smoke (Kiraz et al., 2003).

Despite these convincing epidemiological data in children, major uncertainties remain, mainly with exposure assessment. It is unclear to what extent PM_{10} measured at a point distant from the home or school, misclassifies individual exposure. For example, a fixed

monitoring station cannot capture exposure variations resulting from time spent outside, or proximity to main roads. Also the availability of the sophisticated equipment required for exposure assessment is more easily available in developed countries as compared to developing countries, as part of regulatory requirement.

1.4 Exposure assessment methods – PM

1.4.1 MONITORING OF PM

Actual monitored PM levels (fixed monitors or personal monitors) can assess exposure. Several fixed monitoring sites have been traditionally used to assess ambient air pollution levels. In practice a size specific sampling inlet is used which collects 50% of 10μm aerodynamic diameter, more than 95% of 5μm aerodynamic diameter particles. There are 2 different sampling methods available in Leicester; 1) Tapered Element Oscillating Microbalance (TEOM), 2) Beta Attenuated Monitor. TEOM is expensive equipment and preheats the air stream resulting in loss of semi-volatiles. Because of the spatial variations within the study area, data from fixed sites is not accurate for individual exposure estimation (Nerriere et al., 2005). Personal monitors are ideal, but are expensive and not suitable for long-term monitoring.

1.4.2 MODELLING OF PM

An alternative to monitoring is using the pollution modelling, which incorporates PM contribution from different sources and meteorological data into the Geographic Information System (GIS). In contrast to fixed site monitoring, this method is better at addressing spatial variations and is also suitable for long-term exposure assessment. However the model should be validated using the monitored data. Geographical information systems technology and dispersion modelling of pollutants (Moschandreas et al., 2002) estimates PM_{10} exposure at any geographical location for large numbers of

children. However, to date, it is unclear whether GIS modelling techniques reduce exposure misclassification. A further problem with purely epidemiological data is that combustion-derived PM_{10} is spatially correlated with other pollutants (Gauderman et al., 2004). Health effects attributed to PM_{10} may therefore be caused by other fossil fuel-derived pollutants (e.g. gases). A causal relationship between PM_{10} and growth of lung function would be strengthened by data showing: i) that reduced lung function is associated with increased particle burden in the lower airway, and ii) a plausible biological mechanism.

Leicester is one of the largest cities in the East Midlands of England, designated as First Environment City in 1988. The city stands in the broad, shallow valley of the River Soar, with major radial and tangential roads without a "heavy" industrial area. There are a few high-rise buildings near the centre with the majority of people living in one-storey houses. Leicester has 5 PM_{10} monitoring stations and 2 dispersion models (ADMS and AIRVIRO). AIRVIRO (developed by SMHI) operates on a countywide basis (Leicester Air Quality Report Review and Assessment, 2000). The levels of PM_{10} measured at the City Centre site in 2003 (when the majority of children in this study were tested), showed an annual mean of 25μg/m^3 and the daily mean of 50μg/m^3 was exceeded only on 15 days in a year. The current UK Air Quality Objectives (National Air Quality Strategy) are; a maximum annual mean of 40μg/m^3 and a maximum 24-hour mean of 50μg/m^3, with upto 35 exceedances allowed per year (Defra UK).

1.5 Exposure assessment – biomass smoke

Indoor cooking with biomass fuels can produce PM levels upto 2000μg/m^3 (Balakrishnan et al., 2002). In the same study Balakrishnan et al also found fuel type, type and location of kitchen and time spent near kitchen while cooking were most important determinants of exposure. Similarly indoor cooking was found to have higher concentrations than

outdoor cooking in two rural Bolivian Villages (Albalak et al., 1999). In the absence of expensive sophisticated equipment, these determinants can be used as proxy markers of individual exposure.

1.6 Role of alveolar macrophages

Alveolar macrophages are the cells of innate immune response and the first line of defence against inhaled particles that escape the mucociliary clearance. AM also acquire particles by engulfing other particle containing AM or by re-uptake of particles released by dead AM. The predominant mechanisms of clearance of insoluble particles is by cephalad transport of AM with their phagocytized burdens up the conduction airways (Lehnert, 1992). The lifespan of AM and kinetics of chronically inhaled particles in AM in humans is not exactly known. However there is some evidence from instillation experiments that AM are long lived. Particles instilled experimentally into the normal human lung are cleared in two phases: 1) a rapid-phase clearance half time of 0.5 days and 2) a long-term clearance half time of 110 days(Lay et al., 1998).

1.7 Quantification of particles

The capacity of AM to phagocytose and store particles over time has been used to detect occupational exposure to hazardous dusts (Rainey et al., 1994;Fireman et al., 1999). Is there any evidence that increased exposure increases AM particle burden? In an earlier study in children it was found that the percentage of particle containing AM were increased in children reported to be living near a main road (Bunn et al., 2001). Finch et al (Finch et al., 2002) exposed rats to biodiesel by inhalation for 13 weeks and there was a dose-related increase in the number of particles in AM. The number of rats with higher loading was more in the high exposure group (Table 1). After a 28-day period of recovery after exposure, only 27% of rats had moderate amounts of loading as compared to 85%

immediately post exposure. In a similar study, when rats were exposed for 30 or 90 days to wood smoke the number of AM with >10 particles was higher in the group exposed to 10mg/m^3 as opposed to 1mg/ m^3 (Tesfaigzi et al., 2002). Similarly the mean number of carbon-laden macrophages was significantly higher in Roman traffic policeman as compared to residents in rural area in Italy (Giovagnoli et al., 1999). The carbonaceous PM from ambient air can be seen as black particles in the alveolar macrophages (Calderon-Garciduenas et al., 2001).

Table 1: Chronic exposure of rats to biodiesel and AM particle loading

Varying degrees of particle loading in AM and number of rats exposed to bio-diesel (Soya- bean oil) for 13 weeks. (Finch et al., 2002)

Alveolar macrophage particle loading	**Control (n = 39)**	**Low (0.04mg PM /m^3) (n = 40)**	**Intermediate (0.2mg PM /m^3) (n = 40)**	**High (0.5mg PM /m^3) (n = 40)**
NAD	37	10	0	0
Minimal	2	28	7	0
Mild	0	2	26	6
Moderate	0	0	7	34

NAD – no particles in cytoplasm

Minimal – A few particles scattered in cytoplasm

Mild – moderate number of particles in cytoplasm ($\leq$10): do not obscure the nucleus

Moderate – many particles (too many to count) in cytoplasm cover the nucleus; slightly enlarged nucleus

1.8 Determinants of AM carbon loading

Apart from the amount and duration of exposure, the quantity of AM carbon depends on a series of interrelated physiological variables. Upper airway defences, mucociliary clearance and the ratio of tidal volume to lung surface area, all determine the number of particles reaching the lower airway. Therefore any factor affecting the tidal volumes for example exercise, age etc should increase the amount of PM inhaled. AM properties like phagocytic capacity, residence time of AM before moving out onto the mucociliary escalator, and "recycling" of PM by AM phagocytosis of apoptotic carbon-containing AM also factor in.

The reasons why AM were thought to be suitable to measure PM are: 1) in several studies carbon particles in AM indicate the amount of particles reaching the lower airway and alveoli, 2) AM associated clearance is a major mechanism for removal of insoluble particles, 3) AM can be sampled easily either by bronchoalveolar lavage (BAL) or a less invasive procedure of sputum induction.

1.9 Sampling of alveolar macrophages

BAL has been used in human and animal studies to sample AM. This procedure requires intubation and anaesthesia and is therefore considered to be an invasive procedure, which is difficult to use in epidemiological studies. In contrast, sputum induction is a non–invasive technique of collecting secretions from lower airways in subjects who do not produce sputum spontaneously. This consists of inhaling an aerosol of saline over different time periods and subjects are instructed to expectorate in a container. AMs are the predominant cell type (Spanevello et al., 2000) in these samples from normal individuals, and thereby the measurement of AM carbon loading, is now feasible using induced sputum. Induced sputum can be safely performed in children over 6 yrs, with a success rate of between 68 and 100%(Wilson et al., 2000;Gibson et al., 2000;Jones et al.,

2001), and few side effects. Hypertonic saline-induced airway obstruction can be prevented by pre-treatment with a β_2 adrenergic receptor agonist (e.g. salbutamol) (Gibson et al., 2002): a strategy that also improves success rate (Jones et al., 2001). Induced sputum also samples other inflammatory cells and mediators that can be used to detect inflammation. Because of all the advantages described above, induced sputum is being increasingly used in air pollution studies (Nordenhall et al., 2000;Gong, Jr. et al., 2003).

Induced sputum has been used in developing countries in the diagnosis of pulmonary infections (Zar et al., 2000b;Hartung et al., 2002), and hemosiderin-laden macrophages have been described in spontaneously produced sputum samples from traffic policeman in India (Roy et al., 2001). There is no data on the use of differential count for assessing airway inflammation or AM. One of the limitations of the sputum processing in the developing countries is the cost of the equipment and refrigeration. In the absence of cyto-centrifuge, the sputum processing method needed to be modified.

1.10 Toxicity of particulate matter

Although, the cellular mechanisms for PM_{10}-induced impairment of lung function are unknown, AM-induced inflammation may be a key step in PM_{10}-induced cardiovascular mortality in adults (van Eeden et al., 2001). Indeed, increased levels of the AM-derived neutrophil chemoattractant, interleukin-8 (IL-8), and airway neutrophilia, have been reported in healthy volunteers exposed to diesel exhaust (Salvi et al., 2000). Furthermore, impairment of AM function may be responsible for other health effects. For example, particulate loading of AM impairs their phagocytic ability (Renwick et al., 2001;Becker et al., 2003): a mechanism important for the maintenance of sterility at the air/tissue interface. Phagocytosis requires the surface expression of a range of receptors (Peiser et al., 2002). The macrophage receptor of collagenous origin (MARCO) has been identified as a common pathway for the removal of unopsonized environmental particles and

bacteria by AM (Palecanda et al., 1999). It is unknown whether downregulation of MARCO expression on AM is responsible for the attenuated phagocytosis for other unopsonized particulates induced by carbon loading.

1.11 Hypothesis

The main hypothesis was that the AM carbon is a better indicator of lower airway exposure. An increase in exposure to PM at residence (assessed by proxy markers) increases AM carbon. The annual mean primary modelled PM_{10} at residence is used as a main proxy marker of exposure in this study. The increase in AM carbon is associated with decrement in lung function and increase in neutrophilic and eosinophilic sputum inflammatory markers.

1.12 Aims

- To describe the morphology of carbon in AM
- To establish a method of measuring carbon in AM using light microscopy digital images
- To quantify carbon in AM in conditions of extreme exposure e.g. biomass smoke
- To establish relationships between carbon in AM and
    - Exposure parameters – annual mean primary modelled PM_{10} at residence
    - Demographic parameters – age, height, Body Mass Index (BMI)
    - Exercise parameters – MET score, Vig Score
    - Lung function parameters – FEV_1, FVC, FEF_{25-75} and FEV/FVC
    - Sputum inflammatory parameters – sputum neutrophil and eosinophil differential, supernatant IL-8, exhaled nitric oxide.
- To explore the relationships between carbon in AM and other proxy markers of exposure e.g.- distance from home to main road, primary modelled exposure at school, primary modelled exposure at residence for a month and week prior to sampling.

1.13 Summary

There is increasing evidence from epidemiological studies of adverse respiratory health effects of particulate matter. To date all the epidemiological studies have used either data from few monitoring stations or computer generated modelled data to assess individual exposure. For biomass exposure, the type of fuel used along with type of kitchen is used as proxy markers of exposure. However these measures do not accurately estimate the amount of PM entering the lower respiratory tract, the site more relevant for development of adverse effects. AM as a part of innate immune response ingests inhaled particulate matter. Animal and human studies indicate that the carbon in AM increases with increase in exposure. Therefore the hypothesis is that, the amount of carbon (as a measure of PM) in AM indicates lower airway exposure.

Sampling of AM has been done in the past by BAL, but being an invasive procedure, is not suitable for large epidemiological studies. Induced sputum is a non-invasive procedure with AM as a major cell type in normal individuals and also samples of inflammatory mediators, like IL-8. Therefore I set out to examine the morphology and quantity of carbon in induced sputum AM in conditions of extreme exposure and traffic derived primary PM exposure. The aim was to compare the AM carbon load to exposure, lung function and sputum inflammatory parameters.

Chapter 2: Development of simplified processing of sputum

2.1 Introduction

Induced sputum has been used in developing countries for microbiological diagnosis, but not for assessing airway inflammation or AM carbon quantification. This could be because the expensive equipment (cyto-centrifuge) and ice are not available. Therefore a simplified method of processing was required, in order to use the technique in Ethiopia.

2.1.1 AIM

The aim was to develop a method without the use of cyto-centrifuge or ice, which would enable me to identify different cells with well preserved AM morphology, for performing the differential count and quantify carbon in the AM. The morphology and the differential count of cells in the simplified technique was compared to those processed by standard technique (Section 2.2).

2.2 Methods

These methods were developed in the United Kingdom (University of Leicester) for use in Ethiopia. Sputum induction was performed on healthy adults and the sample processed by a simple and standard method. In the first trial, the blood smear technique was used to make a smear. In the second trial, samples were obtained from the same adults on two occasions, 5 days apart and the smear technique was further modified.

2.2.1 LUNG FUNCTION AND SPUTUM INDUCTION

A Vitalograph 2120 spirometer (Vitalograph Ltd, Buckingham, UK) and Vitalograph 2120 Spirotrac® IV (Vitalograph Ltd, Buckingham, UK) were used to record baseline spirometric measurements. Vitalograph 2120 had a Fleisch Type pneumotachograph to

detect flow and Spirotrac® IV was a fully integrated spirometry data management system compliant with American Thoracic Society (ATS 1994 update) and European Respiratory Society (ERS 1993) Guidelines (http://www.vitalograph.co.uk/2120_td.html). The software calculated the % predicted values after entering the subject's age, gender, ethnic origin, height and weight.

In subjects with FEV_1 ≥80% predicted, the coughing technique to obtain induced sputum was demonstrated. They were asked to rinse their mouth and blow noses prior to sputum induction. Nebulised 4.5% saline was administered using ultrasonic nebuliser with an output of approximately 1ml/min (Sonix 2000 nebuliser, Clement Clarke International, Harlow, UK) as sequential 5 min inhalations (Cataldo et al., 2001). After every 5 minutes, FEV_1 was measured to detect saline-induced bronchoconstriction. If the FEV_1 fell to more than 10% of baseline, additional bronchodilator (salbutamol) was given. Nebulised saline was discontinued if the fall in FEV_1 was >20%, followed by 2.5% nebulised salbutamol. FEV_1 had to be with in 5% of the baseline value before discharging from the laboratory. The sputum sample obtained was immediately stored on ice and processed.

2.2.2 SPUTUM PROCESSING

Standard technique

Induced sputum samples were processed within 2 hours of collection at 4^0C as described previously (Brightling et al., 2000a) with some minor modifications. Sputum was placed on a petri dish and plugs selected and weighed. Freshly prepared 0.1% Dithiothrietol (DTT, Sigma, Poole, UK) at 4 times the weight of sputum plugs was added and sample homogenised by rocking on spiramix roller mixer (Denley Spiramix 5) for 15 minutes. Equal volume of Dulbecco's phosphate buffered saline (PBS) (Sigma, Poole, UK) was then added and the sample mixed by vortexing for 15 seconds. The sample was filtered using pre-wet 48μm gauze (Sefon Ltd, UK) and the volume was recorded. The total cell

count, cell viability and level of squamous cell contamination were assessed using a Neubauer haemocytometer and the Trypan blue exclusion method. A cell pellet was obtained by centrifuging the sample at 2000 rpm (790g) for 10 minutes. The supernatant was gently aspirated and stored in aliquots of 1ml for cytokine analysis at -70^{0}C. The cells were resuspended in PBS to get a cell concentration of 0.5 x 10^6/ml for cytocentrifugation. Two cytospins per subject were prepared using 75µl of cell suspension at 450rpm (18.1g) for 6 minutes using a Shandon III cytocentrifuge (Shandon Scientific, Runcorn, Cheshire, UK). The air-dried slides were stained with Diff Quik stain (Dade Behring, Deerfield, IL USA). When the slides were dry they were covered with a drop of XAM and coverslip. An operator blinded to median carbon area in AM status performed differential count on 400 non-squamous cells at a magnification of x 40.

Blood smear and simplified technique

Sputum plugs were selected and weighed. Freshly made 0.1% DTT (Dithiothrietol) equivalent to four times the amount of sample was added. This mixture was allowed to stand at room temperature for 15 minutes after which it was filtered. The sample was placed at room temperature for 15 minutes to allow homogenisation, and then filtered with 48µm gauze (Sefon Ltd, UK), microcentrifuged (Jencon's Force 12 Microcentrifuge) at 10000 rpm (8000g) for 10 minutes, and the cell free supernatant discarded. The plug of cells was very gently mixed and instead, of cytocentrifugation, a smear made. The smear was air dried, fixed and stained with Diff-Quik stain. The leukocyte differential count was obtained by counting ≥300 non-squamous cells. In the first trial, the smear was made by blood smear technique(Blood smear technique, 2004). A similar technique of sputum smear has been used by Roy et al to study the sputum siderophages (Roy et al., 2001). In subsequent trial, smear was made by placing the cell pellet between two microscope slides and drawing them apart, thus evenly distributing the cells and avoiding the formation of clumps.

2.3 *Results*

2.3.1 BLOOD SMEAR TECHNIQUE

Sputum induction was done on 7 normal adults (5 females). One sample was inadequate (containing only saliva). In the remaining 6 smears, AMs were the predominant cell type (median 86.63%, range 63-95%) followed by the neutrophils (median 12%, range, 0-36.5%). All smear values were within normal range for cytocentrifuged samples from normal adults(Spanevello et al., 2000;Belda et al., 2000).

2.3.2 SIMPLIFIED TECHNIQUE

Five of 6 paired samples showed leucocyte counts within the normal range when processed by either the simple or standard technique. Excellent leucocyte morphology was obtained with the simplified technique (Figure 1) and was satisfactory for quantification of carbon in AM. Median (range) differential counts (%) for simplified and standard techniques are shown in Table 2. The Spearman's correlation coefficient (rho) for simplified and standard for macrophage % was 0.829 and $p = 0.042$.

Figure 1: Cell morphology by simplified and standard technique

A) Smear at x40 and B) Cytospin at x40, both are showing macrophages and neutrophils. The images of AM by C) Smear method, D) Cytospin, both are showing carbon areas. E) Neutrophils by smear technique. All slides stained with Diff-Quik.

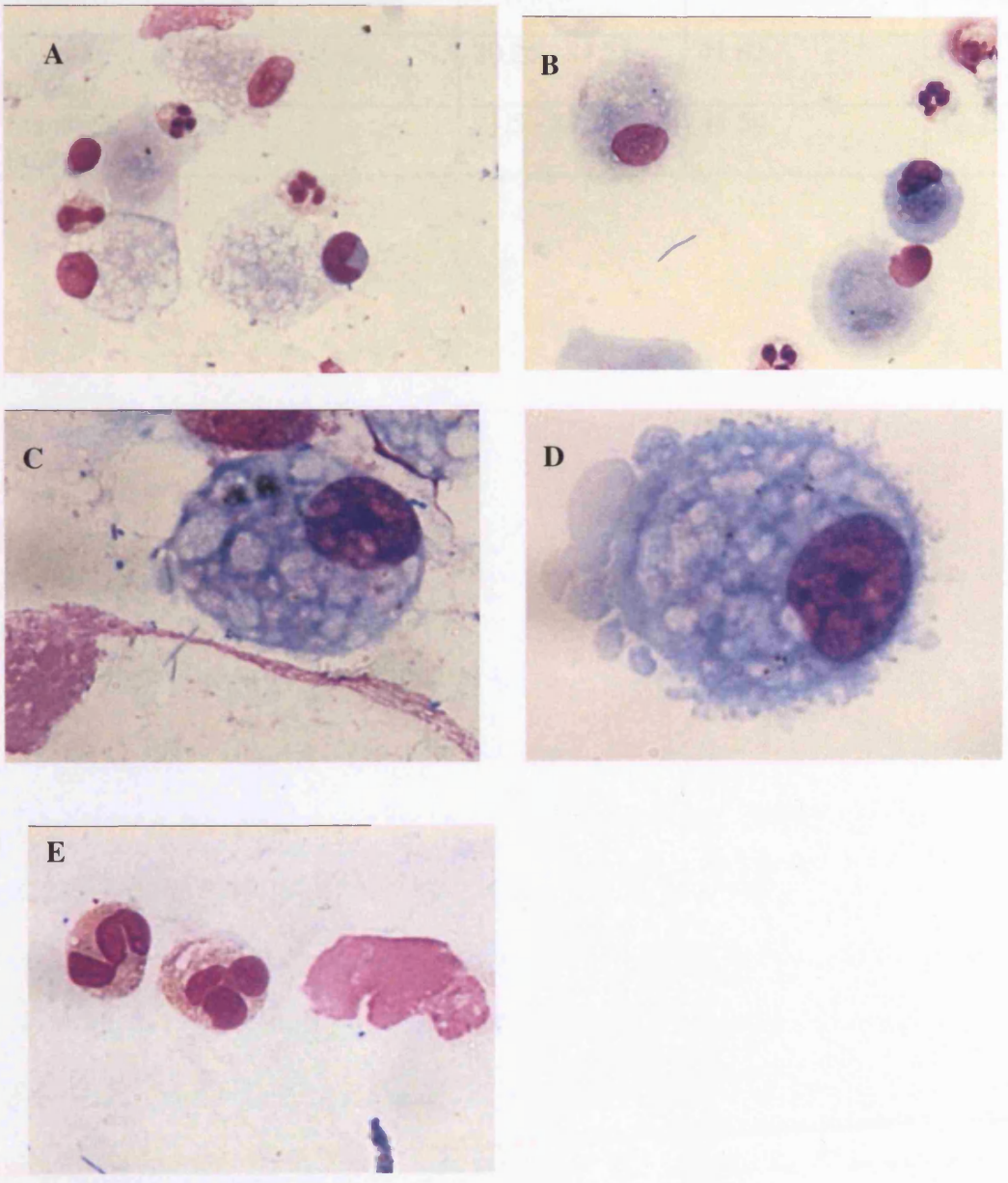

Table 2 - The median and range of macrophage and neutrophil % by simplified and standard method

	Macrophage% (Median)	Macrophage % (Range)	Neutrophil % (Median)	Neutrophil % (Range)
Simplified method	57.37	20.25 - 84.21	41.62	6.3 - 78.5
Standard method	47.25	21.5 - 87.3	48.50	12.25 - 78.25

2.3.3 FINAL METHOD

Induced sputum samples were processed within 2 hours. Sputum was placed on a Petri dish and plugs selected and weighed. Freshly prepared 0.1% Dithiothrietol (DTT, Sigma, Poole, UK) at 4 times the weight of sputum plugs was added. The sample was placed at room temperature for 15 minutes to allow homogenisation, and then filtered with 48μm gauze (Sefon Ltd, UK), microcentrifuged (Jencon's Force 12 Microcentrifuge) at 10000 (8000g) rpm for 10 minutes, and the cell free supernatant discarded. A cell smear was then made by placing the cell pellet between two microscope slides and drawing them apart, thus evenly distributing the cells and avoiding the formation of clumps. Slides were then air dried, and stained with Diff-Quik (Dade Behring, Switzerland). The leukocyte differential count (% AM, neutrophils, lymphocytes and eosinophils) was obtained from ≥300 cells.

2.4 Comments

The excellent morphology of the cells obtained by the modified smear method (simplified method) was adequate for quantification of carbon in alveolar macrophages. Compressing the pellet between two slides more evenly distributed the cells (vs the standard blood film smear technique) and improved leukocyte identification. The article on processing induced sputum by Beatriz and colleagues(Saraiva-Romanholo et al., 2003) rightly pointed out that simplification of the technique will encourage its use as a practical tool for assessing lower airway inflammation, even in developing countries. My simplified method was independently developed and the centrifugation step was essential since it increased the probability of acquiring adequate numbers of cells when the sputum sample was small as in those from children and normal adults. Most laboratories in developing countries have access to a centrifuge, but not a cyto-centrifuge. The method was ideal to be used in Gondar for processing samples from children and adults.

2.5 Summary

I set out to develop a method of processing the sputum sample without cooling or cyto-centrifugation. This was required to process samples in Ethiopia, a developing country, where both of these facilities were not available. I achieved this by processing the samples at room temperature and using a smear technique instead of cyto-centrifugation. The morphology of AM and other cells was well preserved, enabling me to assess the carbon load in AM. Further modification of the smear technique (compressing the cell pellet between the 2 slides) evenly distributed the cells, improving the quality of the smear for imaging and differential counts. Therefore this technique was suitable for use in Ethiopia.

Chapter 3: Carbon loading in extreme conditions of exposure - biomass smoke

3.1 Hypothesis and aims

Women and children exposed to biomass fuel smoke in Ethiopia inhale very high quantities of PM. The hypothesis of this study was that, the carbon area in macrophages of women and children exposed to biomass smoke is higher compared to adults and children not exposed to biomass fuel smoke. Therefore the AM carbon is a marker of lower respiratory tract exposure to PM. The aim was to quantify the AM carbon area in women and their children exposed to biomass smoke and to compare it to adults and children not exposed to biomass smoke.

3.2 Method

The study was conducted at the Gondar Institute of Medical Sciences, Ethiopia, and at the University of Leicester, UK. Ethical approval was obtained from Leicestershire Health Ethics Committee and in Gondar and informed consent was obtained from individuals or parents and guardians.

3.2.1 SUBJECTS

Women and children in Gondar were recruited from the administrative area *Kelebe* 16. They lived in mud huts and cooked using only biomass fuels. The inclusion criteria for Gondar women and children were: i) had not spent more than 5 days away from home in the preceding 3 months, ii) non-smoking households, iii) unremarkable clinical histories, iv) no respiratory illness within the last 3 weeks, and v) exclusive use of biomass fuels. I set out to assess normal individuals because 1) effect of lower respiratory infection on AM carbon is unknown 2) there are no previous studies establishing the quantity of AM

carbon as a baseline. Subject age, height, weight, and size of their family were recorded, along with details of household cooking (e.g. position of the cooking site, fuel used, and the members of the family who were involved in cooking). Adults and children recruited in the UK had the same inclusion criteria, except that adults could be both male and female and could not be exposed to biomass smoke. Subjects exposed to cigarette and coal fire smoke were excluded.

3.2.2 STUDY DESIGN

Sputum induction was performed using an ultrasonic nebuliser (Sonix nebuliser, Clement Clarke International, UK) and sequential 5-minute inhalations of 4.5% saline. Spirometry was not available in Gondar, and the peak flow rate (Mini-Wright peak flow monitor, Clement Clarke International, UK) was therefore used to detect significant bronchial obstruction (>10%) during the procedure. In the UK, the forced expiratory volume in 1 sec (FEV_1) (Vitalograph 2120 spirometer, Vitalograph, UK) was used to monitor lung function. All subjects were pre-treated with salbutamol (400μg inhaled via metered dose inhaler and Volumatic™ spacer). Induced sputum samples were processed using a modified technique, which did not require cyto-centrifugation. Sputum plugs were selected and 0.1% DTT (Sigma Aldrich, USA), at 4 times the weight of sample added, and mixed with a plastic pipette. The sample was placed at room temperature for 15 minutes to allow homogenisation, and then filtered with 48μm gauze (Sefon Ltd, UK), microcentrifuged at 10000 rpm (8000g) for 10 minutes, and the cell free supernatant discarded. I had previously determined that this centrifugation speed did not alter AM morphology. A cell smear was then made by placing the cell pellet between two microscope slides and drawing them apart, thus evenly distributing the cells and avoiding the formation of clumps. From each sample 2 to 4 slides were prepared and air-dried. One slide was stained with Wright's stain in Ethiopia to rapidly assess smear quality (poor quality slides were repeated). The remaining unstained air dried slides were

transported to the UK and both the UK and Ethiopian slides stained with Diff-Quik (Dade Behring, Switzerland). Differential count was done by counting a total of 300 cells on slides with an adequate number of cells and no clumping of neutrophils.

Image analysis of all slides was performed in the UK. Digital colour images of 50 randomly chosen AM per subject were obtained using an Olympus BX50 microscope (Olympus Optical Co. UK), at 1000x magnification under oil immersion. An image of a stage micrometer graticule (S-12S stage micrometer, 0.1mm/50 division, Pyser –SGI Limited, UK) was obtained at the same time using the same magnification. Analysis for cytoplasmic carbon was performed blinded to the country of origin using the Scion image grabber and software (Scion image, Scion Corporation, USA). The analysis steps are illustrated in Figure 2 (A, B). Each AM image was initially processed using Jasc Paint Shop Pro software (Paint Shop Pro 7, Jasc Software, MN, USA). First, the nucleus was removed from the image since the stained nucleus was identified as a "large particle" by the image analysis software. Second, Scion image software was used to calculate carbonaceous particle area. Software scaling was calibrated using the image of the stage micrometer graticule (246 pixels = 20μm). The "density slice" command was adjusted to obtain the "best fit" of the particles visible on the colour image. If the software selected non-black areas (usually areas of intense blue staining), these were manually excluded from the analysis. The individual particle areas identified were added together to produce a sum for each AM. The median cytoplasmic carbon per subject (the primary measure), and the percentage of AM containing particles were subsequently calculated from 50 cells. Analysis of each slide took approximately six hours of processing time.

3.3 Results

Induced sputum samples containing AM were obtained from Ethiopian women and children, UK adults (5 women) and UK children (n=10 for all groups). Although matched for age, Ethiopian children (6 boys and 4 girls) were lighter (mean 30 *vs* 48 kg, $p<0.01$) and smaller (mean 140 *vs* 155 cm, $p<0.01$) than UK children (n=10, 6 boys). Ethiopian mothers used a variety of biomass fuels, often in combination, and most families cooked outside in an outdoor fenced off area (Figure 3A). Four mothers cooked in a separately constructed cooking hut (Table 3 and Figure 3B).

Carbon was visible in the cytoplasm of a proportion of AM in all subjects. Representative AM with high (Ethiopian) and low levels of carbon loading (Leicester) are shown in Figures 4 and 5 (A and B respectively). Ethiopian women had the highest level of cytoplasmic carbon loading, with markedly increased levels compared with UK adults (median 9.19 *vs* 0.71 μm^2/AM, p=0.0002, CI 3.3,11.5; Figure 6A). Ethiopian children had lower levels of loading compared with maternal levels (3.32 *vs* 9.19μm^2/AM, p =0.011, CI 1.1, 9.1), with no association between loading in maternal-child pairs (rs, p=NS). AM carbon loading in Ethiopian children was, however, higher than UK children (3.32 *vs* 0.44μm^2/AM, p=0.0002, CI 1.57,6.77; Figure 6B).

For all 40 subjects, there was a correlation between the median area of cytoplasmic carbon and the median percentage of AM containing any carbon particle (Rs=0.81, p=0.01). The median percentage of AM containing particles in Gondar women was therefore significantly higher than in UK adults (100 *vs* 86%, p=0.002) and Gondar children also had an increased percentage positivity compared to UK children (96 *vs* 82%, p =0.001). Twenty-three individuals had adequate numbers of leukocytes (≥300) for a differential count. There was a trend for an increased proportion of neutrophils in Gondar women compared to UK adults (median neutrophils; 79.0 (n=4) *vs* 32.6 % (n=8),

p=0.05 CI= -8.52, 78.51). There was no difference in the proportion of neutrophils between Gondar and Leicester children (13.6 vs 10.4% p=NS).

Figure 2: Image analysis methodology

Median carbon area in AM analysis using Scion image software. A) AM showing carbonaceous particles and with nucleus deleted (Stained with Diff-Quik and imaged under oil immersion). B) Use of 'density slicing' to highlight particles. The white boxes represent the blue non-carbon areas picked up by software, which are erased prior to analysis of carbon area.

A)

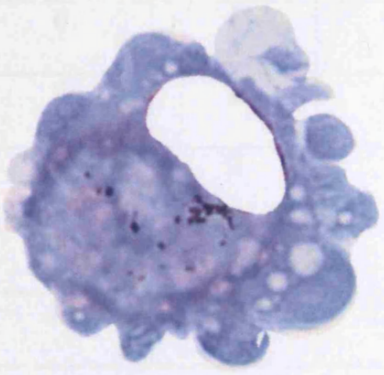

B)

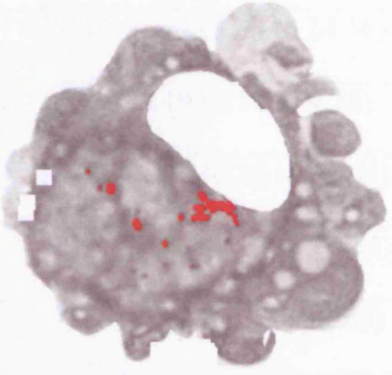

Table 3: Individual data of Ethiopian women

Subject number	Kitchen type*	Biomass fuel used†	Baseline peak flow (L/min)	Median (IQR) area of carbon (μm^2/AM)
1	I	D, W, E	430	16.95 (10.34 to 28.83)
2	II	W, D	430	7.10 (1.59 to 15.49)
3	I	W, D	430	3.72 (1.81 to 7.91)
4	II	W, Ch	360	3.81 (1.5 to 8.52)
5	I	W, D, Ch	400	11.28 (6.24 to 11.28)
6	I	D, W	470	12.22 (8.03 to 24.56)
7	I	D, W	430	4.19 (2.12 to 9.56)
8	II	W, E	370	11.32 (6.36 to 23.44)
9	II	W, D	370	14.24 (7.11 to 25.54)
10	I + III‡	W, D, Ch	430	6.20 (1.32 to 12.85)

*I=Cooking outside in the open air, II= cooking in a 'kitchen building' outside the house, III = cooking inside the living area.

†D=cow dung, W= wood, E= eucalyptus leaves, Ch= charcoal, order given is the priority of fuel use.

‡ Kitchen type III was used for cooking the main meal once every 3 days (*Injura*)

IQR –Interquartile Range

Figure 3: Cooking areas in Gondar

A) Cooking injura on a stove outside the hut. B) Special cooking hut.

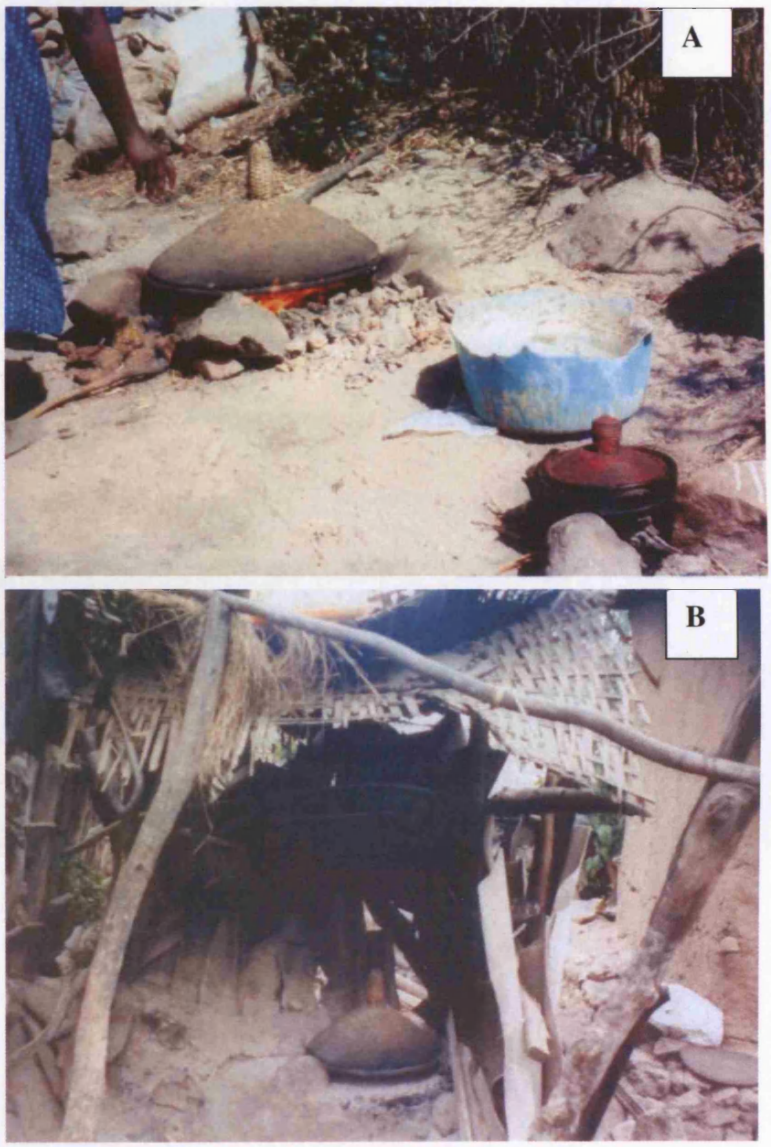

Figure 4: Representative AM from A) women in Ethiopia and B) adults in Leicester

A)

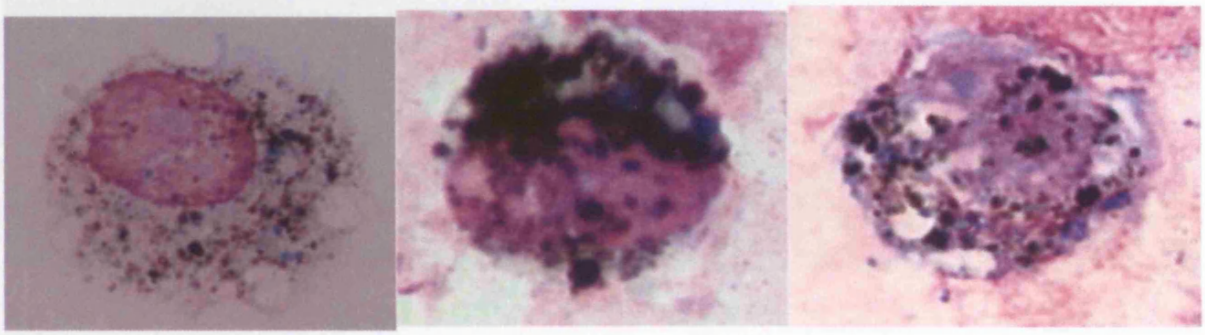

B)

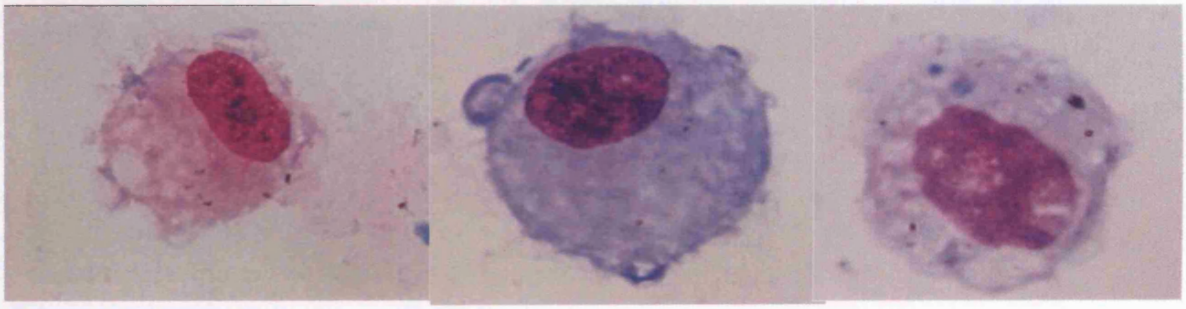

Figure 5: Representative AM from children in A) Ethiopia and B) Leicester

A)

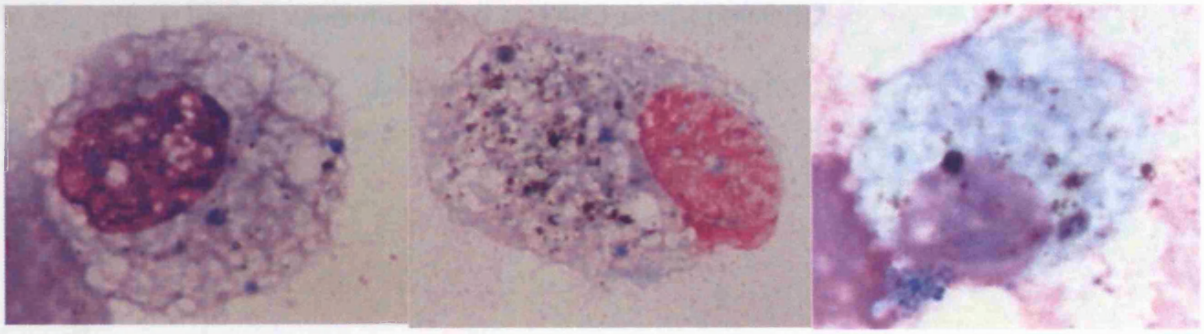

B)

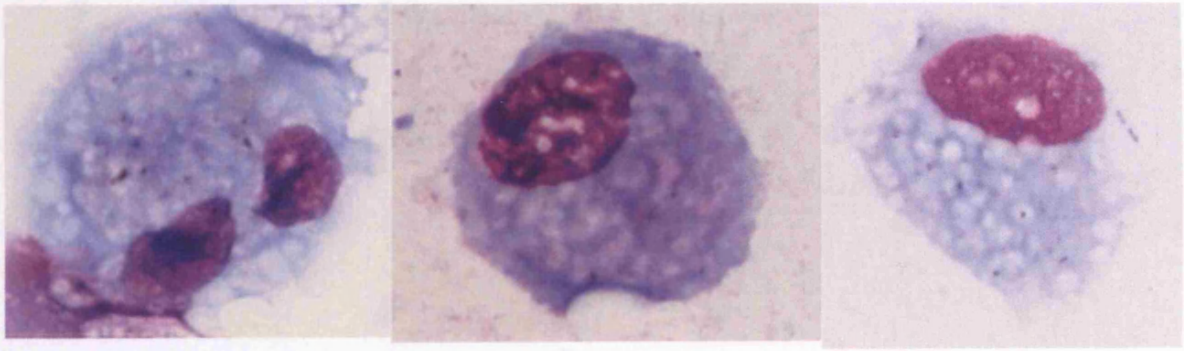

Figure 6: Comparison of carbon area in AM between Ethiopia and the UK

Data are compared using the Mann Whitney U test. n =10 in all groups.

(A) Ethiopian (Gondar) women *vs* UK (Leicester) adults; p=0.0002,

(B) Ethiopian children *vs* UK children p = 0.0002. Bars represent medians.

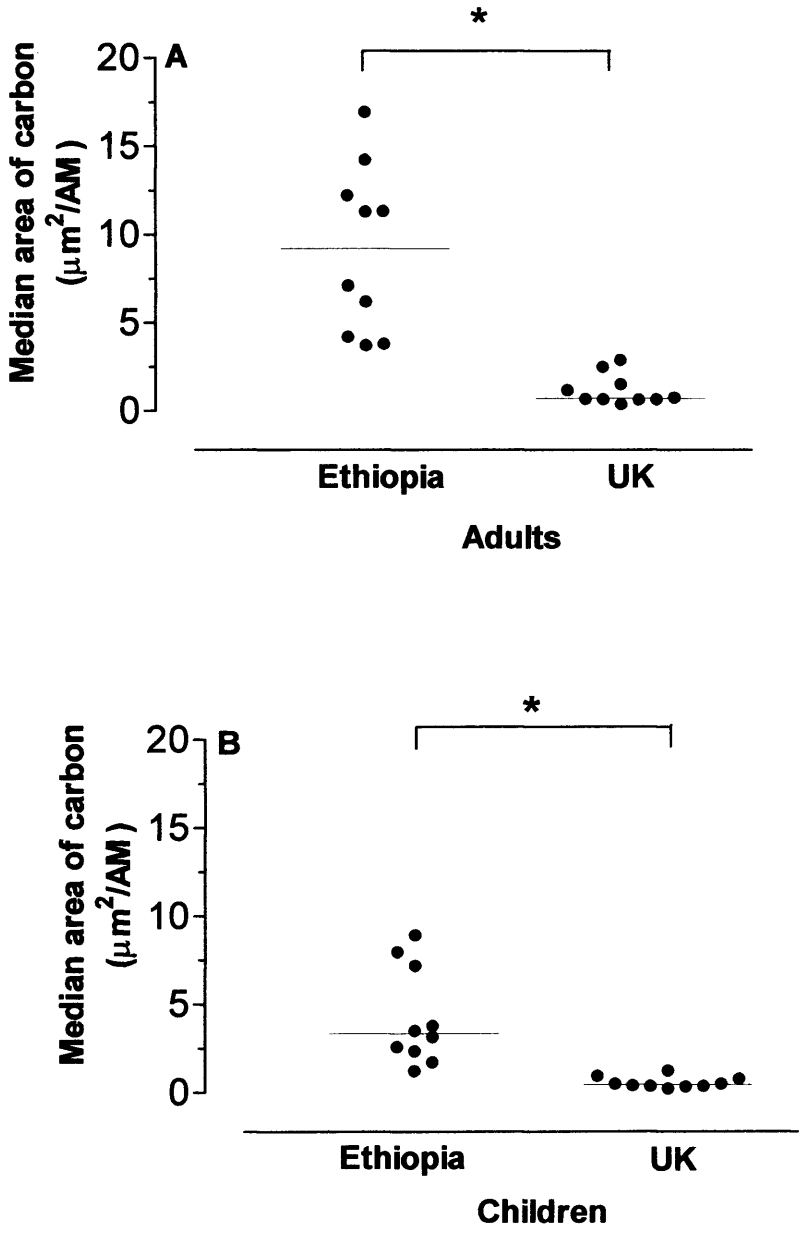

3.4 Summary

My aim in this study was to quantify AM carbon in healthy women and their children, with use of biomass fuels as the main source of energy used for cooking, and compare it to healthy adults and children in Leicester. AM were sampled by induced sputum and carbon in AM quantified by image analysis using Scion Image software. The amount of carbon in women from Ethiopia (biomass exposure) was significantly higher than adults from the UK and their children. Though children from Ethiopia had lower amounts of carbon in the AM than mothers, it was higher compared to children living in the UK. The results are discussed in detail in Chapter 5.1.

Chapter 4: AM Carbon in traffic derived PM exposure

4.1 Hypothesis and aims

The main hypothesis of this study was AM carbon is a better indicator of lower airway exposure and increases in primary modelled PM_{10} at residence. The quantity of AM carbon is determined by age, height, exercise and Body Mass Index (BMI). The AM carbon is associated with decrease in lung function and increase in sputum inflammatory markers.

Aims

- To describe the morphology of carbon in AM of children exposed to ambient PM
- To establish relationships between carbon in AM and
    - Exposure parameters – annual mean primary modelled PM_{10} at residence
    - Demographic parameters – age, height and BMI
    - Exercise parameters – MET score, Vig Score
    - Lung function parameters – FEV_1, FVC, FEF_{25-75} and FEV/FVC
    - Sputum inflammatory parameters – sputum neutrophil and eosinophil differential, supernatant interleukin -8, exhaled nitric oxide.
- To explore the relationships between carbon in AM and other proxy markers of exposure
    - Distance from home to main road
    - Primary modelled exposure at residence for a month and week prior to sampling
    - Primary annual mean modelled exposure at school

4.2 Methods

4.2.1 SUBJECTS

The study protocol and the informed consent forms were approved by the Institutional Review Board (Leicestershire Research Ethics Committee). All parents gave written, informed consent and were financially compensated for expenses associated with their participation. All children gave assent after the procedure was explained to them.

Permission was obtained from the Local Education Authority to approach the schools and subsequently from school Head Teachers to distribute invitation letters to children aged between 8 to 15 years. Parents and children who expressed a wish for more information were contacted, and asked questions related to the inclusion and exclusion criteria. To be invited to attend for induced sputum, children had to be: i) aged between 8 to 15 years, ii) residing in Leicestershire, iii) residing in the same house during the previous year, iv) have normal reported levels of activity. In order to achieve the broadest range of exposures, modelled levels of primary PM_{10} (description of primary PM in section 1.1.3) in 1997 for the home address had to be either the low or high exposure tertile (the "screening" PM_{10}). Thus children in the mid-tertile of exposure were excluded. The lower tertile was initially defined as mean modelled primary PM_{10} of $\leq 1.92 \mu g/m^3$ or below, and high tertile as $>3.82\ \mu g/m^3$, but due to difficulties in recruiting children, the upper limit for the lower exposure group was increased to PM_{10} of $\leq 2.3 \mu g/m^3$. The exclusion criteria were; i) any chronic respiratory illness (e.g. asthma), ii) a history of an acute respiratory tract infection in the last 3 months, iii) exposure to tobacco smoke at home or any personal smoking, iv) use of open coal fired heating in the home, v) a holiday outside Leicestershire >5 days during the previous 3 months, vi) living in an apartment above the first floor (as modelled data is applicable for first floor). Since the half-life of particles in AM after a single instilled dose is 110 days(Lay et al., 1998), I excluded children who

had a holiday outside Leicester for more than 5 days in the previous 3 months. I set out to assess normal individuals because 1) effect of lower respiratory infection on AM carbon is unknown, 2) there are no previous studies establishing the quantity of AM carbon as a baseline. Addresses of children fulfilling the inclusion criteria were converted to grid coordinates to obtain the "screening" primary mean modelled PM_{10}.

116 healthy children were recruited. The recruitment was mainly from school. Some healthy siblings of children attending asthma clinic or on the asthma database were also recruited (details in Figure 7). Because of difficulties in recruiting children from low tertile, families on the Leicestershire Health Authority Child Health Database were approached. The primary annual mean modelled PM_{10} was available for these children (as a part of an ongoing project in the department), which enabled me to identify children living in the lower tertile.

4.2.2 STUDY DESIGN

This was a cross-sectional study and children fulfilling the inclusion criteria were invited to attend for sputum induction, which was performed from November 2002 through December 2003 at the Leicester Royal Infirmary (UK). Children and parents were asked about age, gender, number of siblings, birth order, parental conception of living near main or quiet road, details of other potential sources of pollution near the homes apart from traffic, and the address of the school that the child attended in the last year. Children were also asked to fill in a questionnaire related to the leisure time physical activity for calculation of MET hr/wk and VIG (vigorous) hours/week (Aaron et al., 1993). The number of days children performed hard and light physical exercise over the previous 2 weeks, and time spent watching television was also recorded. The characteristics, and the screening exposure data, of the 66 children in whom adequate induced sputum samples were obtained is summarised in Appendix 2. Four children with the revised screening criteria of an annual modelled mean PM_{10} in 1997 between 1.92 and 2.3$\mu g/m^3$ were

recruited, in whom 3 produced an adequate sputum sample. When adequate sputum was obtained, children were asked if they would attend in 6 months for a further sample in order to study the long-term variation in median carbon area in AM.

Figure 7: Recruitment and number of healthy children attending the sputum induction

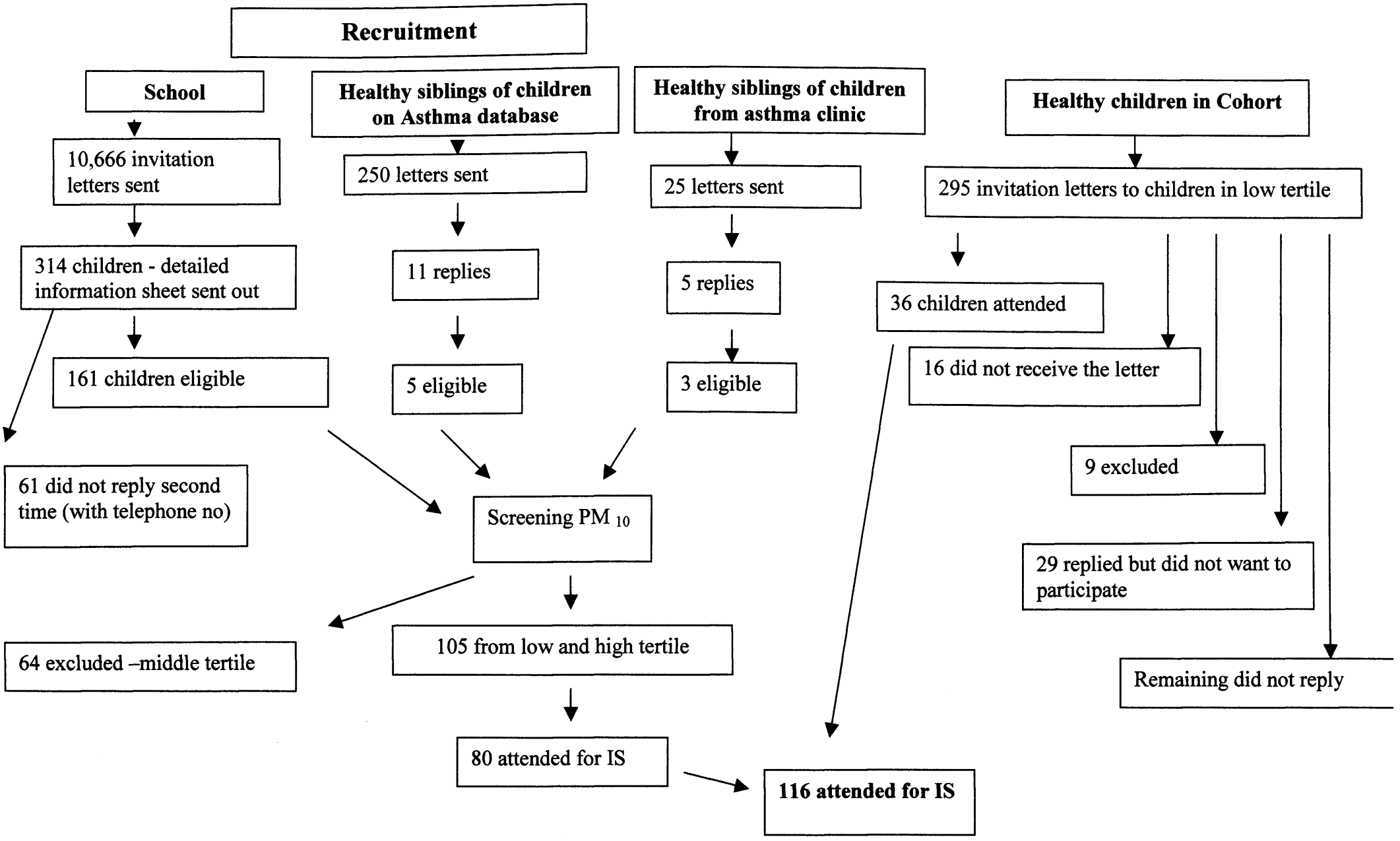

Figure 8: Number of adequate samples from recruited children

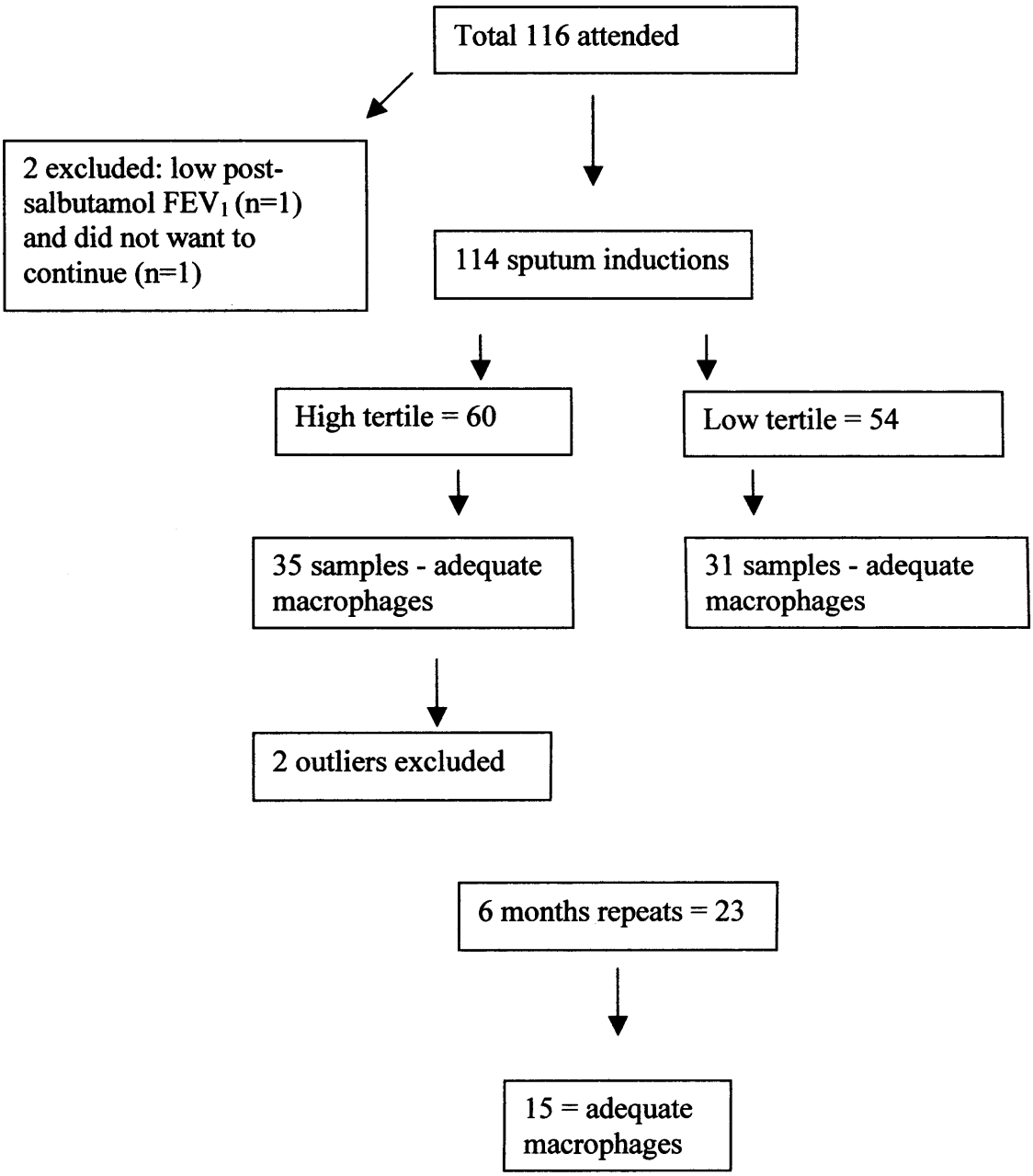

4.2.3 EXERCISE

Children filled in details of frequency and duration of all activities that they had participated in for at least 10 times during the past year. An estimate of the average number of hours per week spent in each activity was then calculated. The hours/week estimate for each activity was also multiplied by the metabolic cost of that activity (expressed as MET and obtained from existing tables) (Andrea M.Kriska and Carl J.Caspersen, 1997), in order to weight each activity by a crude estimate of its relative intensity. MET (hr/wk) for each activity were summed to determine a composite estimate over the past year. A higher score indicated increased activity. One MET represents energy expenditure at rest (1 kcal/kg/hr). VIG was estimated by tallying the average hours of activity with METs $\geq$6.

The calculation of MET- hr/wk from Kriska's Modifiable Activity Questionnaire was done using the following formula:

MET hr/wk for each activity:

$$\frac{(\#\text{ months/year}) \times (4.3\text{ wks/month}) \times (\#\text{ days/wk}) \times (\#\text{ min/day}) \times \text{MET value}}{60(\text{min/hr}) \times 52(\text{wk/yr})}$$

4.2.4 SALIVARY COTININE

To exclude significant exposure to cigarette smoke, salivary samples for cotinine from 114 children were tested (2 insufficient for analysis). Samples were collected in a 1ml ependorf container using a straw to drip in the sample. Samples were labelled and immediately frozen at -70^{0}C, then were transported in batches to ABS laboratories (London UK), on frozen gel pads for salivary cotinine analysis by gas-liquid chromatographic method with a detection limit of 0.1ng/ml (Feyerabend and Russell, 1990). Salivary cotinine was expressed as ng/ml. In this assay, a level $\leq$14.3ng/ml

excludes active smoking (McNeill et al., 1987), and a level ≤1.2ng/ml represents the 90th percentile for children with no adult smokers in the household (Jarvis et al., 1992).

4.2.5 EXHALED NITRIC OXIDE

A Sievers Nitric Oxide (NO) Analyser 280 was calibrated using a zero filter and known concentrations of NO. Exhaled NO (eNO) in children >12 years was measured by a technique described for adults (American Thoracic Society, 1999). For children <12 years a 2s plateau duration and exhalation time of at least 4 seconds was used. Repeated exhalations were performed until three NO plateaus agreed at the 10% level or 2 at the 5% level. The mean eNO value was measured according to the American Thoracic Society (ATS) Guidelines at 50ml/sec flow rate and expressed as parts per billion (ppb). Satisfactory exhalations were obtained from 37/42 children (26 with adequate AM in sputum) who did the test during their first visit.

4.2.6 LUNG FUNCTION

A Vitalograph 2120 spirometer (Vitalograph Ltd, Buckingham England) and Vitalograph 2120 Spirotrac® IV (Vitalograph Ltd. Buckingham UK) were used to record baseline spirometric measurements. Vitalograph 2120 had a Fleisch-Type pneumotachograph to detect flow and Spirotrac® IV was a fully integrated spirometry data management system compliant with ATS 1994 update and ERS 1993 Guidelines http://www.vitalograph.co.uk/2120_td.html). The equipment was cleaned according to manufacturers instructions and was serviced on site annually. The software calculated the % predicted values after entering the child's age, gender, ethnic origin, height and weight. The spirometer was calibrated for the room temperature prior to testing every day. Each child was asked to perform 3 satisfactory blows with a minimum of 2 acceptable ones. A disposable mouthpiece (Safe Tway mouthpieces, Vitalograph, UK) was used for each individual. The acceptability and reproducibility criteria were based on the ATS

recommendations (1995), modified for children. The reproducibility criteria were that the largest and second largest FEV_1 and FVC could not vary by more than 0.2L, with no false start, coughing, or early end of expiration, to accept the FVC. A plateau in the volume time curve had to be observed, defined by no change in volume for at least 1 second or reasonable time. A maximum of 8 blows were attempted for baseline spirometry. The use of nose clips was optional. The forced expiratory volume in 1 second (FEV_1), forced vital capacity (FVC), FEV_1/FVC and mid-expiratory flow between 25% and 75% of the forced vital capacity (FEF_{25-75}) were calculated. Each flow volume loop was visually examined. If the final expiratory phase stopped due to Valsalva manoeuvre or hesitation, but the first portion of the loop was acceptable, only FEV_1 was calculated. The software used the LAM/Polgar regression equations for predicted values for Asian children. In addition, Z (standard deviation)-scores were calculated for all baseline parameters as previously described (Rosenthal et al., 1993), using equations derived from normal healthy cohort of UK Caucasian children. After obtaining a "baseline" lung function, children were treated with 200μg salbutamol administered via a metered dose inhaler and Volumatic (Volumatic® Allen and Hanburys, Uxbridge, Middlesex, UK). "Post-bronchodilator" lung function measurements were obtained at 15 minutes. Children with post bronchodilator FEV_1 <80% were excluded. FEV_1 was used to assess the intrathoracic airways obstruction, mainly larger airways and FEF_{25-75} for smaller more distal airways.

4.2.7 SPUTUM INDUCTION

In children with FEV_1 ≥80% of predicted, the coughing technique to obtain induced sputum was demonstrated. Children were asked to rinse their mouth and blow noses prior to sputum induction. Nebulised 4.5% saline was administered using ultrasonic nebuliser with an output of approximately 1ml/min (Sonix 2000 nebuliser, Clement Clarke

International, Harlow, UK) as sequential 5 minute inhalations (Cataldo et al., 2001). After every 5 minutes, FEV_1 was measured to detect saline-induced bronchoconstriction. If the FEV_1 fell by more than 10% of baseline, additional bronchodilator (salbutamol) was given. Nebulised saline was discontinued if the fall in FEV_1 was >20%, followed by 2.5% nebulised salbutamol. FEV_1 had to be within 5% of the baseline value before discharging the child from the laboratory. The sputum sample obtained was immediately stored on ice and processed. No child had a significant drop in FEV_1 or symptoms that needed "rescue" salbutamol. Some children reported mild throat discomfort after sputum induction.

4.2.8 SPUTUM PROCESSING AND LEUKOCYTE DIFFERENTIAL

Induced sputum samples were processed within 2 hours of collection at 4^0C as described previously (Brightling et al., 2000a) with some minor modifications. Sputum was placed on a petri dish and plugs selected and weighed. Freshly prepared 0.1% Dithiothrietol (DTT, Sigma, Poole, UK) at 4 times the weight of sputum plugs was added and sample homogenised by rocking on spiramix roller mixer (Denley Spiramix 5) for 15 minutes. Equal volume of Dulbecco's Phosphate Buffered Saline (PBS) (Sigma, Poole, UK) was then added and the sample mixed by vortexing for 15 seconds. The sample was filtered using pre-wet 48μm gauze (Sefon Ltd, UK) and the volume was recorded. The total cell count, cell viability and level of squamous cell contamination were assessed using a Neubauer haemocytometer and the Trypan blue exclusion method. A cell pellet was obtained by centrifuging the sample at 2000 rpm (790g) for 10 minutes. The supernatant was gently aspirated and stored in aliquots of 1ml for cytokine analysis at -70^0C. The cells were resuspended in PBS to get a cell concentration of 0.5 x 10^6/ml for cyto-centrifugation. Two cytospins per subject were prepared using 75μl of cell suspension at 450rpm (18.1g) for 6 minutes using a Shandon III cyto-centrifuge (Shandon Scientific,

Runcorn, Cheshire, UK). The air-dried slides were stained with Diff-Quik stain (Dade Behring, Deerfield, IL USA). When the slides were dry they were covered with a drop of XAM and coverslip. An operator blinded to median carbon area in AM status performed differential count on 400 non-squamous cells at a magnification of x 40.

The remaining airway cell suspension was stored in 4.5% buffered gluteraldehyde at 4 - 8°C for electron microscopy (EM). 4 to 10 cytospins were prepared for MARCO (Macrophage Receptor of Collagenous Origin) immunostaining using labelled slides using 75µl at 800rpm(80g) for 5 minutes at low acceleration(Bunn et al., 2002). Slides were air dried for 1 hour and dipped in chloroform and acetone mixture (50:50) for 10 minutes (in a fume cupboard). The slides were then air dried for 1 hour, wrapped in foil and stored in a freezer at –70°C.

4.2.9 INTERLEUKIN-8

Interleukin-8 (IL-8) in unfrozen induced sputum supernatants was analyzed (by Lucy Woodman and Ananth Tellabatti) according to an established bioassay, using a BD OptEIA™ set for human IL-8, BD Biosciences Pharmingen, San Diego, CA, US)(Brightling et al., 2000b).

Principle of the test

The BD OptEIA test is a solid phase sandwich ELISA (Enzyme-Linked Immunosorbent Assay). It utilizes a monoclonal antibody specific for IL-8 coated on a 96-well plate. Standards and samples are added to the wells, and any IL-8 present binds to the immobilized antibody. The wells are washed and streptavidin-horseradish peroxidase conjugate mixed with biotinylated anti-human IL-8 antibody is added, producing an antibody-antigen-antibody "sandwich". The wells are again washed and TMB substrate solution is added, which produces a blue colour in direct proportion to the amount of IL-8

present in the initial sample. The Stop Solution changes the colour from blue to yellow, and the microwell absorbances are read at 450nm. The IL-8 concentration is quantified in comparison with a standard curve for IL-8 and is expressed as ng/ml, after correction for dilution of the supernatant. The sensitivity level of the assay is 0.8×10^{-3} ng/ml.

Assay procedure summary

To each of the wells, 50µl of ELISA Diluent was added, followed by 100µl of standard or sample and incubated for 2 hours at room temperature. The wells were aspirated and washed 5 times, and 100µl of prepared Working Detector was added to each well and incubated for 1 hour at room temperature. The wells were aspirated again and washed 7 times. Finally 100µl TMB One-Step Substrate Reagent was added to each well and incubated for 30 minutes at room temperature, followed by 50µl Stop Solution. The absorbances are read at 450nm within 30 minutes.

Calculation of Results

The mean absorbance for each set of duplicate standards, controls and samples was calculated. The mean zero standard absorbance (ie, plate background) was subtracted from each. The standard curve was plotted on log-log graph paper, with IL-8 concentration on the x-axis and absorbance on the y-axis. The best-fit straight line through the standard points was drawn. If samples were diluted, the interpolated IL-8 concentration was multiplied by the dilution factor.

4.2.10 AM CARBON LOADING

Digital colour images of 100 AM from each individual were captured using JVC digital camera and Olympus BX50 microscope (Olympus Optical Co. Ltd, UK), at x1000 magnification (under oil immersion). Prior to each imaging, the microscope was adjusted for Kohler illumination, and the slide and lenses cleaned to remove any contaminating dust particles. All AM in randomly selected fields were identified by their characteristic

features and imaged to include whole cells, with the cell borders clearly seen. Images were obtained with the AM nucleus in focus to ensure that there were no artefacts in the image. Scion Image grabber software (Scion Corporation, USA) was used to acquire the images, which were stored as tiff files. An image of a stage micrometer graticule (S-12S stage micrometer, 0.1mm/50 division, Pyser –SGI Limited, UK) was also obtained at the same magnification. Scion software scaling was calibrated using the image of the stage micrometer graticule (246 pixels = 20μm).

Each AM image was initially processed using Jasc Paint Shop Pro software (Paint Shop Pro 7, Jasc Software, MN, USA) and PC USB Graphics Tablet (Medion). First, each AM was "cut and pasted", then the nucleus removed - since it was identified as a "large particle" by the image analysis software. The Scion Image software was used to measure carbonaceous areas in μm^2, using an in-house macro to reduce the number of manual steps (Appendix 1). The "density slice" command was adjusted to obtain the best fit of the carbon areas visible on the colour image (Figure 2, page 40). Examination of the colour image identified bacteria and dense cell wall areas that had been erroneously selected as "black" by the software. These were manually removed using the "erase" feature or excluded by selecting only the true carbon areas. The total carbonaceous area for each AM was calculated and the summary variable calculated from 100 randomly selected AM. To measure AM cytoplasmic area the "density slice" was set to maximum. The maximum diameter of the carbonaceous area was also measured in 36 of the individuals. Intra-and inter-observer variability was assessed by i) the same operator repeating measurements on 40 AM (intraobserver), and ii) a second operator calculating loading on the same 40 AM (interobserver –Ananth Tellabatti). For all analyses, the median area of carbonaceous material per AM per child (median carbon area in AM) was chosen *a priori* as the primary loading variable. The mean carbon area, median and mean

number of carbon areas per AM, and the percentage of AM with any area of carbon, were used in exploratory analyses.

4.2.11 MARCO EXPRESSION

Two slides per child were processed in batches along with a control for MARCO. The frozen slides were air dried for 1 hour, marked with PAP pen (DAKO), washed in PBS. The section was covered with 100µl monoclonal MARCO antibody (supplied by Dr Lester Kobzik, Boston, USA) at 1:50 concentration and left overnight at 4^0C. Then goat serum in 1/5 concentration (Normal – Dako Cytomation Denmark) was added and left for 25 minutes. Slides were washed in PBS thrice before incubating with 100µl of secondary antibody at concentration of 1:300 (Biotinalated Goat Antimouse Immunoglobulin Dako Cytomation Denmark) at room temperature in the dark for 1 hour. The slides were then washed again and incubated with ABC (Avidin Biotinalated Complex, Vector Laboratories UK) for 30 minutes. 100µl of DAB solution (Peroxidase Substrate Kit, Vector Laboratories UK) was added after washing and reaction observed under microscope. Finally, counterstaining was done using Erhlich's haematoxylin. Slides were then air-dried, mounted using DPX and a coverslip. Positively stained cells were identified by the brown colour (Figure 9) and a maximum of 300 cells were examined under x400 magnification. Only cells with intact cell membrane were included. An operator blinded to median carbon area in AM status (Ananth Tellabatti: see acknowledgments) assessed MARCO staining as percentage of positive cells.

Figure 9: AM stained with MARCO antibody

AM stained with MARCO Monoclonal antibody showing one positively stained (brown) and one negatively stained AM, imaged under oil immersion.

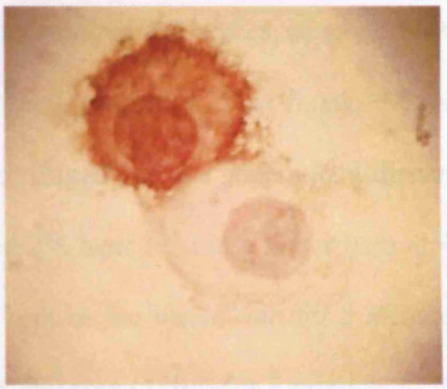

4.2.12 ELECTRON MICROSCOPY

AM were fixed in 4% gluteraldehyde in (Sørensons) phosphate buffer. After fixation, the samples were centrifuged for 5 minutes at 750 rpm (120g) on a bench top centrifuge, and re-suspended in the phosphate buffer; the cells were rinsed in fresh buffer. This was repeated 3 times to remove the traces of gluteraldehyde. AM were post-fixed in 1% Osmium tetroxide for 60 minutes. Post-fixed AM were centrifuged, and rinsed twice in distilled water, centrifuged and the supernatant discarded while the cells were suspended in 5 drops of liquid 2% agar held in a water bath at 45°C. AM in each tube were mixed with the agar and kept in the water bath for 5 minutes for equilibration and full mixing, then centrifuged at 750 rpm (120g) for 5 minutes to form a pellet of cells in the agar. The AM-containing agar was removed from the tubes and processed for Transmission Electron Microscopy (TEM) following standard ethanol dehydrating and Araldite embedding protocols. 70nm thick sections were cut, stained by uranyl acetate and lead citrate and examined in the TEM, Jeol 100 Electron Microscope (Jeol Ltd, Welwyn Garden City, UK) with calibrated images of AM being captured at a magnification of x 8300 using a AMT Advantage digital camera system (Deben UK Ltd, Suffolk, UK). Images of at least 20 AM sections from each individual were obtained, and examined with special attention to lysosomal electron dense material.

4.2.13 MARKERS OF PM_{10} EXPOSURE

The AIRVIRO Version 2.21 dispersion model (described in detail in the next section) was used since it operates on a countywide basis. To obtain PM_{10} concentrations for exposure at the home and school, addresses were converted to grid co-ordinates (Ordinance Survey UK), and the model output interrogated using these co-ordinates. The Leicester Pollution Control Team supplied hourly-modelled primary (i.e. locally generated) PM_{10} for home and school co-ordinates for the year prior to the date of

obtaining the induced sputum sample. The primary variable was the mean annual exposure of the home to modelled primary PM_{10}. Exposures for shorter (exploratory) time periods were also calculated. In the exploratory analyses, it was assumed that children attended all the days at school except holidays and weekends. Exploratory mean modelled primary PM_{10} exposures were calculated for only the hours the child attended school, and a combination of school and at home. Further exploratory variables, included the mean annual actual TEOM monitored total PM_{10} for the previous 12 months from the city centre, and a combination of the primary modelled PM_{10} for the home and "background" actual measured total PM_{10} from a rural monitoring TEOM station.

4.2.14 AIRVIRO INPUTS

AIRVIRO is a dispersion model, developed by Swedish Meteorological and Hydrological Institute, Norrköping, Sweden (Leicester Air Quality Report Review and Assessment, 2000). The model is capable of grid, gaussian, or canyon dispersion calculations. The model operates on a UNIX workstation, and includes modules for data collection, dispersion calculations, and an emissions database. Dispersion calculations are performed in the dispersion module using meteorological data together with local emissions data from the emissions database. For meteorological information, AIRVIRO used the output from a meteorological mast installed to provide data for the AIRVIRO model. Emission sources for modelling using AIRVIRO are defined as point (e.g. industrial and commercial buildings), line (roads), or area (residential, or large industrial estates) sources. The AIRVIRO model can be run on either a City or County map, zooming into a smaller area where greater detail is required. Emissions from the entire selected map are used for dispersion calculations, even where the zoom function has been used to select a smaller area for subsequent display. For this study, the run was done at a resolution of 50m x 50m.

Emission factors were obtained from the Strategy Directorate of the Greater London Authority. For this study, modelled primary concentrations of PM_{10} for 2002 and 2003, were obtained using an updated emission inventory package EMIT 2.0 (Emission Inventory Toolkit) (Leicester City Council Air Quality Review and Assessment 2003). EMIT 2.0 was inputted with up to date National Atmospheric Emission Inventory emission factors(Leicester City Council., 2003). In the model, emissions were defined as from either lines, point or area sources. For line sources (i.e. roads), AIRVIRO first calculated hourly emissions for each road link using hourly traffic flows multiplied by emission factors for each vehicle. Traffic flow data were obtained from Greater Leicester Traffic Model (GLTM), which is a TRIPS-type model. Six vehicle types for which emission factors were available from the London Research Centre were used in output calculation. The traffic allocated to each link was described according to peak flows, road type and traffic type. The speed allocated to each link was the statutory speed limit for the link, but was amended as appropriate. Point source was defined as any source that has well defined position and an emission of small-restricted volume. To reduce the time of full data entry, the time variation of emissions for each source was limited to "standard" of emission variations according to the daily, weekly, and seasonal pattern of emissions. Area sources were regarded as diffuse emissions from a defined area, and AIRVIRO modelled the dispersion of emissions from area sources at a height of 2 metres.

To calculate the dispersion of modelled primary PM_{10}, the grid reference point for each child's home and school, and desired year of meteorological data (year prior to study date) were selected. Each yearly model run expressed calculated hourly PM_{10}. Figure 10A shows an example of the modelled PM map for Leicester.

AIRVIRO validation

The Leicester City Council Pollution control group supplied hourly data at three PM_{10} monitoring sites for the years 2001, 2002 and 2003. The data available was incomplete due to technical problems at two monitoring stations during this period. Therefore the summary data was insufficient to validate the modelled data at the monitoring stations.

4.2.15 HOME-TO-MAIN ROAD DISTANCE

Address data were supplied in Excel format and imported into MS Access database software to allow easy comparison with the Address-point (Ordnance Survey, Southampton, UK) database for Leicestershire. The Address-point database provides full address and National Grid co-ordinate data for all postal addresses in the UK. Address data from the study were matched with corresponding data in the Address-point database and their grid co-ordinates to 1 metre resolution, extracted. The grid co-ordinates were imported into the ESRI ArcView (v3.2) Geographical Information System (GIS) software for analysis. The distance from each child's home address to the nearest main road (classed as Motorway, A or B road) was calculated using a Meridian digitized map of all the main roads in Leicestershire and ArcView Avenue scripts (Figure 10B).

In summary the main variables of exposure were:

- Annual mean modelled primary PM_{10} at home address
- Month, week modelled primary PM_{10} at home
- Annual mean modelled primary PM_{10} for school hours
- Annual mean modelled primary PM_{10} home and school hours
- Addition of secondary (background PM from rural sulfate monitoring) PM to all the primary modelled variables
- Annual mean monitored PM_{10} from Leicester City Centre site
- Home to major road distance

Figure 10: AIRVIRO and distance from road – examples

A) Mean annual modelled primary PM_{10} output of the AIRVIRO model for Leicester. Increased to decreased concentrations are represented as red, orange, yellow, blue.

B) Map showing the location of some school children in north Leicester and their distance to nearest main road (red line).

A

B

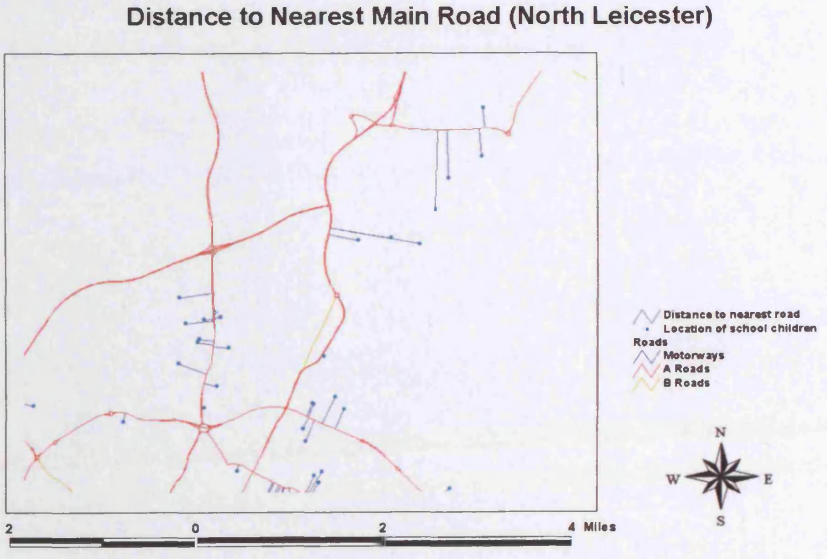

4.3 Statistical methods and data analysis

Of the 116 children invited to the laboratory, 2 were excluded (one child had a baseline FEV_1 less < 80%, even after salbutamol, and one child did not wish to continue with the test). Of the 114 children who had sputum induced, 35/60 and 31/54 adequate numbers of AM were obtained from high and low "screening" tertiles using 1997 data, respectively (Figures 7 and 8). In the long-term repeat analysis, adequate numbers of AM were obtained in 8/15 from high "screening" tertile of the 13/23 from the low "screening" tertile.

S-plus version 6.2 (Insightful Corp., Seattle, Washington, USA) was used to carry out all statistical analyses, and GraphPad Prism (GraphPad Software, CA, USA) used for graphical representation. From the carbon loading data available, in each child the median and the mean carbon area, the median and mean number of carbon areas and the percentage of cells with any carbon, were calculated. Although the median area of carbon was chosen *a priori* as our loading measure, whether it was indeed the most appropriate measure (*vs* mean) was assessed by "bootstrapping"(A.C.Davison, 2003). For bootstrapping, the total of carbon areas from 100 AM (i.e. 100 data points) were repeatedly sampled by the software (S-plus). In this procedure, data points could be taken (from within the observations) more than once. 100 observations were chosen with replacement from the data points. This was done 1000 times for each child. The mean and median of these re-sampled observations were then calculated. The mean of the squared difference between the actual mean or median and the resampled mean or median was analysed. The summary statistics for resampled means and the medians was compared. Median carbon area in AM, and the exploratory loading variables (i.e. number of particles and percentage of positive cells) were compared to mean annual, monthly, and weekly modelled primary PM_{10}, and measured PM_{10}, using normal linear models and Spearman's rank correlation test.

Although screened children were identified as living in the high and low exposure tertiles using the model run for 1997, modelled exposure of the home to PM_{10} in 12 months prior to sputum induction did not separate into two distinct categories (Figure 11), probably because an updated emissions inventory introduced between 1997 and 2001. I therefore used normal linear models. Suitable confounders were added to the normal linear model if they had a p value of <0.05, or in the models where the main effect was significant and they changed the slope of the main effect by more the 10%. 2 children, living at the same address, had unusually high median carbon area in AM, suggestive of an unexpected source of PM, and were classified as outliers and excluded from the analysis. Intra- and inter-observer variability was assessed using paired t-tests to test for bias and the SD of the difference was used to report on the variation. The percentage of SD of the difference to the SD of the combined results (n=80) was used to compare the tests. The British Standards Institute repeatability co-efficient (2 x SD of the differences) and the limits of the agreement (=mean difference $\pm$ repeatability coefficient) of the test were also calculated for the inter- and intra-observer variability. This is used to assess the agreement in a given situation.

4.4 Results

4.4.1 QUALITATIVE ASPECTS

Adequate samples for median carbon area in AM analysis were obtained from 66 children (36 boys). Their demographic data, exercise scores, lung function parameters, and induced sputum results are summarised in Table 4 (after excluding two outliers, see below) and individual data is shown in Appendix 2. AM showing a representative range of carbon loading are shown in Figure 12 and median carbon area and other exploratory parameters are summarised in Table 5. The carbon area parameters for all children are given in Appendix 3. Carbonaceous areas were not uniformly distributed within the AM of individual children. The distribution of the maximum diameter of carbonaceous areas from 36/64 children is shown in Figure 13.

The morphology of carbon in AM when viewed under light microscopy suggests that the large carbon areas result from aggregates of smaller particles (Figure 14 A and B). Carbon was not seen in other airway cells (neutrophils, columnar cells and eosinophils), consistent with the major role of AM in removing inhaled particles. Free carbon was infrequently observed (Figure 14D). Some AM containing larger amounts of carbon had a morphological appearance strongly suggestive of ongoing phagocytosis. In Figure 12 the AM with the highest amount of carbon area appears to be phagocytosing a neutrophil (which is surrounded by filopodia of AM).

Table 4: Summary of demographic, exercise, lung function and sputum induction data from children who produced an adequate sample of induced sputum

	Mean	SEM	SD	Percentiles		
				25	50	75
Age (years)	11.47	0.29	2.34	9.00	12.00	13.75
Weight (kgs)	45.54	1.68	13.44	35.10	44.60	54.95
Height (cms)	149.77	1.64	13.15	138.68	151.35	158.43
MET-hr/wk	39.93	5.00	39.99	15.38	29.09	54.39
VIG hr/wk	3.37	0.59	4.72	0.29	1.63	4.63
Baseline FEV_1% predicted	100.12	1.38	11.06	91.25	99.15	106.58
FVC % predicted	103.02	1.44	11.21	95.15	103.00	110.85
Leukocyte viability %	69.58	2.24	16.49	60.00	71.40	81.76
Squamous cell %	5.45	0.99	7.31	0.00	2.60	8.48
Neutrophils %	31.85	3.65	29.20	5.67	20.63	56.00
Eosinophils%	1.63	0.63	5.04	0.00	0.25	0.75
Macrophage %	65.95	3.72	29.79	41.38	78.63	93.25
Lymphocytes %	0.15	0.03	0.21	0.00	0.00	0.25
Epithelial cells %	0.41	0.10	0.79	0.00	0.25	0.50
IL-8 (ng/ml)	14.87	3.44	27.33	0.96	6.26	12.06
MARCO (% positive AM)	80.42	2.50	13.90	70.97	83.55	92.46

Figure 11: Screening and study modelled PM_{10}

Comparison of screened (1997) and study period (12 months prior to test) modelled PM_{10} ($\mu g/m^3$).

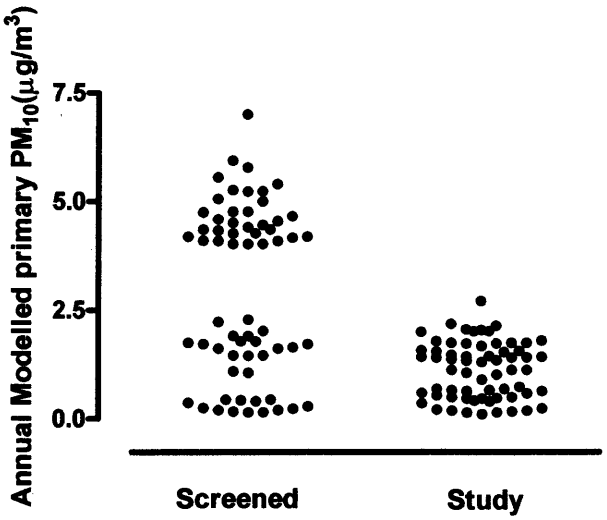

Figure 12: Representative images of AM

AM showing increasing degrees of carbon loading (all from different children). Stained with Diff-Quik and imaged under oil immersion by light microscopy. In the last image, a neutrophil is adjacent to the AM.

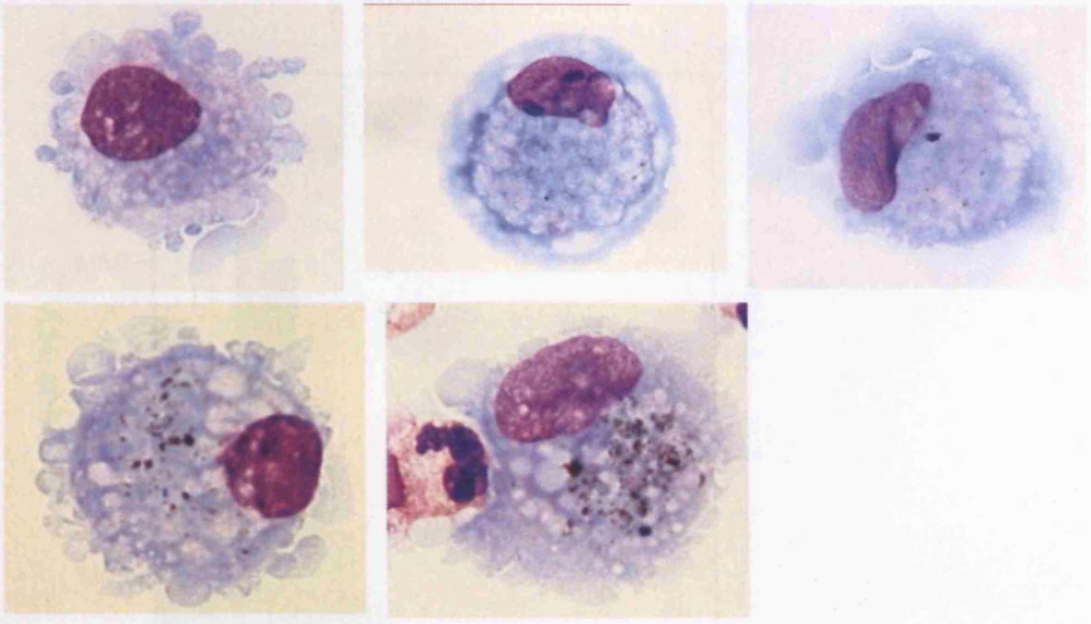

Figure 13: Carbon area size distribution

Distribution of the maximum diameter of individual carbon areas (particle size) in 36 children (n=3,600 AM) measured as the two dimensional diameter (μm). There are very few areas between <2μm and 6μm (not shown in graph). Most particle areas are <2μm.

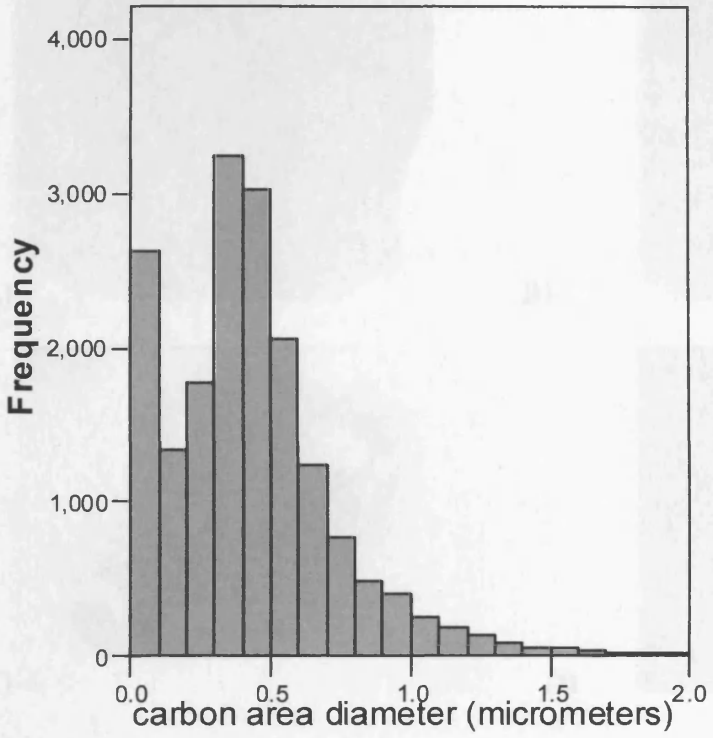

Figure 14: Light microscopic carbon area morphology

A & B) Single "areas" of carbon with a morphology consistent with aggregates of smaller particles in AM cytoplasm (black arrows), C) intracytoplasmic bacteria (dashed arrow) in a neutrophil and AM, D) carbon particle outside AM (arrowhead). Stained with Diff-Quik and imaged under oil immersion (x 1000).

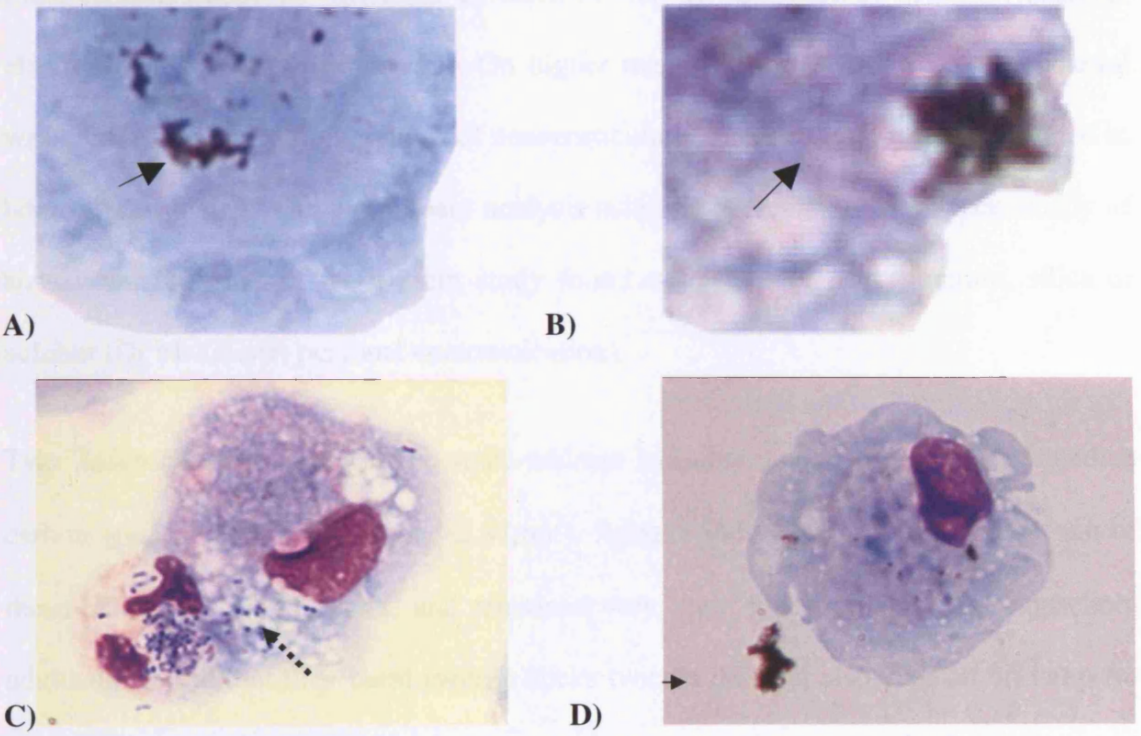

Carbon uptake was not limited to larger AM, since there was no correlation between mean carbon area and the cytoplasmic area of AM (R^2= 0. 014 and p=0.357, rho = -0.001 and p= 0.991 NS). Bootstrap analysis showed that median is less variable than mean and therefore the better statistical descriptor of median carbon area in AM (Table 6).

Electron microscopy of AM from all children showed the presence of intra-lysosomal electron-dense material (Figure 15). On higher magnification (x250, 000) this material was seen to contain agglomerations of nanoparticulate spherules (Figure 16) embedded in homogenous matrix. The preliminary analysis using electron energy loss spectroscopy of airway macrophages in the present study found no signal for iron, titanium, silica or sulphur (Dr M. Geiser, personal communication).

Two Asian children living at the same address had abnormally high levels of median carbon area in AM (4.62μm^2 and 2.87μm^2). Sputum induction was repeated in one of these children 6 months later, and remained very high. Questioning of the household adults did reveal that they burnt incense sticks twice a day and also used an oil lamp for prayers every day. Since there was an unexpected source of exposure, the 2 children were classified as outliers, and excluded form the analysis. This information will be used for future studies.

Figure 15: Transmission electron microscopic (TEM) appearance of AM

TEM appearance of representative AM profiles from children imaged at magnification of X 83,000, showing intralysosomal homogeneous electron dense material (arrow).

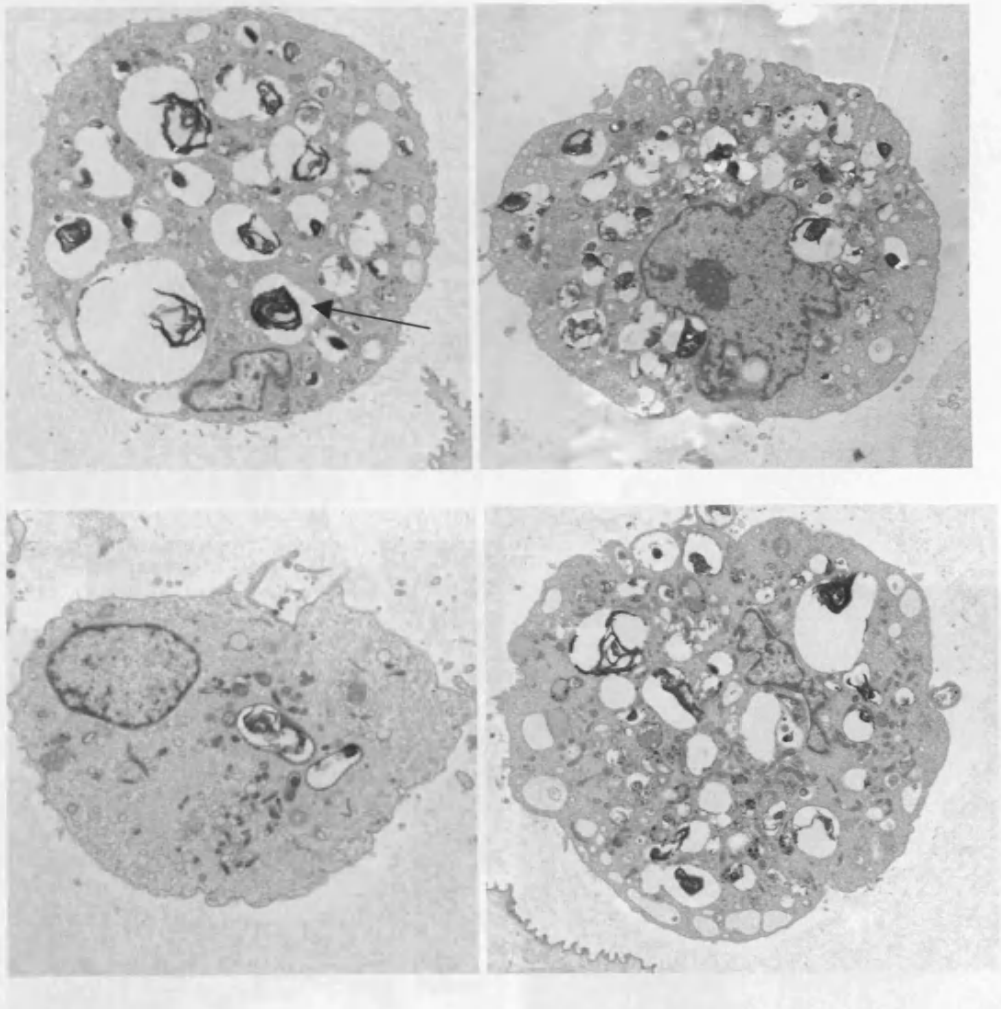

Figure 16: Higher magnification of AM on TEM

TEM of a section of AM (A & B), and at C) higher magnification (x 250,000) showing nanoparticles (white arrows) embedded in the homogeneous electron dense intra lysosomal material.

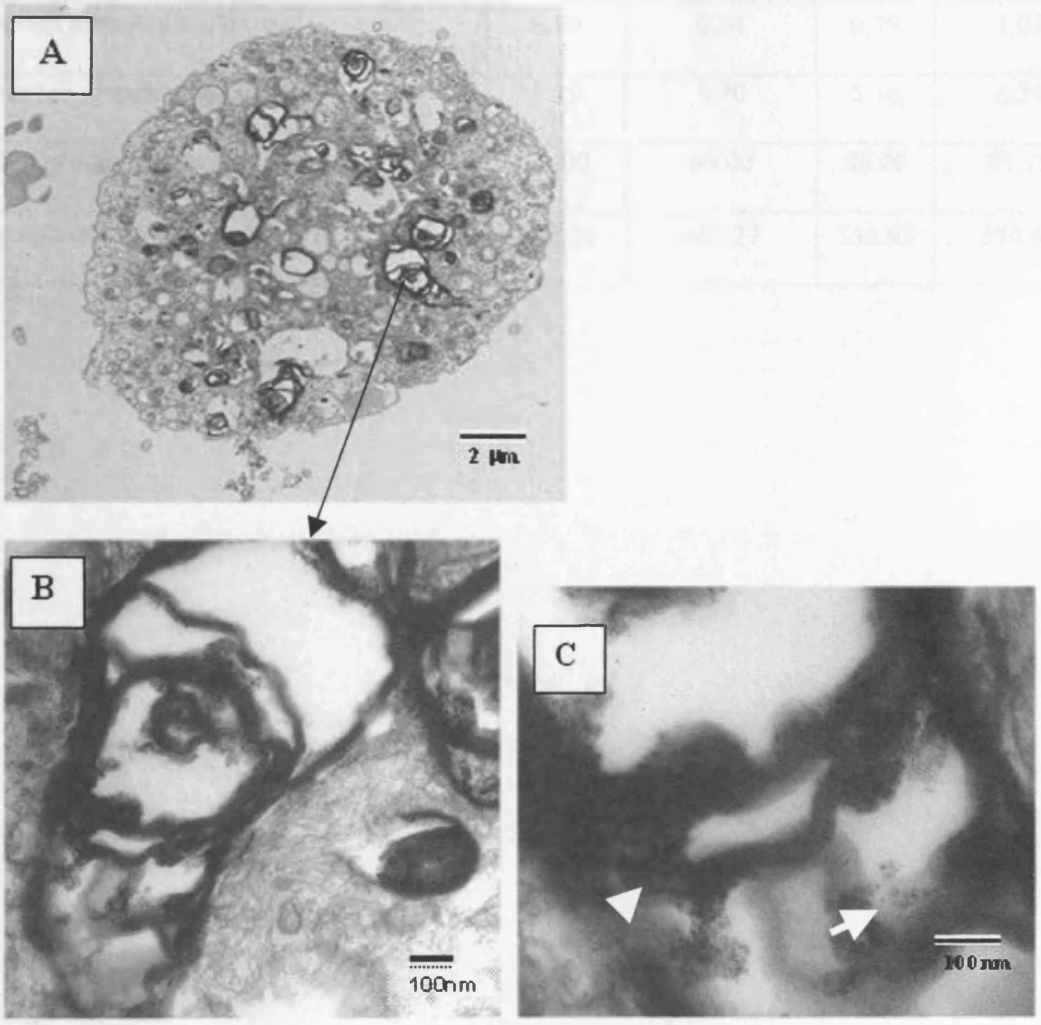

Table 5: Summary of the carbon area variables

	Minimum	25Th Percentile	Median	75th Percentile	Maximum
Median carbon area/AM/child (μm^2)	0.03	0.30	0.41	0.55	1.14
Mean carbon area/AM/child (μm^2)	0.19	0.54	0.75	1.03	2.07
Mean number of carbon areas/AM	1.19	3.70	5.16	6.39	14.20
AM with any carbon area (%)	50.00	80.00	86.00	91.75	99.00
Mean cytoplasmic area (μm^2)	312.26	467.27	536.93	594.98	681.60

Table 6: Result of bootstrapping analysis used to assess appropriateness of median carbon area as the primary loading variable

Summary	Mean*	Median†
Minimum	0.001	0.001
1st quartile	0.008	0.002
Median	0.011	0.004
Mean	0.031	0.013
3rd quartile	0.029	0.008
Maximum	0.321	0.220

* - The mean of the squared differences of the actual mean and the calculated mean of 100 resampled total area of carbon/AM.

† - The median of squared differences of the actual median and the calculated median of 100 resampled observations total area of carbon/AM.

Median area of carbon is a better descriptor of AM loading since it is exhibits less variability.

4.4.2 MEDIAN CARBON AREA IN AM AND MODELLED PM_{10}

There was a weak, positive association between median carbon area in AM and mean annual modelled primary PM_{10} at the home address (Figure 17A). Thus, for each unit increase in modelled primary PM_{10} at the home address, I found a $0.101\mu m^2$ increase in median carbon area in AM. In the exploratory analysis, modelled primary PM_{10} at the school address did not show a significant association with median carbon area in AM. Similarly, no significant association with median carbon area in AM was observed using the combined "home and school" modelled exposure (Figure 17B and C). Adding the measured "imported" (secondary) PM_{10} values from a rural TEOM site, did not improve these associations (Figure 18 and Table 7). The distance of the home to the nearest main road was not associated with median carbon area in AM (Figure 19), and there was no significant difference in median carbon area in AM in children living <150m and >150m from a major road (p=NS). In addition there was no association between median carbon area in AM and centrally measured (total) PM_{10} when expressed as the mean annual value. Appendix 4 provides the individual data of the exposure parameters for all children.

Table 7: Associations between exposure variables and median carbon area in AM

	Median carbon area in AM (μm^2)							
Variable	**Linear Regression**						**Spearman's**	
	R^2	SE (Estimate)	Coefficient	SE (coefficient)	p	95% CI	rho	p
Primary Annual Modelled PM_{10} Home	0.081	0.223	0.101	0.043	0.022	0.015 to 0.187	0.295	0.019
Primary Annual Modelled PM_{10} School	0.012	0.233	0.058	0.071	0.415	-0.084 to 0.200	0.171	0.193
Primary Annual Modelled PM_{10} (H+S)	0.049	0.229	0.094	0.055	0.092	-0.016 to 0.204	0.24	0.068
Primary Annual PM_{10} home + Secondary	0.019	0.230	0.047	0.043	0.273	-0.038 to 0.132	0.204	0.106
Primary Annual PM_{10} school + Secondary	0.003	0.234	0.024	0.048	0.628	-0.073 to 0.121	-0.006	0.963
Primary Annual PM_{10} (H+S) + Secondary	0.004	0.234	-0.021	0.051	0.677	-0.123 to 0.081	0.123	0.353
Primary Annual Central monitored PM_{10}	0.01	0.231	-0.022	0.027	0.430	-0.076 to 0.033	-0.0786	0.53708
Distance from road (km)	0.004	0.232	0.029	0.059	0.623	-0.088 to 0.146	-0.007	0.953

Figure 17: Median carbon area and primary modelled exposure

Median carbon area in AM and annual modelled primary PM_{10} for the: A) home only (the primary exposure variable) B) combination of home and school (H+S) combined, and C) school only.

A)

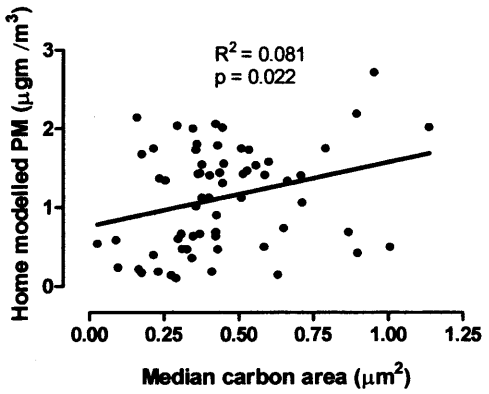

B)

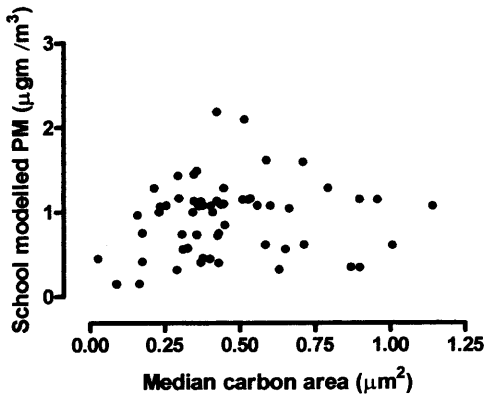

C)

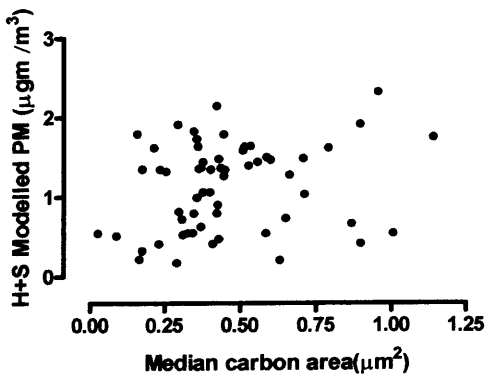

Figure 18: Median carbon area in AM and combined PM

Median carbon area in AM and the combination of "secondary" measured PM_{10} from a rural site with modelled mean annual PM_{10} for the A) home, B) school, and C) combined home and school. All exposures units are $\mu g/m^3$.

A)

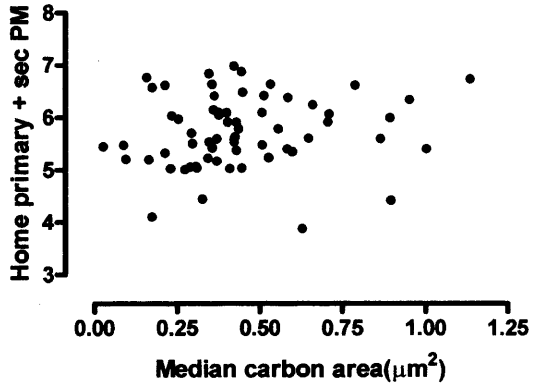

B)

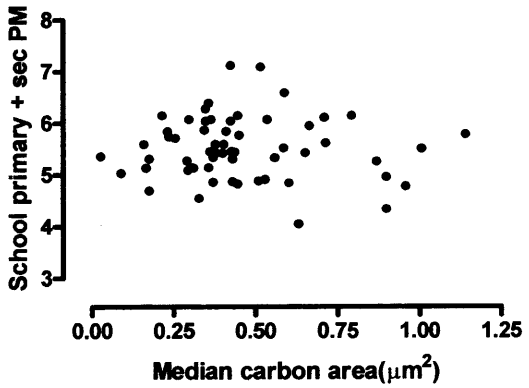

C)

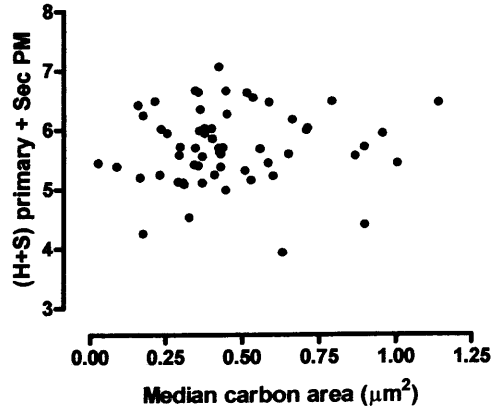

Figure 19: Median carbon area of AM and the home-to-main road distance

(One point outside the range is not shown).

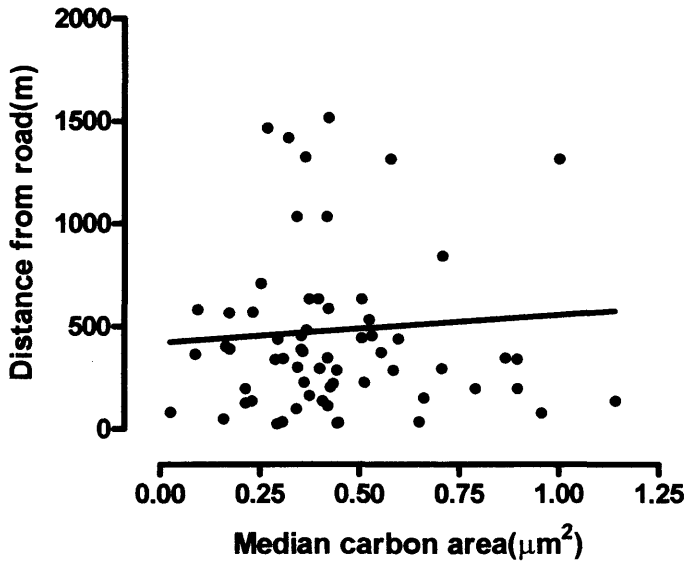

4.4.3 MEDIAN CARBON AREA IN AM AND PHYSICAL ACTIVITY

There were no significant differences in age (years) (11.47 ± 2.34, vs 10.6 ±1.94, p = 0.065), activity levels - MET hr/wk (39.93 ± 39.99 vs 42.08 ± 58.1, p = 0.83), VIG hr/wk (3.37 ± 4.72 vs 3.14 ± 4.56, p = 0.52), and pre-bronchodilator FEV_1 (% predicted) (100.12 ± 11.06 vs 97.39 ± 12.28, p = 0.54) between children included and not included in the analysis. In the group where carbon loading was determined, the median (interquartile range) salivary cotinine was 0.3ng/ml (0.3) and all levels were below the cut-off for active smoking. Only 2 children (1.6 and 1.9ng/ml) were above the 90^{th} percentile of the non-smoking group (Jarvis et al., 1992).

Median carbon area in AM showed no significant association with age, height, weight and number of siblings (Table 8a), body mass index (p = 0.42, 95% CI = -0.022 to 0.009), and there was no difference in loading between males and females (0.45 vs 0.42 μm^2, p = 0.59). A greater proportion of Asian children had higher median carbon area as compared to Caucasians (p difference =0.0001) and lived in areas of higher modelled primary PM_{10} (Figure 20). Median carbon area in AM was not significantly associated with measures of increased activity (Met score, VIG hours per week, number of days active outside in a week, and light and hard exercise) (Table 8b and Figure 21), and decreased activity (time spent watching television and playing video games). The main mode of transport to school had no effect on median carbon area in AM (Figure 22). The majority of AM examined contained at least one area of carbonaceous material (84.3 ± 10 % AM per child, contained carbon). There was no association between salivary cotinine and carbon loading (R^2 = 0.004, p=0.62).

Figure 20: Median carbon area of AM and modelled primary PM_{10} of ethnic groups

The scatter plot of the relationship between modelled annual mean primary PM_{10} ($\mu g/m^3$) at the home address and airway macrophage carbon (μm^2). Open circles represent healthy Caucasian and triangles healthy non-Caucasian children.

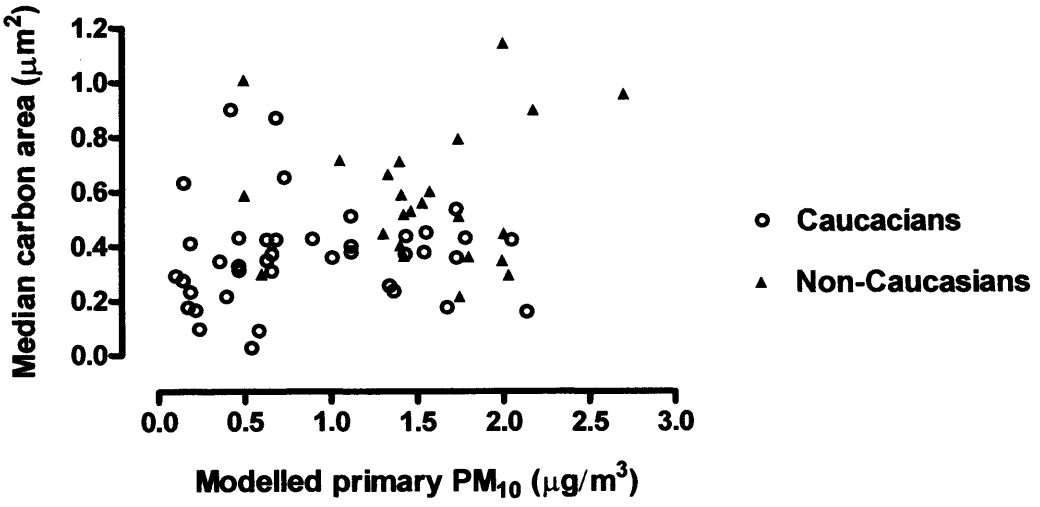

4.4.4 MEDIAN CARBON AREA IN AM AND LUNG FUNCTION

There was a significant dose-dependent inverse association between median carbon area in AM and baseline (pre-bronchodilator) FEV_1 and FEF_{25-75} as % predicted ($p<0.005$), and as Z-score (Figure 23, Table 9). The individual data of the lung function variables is given in Appendix 5. Thus for every $0.1\mu m^2$ increase in median carbon area in AM, there was 1.7% decrement in FEV_1 and a 3.47% decrement in FEF_{25-75} (% predicted). These associations were not affected by bronchodilator treatment, which indicates that the decrement in lung function is not the result of reversible bronchoconstriction, and would explain why there was no correlation between median carbon area in AM and FEV_1/FVC since this is the indicator for reversible obstruction. The association between percent predicted FVC and median carbon area in AM was less consistent. There was however, a significant negative association between median carbon area in AM and FVC when expressed as Z-score. The association between mean annual modelled primary PM_{10} at the home address and FEV_1 was weak ($R^2 = 0.066$, $P= 0.04$), and was nonsignificant for the other lung function variables (Table 10).

Table 8a: Associations of demographic variables with median carbon area in AM

Variable	Median carbon area in AM (μm^2)					
	R^2	SE (estimate)	Coefficient	SE (coefficient)	p	95% CI
Age	0.003	0.232	0.005	0.012	0.690	-0.020 to 0.030
Height	0.000	0.232	0.000	0.002	0.898	-0.004 to 0.005
Weight	0.002	0.232	-0.001	0.002	0.732	-0.005 to 0.004
No of sibling	0.013	0.231	0.026	0.029	0.379	-0.032 to 0.084

Table 8b: Associations of exercise variables with median carbon area in AM

Variable	Median carbon area in AM (μm^2)					
	R^2	SE (Estimate)	Coefficient	SE (coefficient)	p	95 % CI
MET hr/wk	0.011	0.231	0.001	0.001	0.410	-0.001 to 0.002
VIG- hr/wk	0.019	0.230	0.007	0.006	0.283	-0.006 to 0.019
Last 7 days outdoor activity	0.002	0.227	-0.005	0.013	0.708	-0.032 to 0.022
Typical week outdoor activity	0.006	0.226	-0.010	0.017	0.543	-0.043 to 0.023
Hard exercise	0.038	0.230	-0.043	0.027	0.127	-0.098 to 0.012
Light exercise	0.038	0.228	-0.037	0.024	0.124	-0.085 to 0.010
Television/ video games	0.001	0.232	0.008	0.036	0.832	-0.063 to 0.079

Figure 21: Median carbon area in AM and exercise parameters

Association between median carbon area in AM and: A) MET Score B) VIG hr/week. One point in both the graphs is not shown. p = NS for both associations.

A)

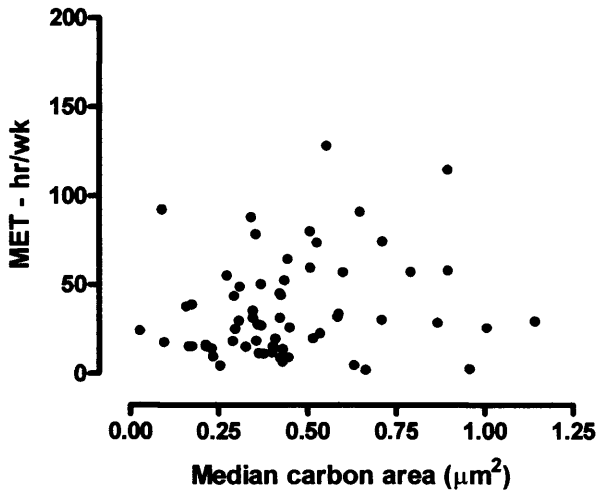

B)

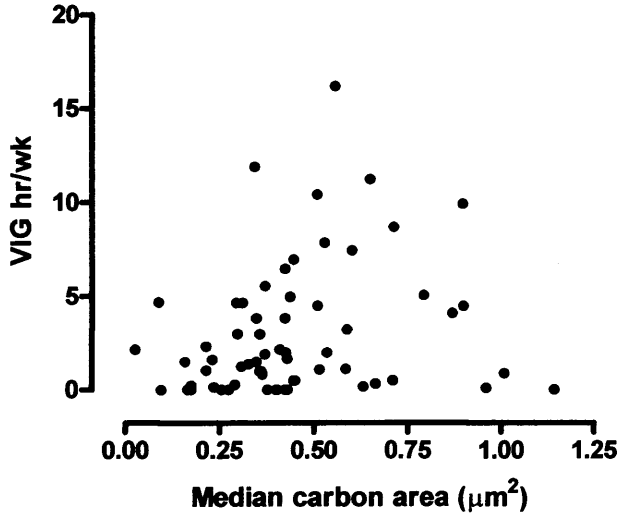

Figure 22: Median carbon area in AM and mode of transport to school

p= NS (ANOVA) . The horizontal lines represent medians.

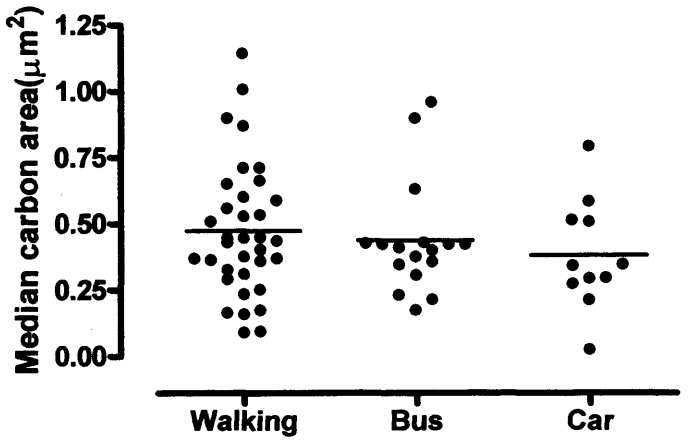

Table 9: Association of lung function with median carbon area in AM

	Median carbon area in AM (μm^2)							
Variable	**Linear Regression**						**Spearman's**	
	R^2	SE (Estimate)	Coefficient	SE (Coefficient)	p	95% CI	rho	P
FEV_1 % pred	0.126	10.420	-17.034	5.691	0.004	-28.411 to -5.658	-0.305	0.015
Z-score FEV_1	0.182	1.022	-2.074	0.558	<0.001	-3.190 to -0.959	-0.407	0.001
FVC % pred	0.074	10.885	-12.925	5.967	0.034	-24.864 to -0.986	-0.249	0.054
Z-score FVC	0.222	1.028	-2.309	0.564	<0.001	-3.437 to -1.182	-0.468	<0.001
FEV_1/FVC % pred	0.042	6.721	-6.102	3.804	0.114	-13.716 to 1.512	-0.124	0.346
Z-score FEV/FVC	0.005	0.746	-0.234	0.422	0.581	-1.079 to 0.610	-0.094	0.476
FEF_{25-75} % pred	0.130	21.336	-34.749	11.696	0.004	-58.152 to -11.346	-0.309	0.015
Z-score FEF_{25-75}	0.101	0.882	-1.244	0.484	0.013	-2.211 to -0.276	-0.310	0.015
Post-bronchodilator FEV1 % pred	0.112	10.477	-15.906	5.724	0.007	-27.352 to -4.461	-0.278	0.027
Z-score Post-bronchodilator FEV_1% pred	0.181	1.002	-2.010	0.547	0.001	-3.105 to -0.916	-0.390	0.002

Figure 23: Median carbon area and lung function

Association between median carbon area in AM and: A) FEV_1 % Predicted, B) FEV_1 Z-score, C) FVC % Predicted, D) FVC Z-score, E) FEF_{25-75} % Predicted, and F) FEF_{25-75} Z-score.

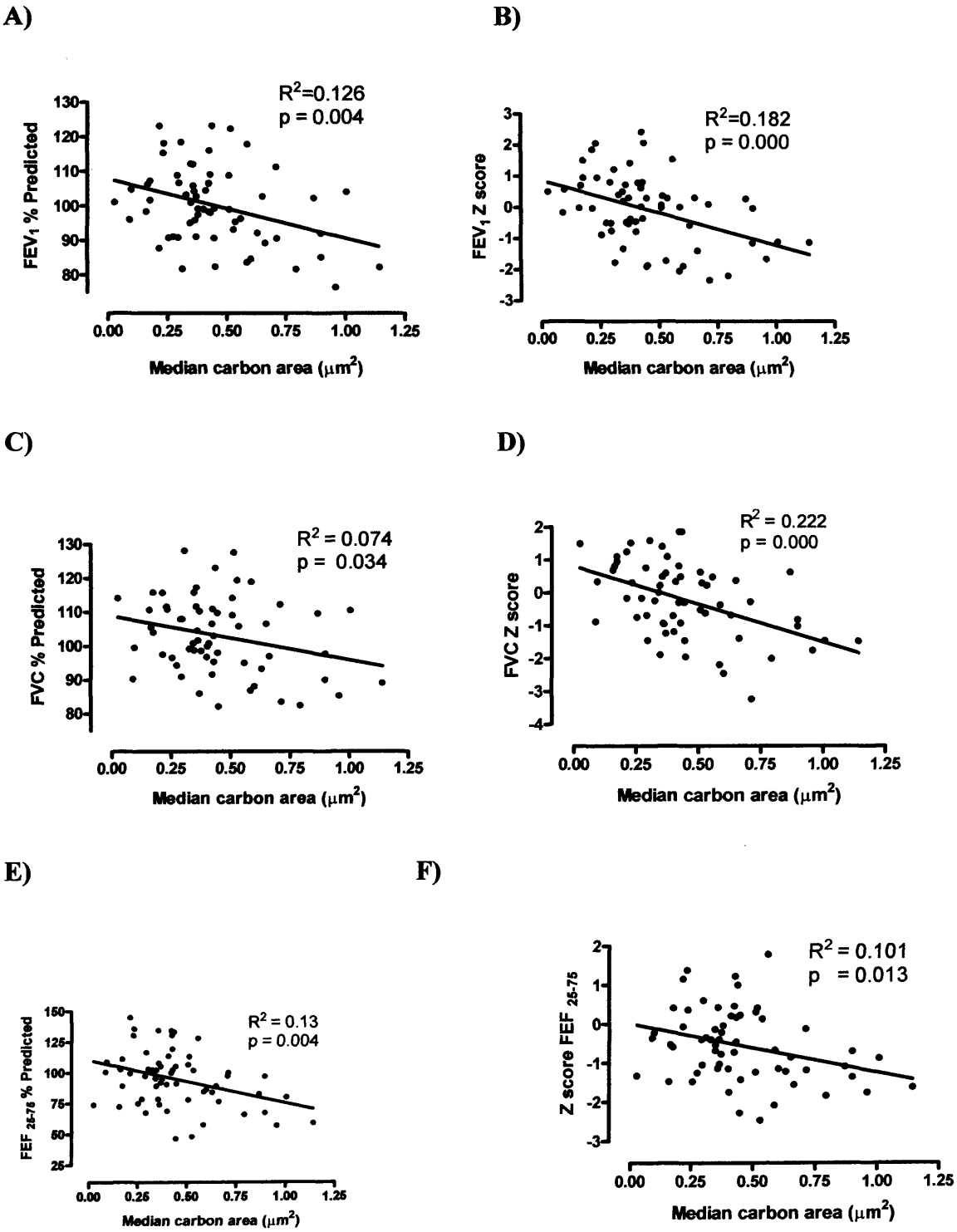

Table 10: Associations between annual PM_{10} exposure and lung function variables

Exposure variables	Lung function	Linear regression						Spearman's	
		R^2	SE (Estimate)	Coefficient	SE (Coefficient)	p	95% CI	rho	p
Home	FEV_1 % Pred	0.066	10.774	-4.346	2.077	0.040	-8.497 to -0.194	-0.254	0.043
	FVC % Pred	0.005	11.281	-1.198	2.208	0.590	-5.616 to 3.220	0.043	0.736
	FEV/FVC % Pred	0.017	6.809	-1.366	1.346	0.314	-4.060 to 1.328	-0.1	0.441
	FEF_{25-75}	0.062	22.151	-8.595	4.335	0.052	-17.270 to 0.080	-0.219	0.089
School	FEV_1 % Pred	0.015	11.017	3.083	3.349	0.361	-3.623 to 9.789	0.027	0.84
	FVC % Pred	0.032	11.302	4.683	3.462	0.182	-2.255 to 11.621	0.167	0.214
	FEV/FVC % Pred	0.001	6.977	0.497	2.174	0.820	-3.862 to 4.856	-0.037	0.788
	FEF_{25-75}	0.003	22.369	2.899	6.852	0.674	-10.833 to 16.630	-0.02	0.882
H + S	FEV_1 % Pred	0.031	10.923	-3.557	2.620	0.180	-8.804 to 1.690	-0.173	0.188
	FVC % Pred	0.001	11.483	-0.663	2.793	0.813	-6.259 to 4.934	0.012	0.931
	FEV/FVC % Pred	0.010	6.945	-1.273	1.717	0.462	-4.715 to 2.169	-0.09	0.505
	FEF_{25-75}	0.031	22.057	-7.095	5.364	0.191	-17.845 to 3.655	-0.174	0.194
Home + Secondary	FEV_1 % Pred	0.011	11.085	-1.716	2.051	0.406	-5.815 to 2.384	-0.159	0.209
	FVC % Pred	0.000	11.309	-0.097	2.114	0.964	-4.327 to 4.134	-0.027	0.838
	FEV/FVC % Pred	0.001	6.867	-0.255	1.325	0.848	-2.908 to 2.398	0.047	0.723
	FEF_{25-75}	0.012	22.742	-3.568	4.251	0.405	-12.075 to 4.938	-0.153	0.238
School + Secondary	FEV_1 % Pred	0.056	10.782	4.312	2.342	0.071	-0.379 to 9.002	0.142	0.282
	FVC % Pred	0.037	11.272	3.589	2.458	0.150	-1.336 to 8.515	0.167	0.214
	FEV/FVC % Pred	0.023	6.899	1.766	1.557	0.262	-1.356 to 4.888	0.167	0.219
	FEF_{25-75}	0.034	22.016	6.723	4.800	0.167	-2.897 to 16.343	0.11	0.417
(H+S) + Secondary	FEV_1 % Pred	0.000	11.098	-0.164	2.299	0.944	-4.768 to 4.441	-0.078	0.555
	FVC % Pred	0.001	11.481	0.630	2.402	0.794	-4.184 to 5.443	-0.006	0.962
	FEV/FVC % Pred	0.001	6.976	0.413	1.518	0.787	-2.632 to 3.457	0.12	0.38
	FEF_{25-75}	0.000	22.404	-0.414	4.687	0.930	-9.806 to 8.979	-0.066	0.626

4.4.5 MEDIAN CARBON AREA IN AM AND AIRWAY INFLAMMATION

There was no significant association between median carbon area in AM and: % airway neutrophils, percentage of airway eosinophils, IL-8 concentration, and a marker of allergic airway inflammation - eNO (Figure 24 and Table 11). There was no significant association between median carbon area in AM and the percentage of AM positive for MARCO - the phagocytic receptor for unopsonized particles (Table 11). The individual data of inflammatory markers is given in Appendix 6.

4.4.6 INTER-AND INTRAOBSERVER VARIATION OF MEDIAN CARBON AREA IN AM

Carbon areas in 40 AM were analysed by myself on two occasions and by a separate operator (Ananth Tellabatti in one occasion (Table 12). I trained Ananth to do the image analysis. No significant systematic bias was seen in either the intra- or interobserver analysis as shown by p value from t-test for bias along with the limits of agreement. The British Standards Institution Repeatability Coefficient was calculated to be 1.49, 2.97 and 2.96 for the intra, and 2 interobserver analyses respectively. The standard deviation of the difference was 21%, 42% and 40% of the overall standard deviation (combined standard deviation of all results n= 80) for the intra-; and first and second inter-observer analysis respectively, indicating good repeatability.

4.4.7 OTHER MEASURES OF CARBON LOADING

Although median carbon area per AM per child (median carbon area in AM) and mean annual modelled PM_{10} exposure at the home was chosen *a priori* as the primary variables of interest, I explored other possible descriptors. The summary data and the associations between other possible descriptors of both carbon loading and modelled exposure are given in Table 13. In general, the association between median carbon area in AM and shorter periods of modelled exposure (week, month) was less significant when compared

with mean annual exposure. Of the other measures of carbon loading, only the mean number of carbon areas in AM showed a better correlation with annual modelled exposure (Table 13). The association between the mean number of carbon areas and lung function parameters was also significant for FEV_1 ($p=0.002$) and FEF_{25-75} ($p<0.001$).

4.4.8 LONG-TERM VARIABILITY

Long-term variability data are shown in Tables 14a and 14b. This showed that median carbon area in AM remains relatively stable over a 6-month period ($R^2= 0.84$) and the SD of the difference of the median was 42%.

Table 11: Associations between inflammatory variables and MARCO with median carbon area in AM (μm^2)

	Median carbon area in AM							
Variable	**Linear Regression**						**Spearman's**	
	R^2	SE (Estimate)	Coefficient	SE (coefficient)	p	95% CI	rho	p
Neutrophil %	0.027	29.028	-20.965	15.854	0.191	-52.656 to 10.727	-0.217	0.084
Eosinophil %	0.000	5.079	-0.139	2.774	0.960	-5.684 to 5.407	-0.085	0.498
IL-8 (ng/ml)	0.010	27.416	-11.847	14.974	0.432	-41.790 to 18.096	-0.124	0.328
eNO (ppb)	0.001	17.606	-2.062	14.994	0.892	-33.009 to 28.885	0.084	0.682
MARCO (%)	0.030	13.917	-10.045	10.525	0.348	-31.571 to 11.480	-0.123	0.499

Figure 24: Median carbon area and inflammatory markers

Association between median carbon area in AM and: **A)** sputum neutrophil percentage, B) sputum IL-8, and C) exhaled nitric oxide (eNO). p = NS for all.

A)

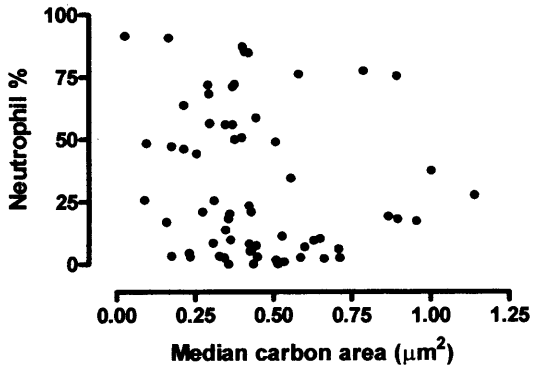

B)

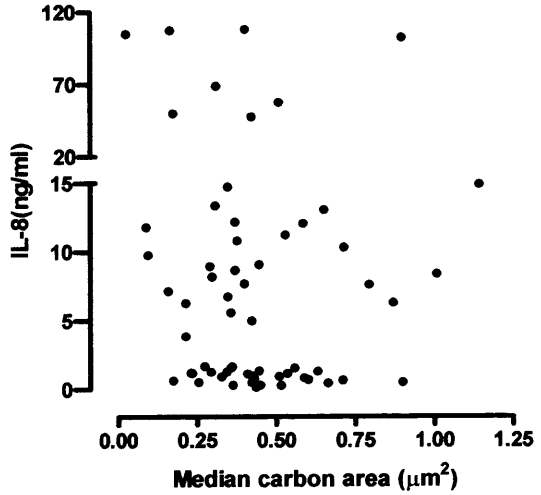

C)

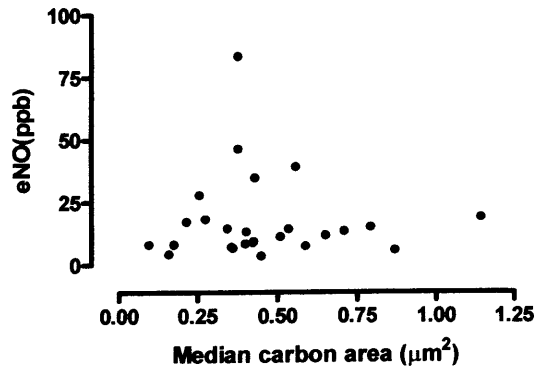

Table 12: The bias, and t-test for bias, for intra- and inter-observer variability

	P-Value from t-test for bias	Mean difference	SD of the difference	SD of the combined Results	Limits of agreement (Upper and lower)
Intra Observer variation	0.08	0.215	0.747	3.655	1.709 to –1.279
Inter Observer variation *	0.5	0.159	1.488	3.580	3.135 to –2.817
Inter Observer variation †	0.81	0.056	1.484	3.688	3.024 to – 2.912

* - Inter-observer variation with first test of observer 1(myself) and test of observer 2(AT)

† - Inter-observer variation with second test of observer 1 and test of observer 2

Table 13: Associations between i) different time periods for modelled primary PM_{10} exposure for the home address, and ii) distance from road (km) with AM carbon loading parameters

Exposure	Linear regression						Spearman's	
	R^2	SE (Estimate)	Coefficient	SE (coefficient)	p	95% CI	rho	P
Annual modelled PM								
Median carbon area in AM	0.081	0.223	0.101	0.043	0.022	0.015 to 0.187	0.295	0.019
Mean carbon area in AM	0.053	0.413	0.148	0.080	0.068	-0.011 to 0.307	0.213	0.090
Mean number of carbon area	0.107	2.437	1.280	0.470	0.008	0.341 to 2.219	0.273	0.030
% AM with carbon	0.054	10.037	3.636	1.935	0.065	-0.232 to 7.504	0.175	0.166
One month modelled PM								
Median carbon area in AM	0.076	0.224	0.087	0.038	0.028	0.010 to 0.163	0.321	0.011
Mean carbon area in AM	0.029	0.418	0.098	0.072	0.179	-0.046 to 0.241	0.197	0.119
Mean number of carbon area	0.095	2.454	1.073	0.422	0.013	0.230 to 1.915	0.214	0.089
% AM with carbon	0.036	10.129	2.665	1.740	0.131	-0.814 to 6.144	0.159	0.207
One week modelled PM								
Median carbon area in AM	0.047	0.227	0.064	0.037	0.086	-0.009 to 0.137	0.275	0.029
Mean carbon area in AM	0.013	0.421	0.062	0.068	0.363	-0.074 to 0.198	0.166	0.188
Mean number of carbon area	0.077	2.477	0.911	0.399	0.026	0.112 to 1.710	0.236	0.061
% AM with carbon	0.034	10.144	2.407	1.636	0.146	-0.863 to 5.678	0.159	0.207
Distance from road (km)								
Median carbon area in AM	0.004	0.232	0.029	0.059	0.623	-0.088 to 0.146	-0.007	0.953
Mean carbon area in AM	0.003	0.423	0.049	0.107	0.652	-0.166 to 0.263	0.013	0.917
Mean number of carbon area	0.004	2.573	0.323	0.651	0.621	-0.978 to 1.625	-0.012	0.923
% AM with carbon	0.016	10.235	2.626	2.590	0.315	-2.551 to 7.804	-0.037	0.766

Table 14a: The bias and t-test for bias for long-term variability of median carbon area in AM (μm^2)

	P-Value (t-test)	Mean difference	SD of the difference	SD of first test	SD of second test	SD of combined results
Median carbon area in AM (μm^2)	0.048	0.151	0.27	0.68	0.64	0.65

Table 14b: Correlations between median carbon area in AM performed on the same individuals 6 months apart (long term variability) (μm^2)

	Pearson's			Spearman's	
	Correlation	R^2	p	rho	p
Median carbon area in AM (μm^2)	0.92	0.84	<0.0001	0.116	0.11

4.5 Summary

This chapter describes the methods and the results of the macrophage carbon loading in children exposed to traffic derived PM. Healthy children from non-smoking families, living in Leicestershire were recruited. Their demographic data was recorded along with the exercise details. Salivary cotinine was measured to exclude personal smoking and exposure to environmental tobacco smoke. Lung function was measured prior to and during the sputum induction and samples were processed by standard technique. Digitized images of 100 AM were analysed for carbon areas using Scion Image software. The sputum neutrophil %, eosinophil %, exhaled nitric oxide and supernatant interleukin-8 were used to assess local inflammation.

The modelled PM_{10} at the residence and school and distance from main road to home were used as proxy markers of exposure. The modelled PM_{10} data was obtained from AIRVIRO model for a year prior to sputum induction. The mean exposure for a week, a month and a year were calculated. The distance from main road was calculated using the GIS software. Linear regression and Spearman's correlations were used to assess the associations between exposure parameters (annual mean modelled PM_{10} used as primary variable) and AM carbon loading (median area of carbon/AM/ individual as primary variable). Similarly associations between carbon loading and demographic, lung function, and inflammatory parameters were calculated.

I found a weak, but significantly positive, association between AM carbon and modelled exposure to annual mean primary PM_{10} at the residence. Annual mean modelled exposure at school and combined home and school exposures were not associated with AM carbon area. Other exploratory markers of exposure like shorter duration of exposure (one week, one month prior to IS), addition of secondary PM_{10} to primary at residence, distance from home to main road and Leicester City Centre monitored data were also not associated with AM carbon area.

A very significant finding was a strong inverse association between median carbon area in AM and % predicted forced expiratory volume in 1 second and mid-expiratory flow between 25% and 75% of the forced vital capacity. The association remained significant after the bronchodilator was used and with the z-scores. The other lung function parameters, like FVC and FEV/FVC were not associated with median carbon area. There was a weak positive association between the annual mean modelled PM_{10} and FEV_1.

There was no significant association between AM carbon and the home-main road distance, age, height, weight, gender, and activity level. The sputum neutrophil and eosinophil percentage, supernatant IL-8 levels, exhaled nitric oxide were not associated with AM carbon area. The percent MARCO positivity of AM was also not associated with the AM carbon area.

Chapter 5: Discussion

5.1 Biomass smoke exposure and AM carbon

This study has demonstrated that it is feasible to noninvasively assess carbon loading of AM in the developing world, and that loading is approximately 13 times higher in women exposed to biomass smoke than adults from a UK city where the majority of inhalable particles are from the combustion of fossil fuels. These data suggest that animal studies of biomass PM-induced disease should achieve at least a loading of 9.0μm^2 /AM, and 100% of AM should contain at least one carbon particle under light microscopy. To date, there are no models for the association between biomass-smoke exposure and increased vulnerability to lower respiratory tract infection: a major threat to global respiratory health (Bruce et al., 2000). It is therefore unclear whether carbon loading of AM *in vivo* directly increases vulnerability to bacterial or viral infection, or is a surrogate marker for more significant exposures of other airway cells. However, phagocytosis of carbonaceous particles by AM impairs a range of antibacterial functions, including phagocytic ability for other non-opsonized particles(Renwick et al., 2001;Monn et al., 2002), release of superoxide radicals(Kleinman et al., 2003), and regulation of pulmonary inflammatory responses to viral infection (Becker and Soukup, 1999).

There are several potential limitations of this study. First, carbon loading may not represent loading in the smaller airways since induced sputum selectively samples cells from the large central airways(Alexis et al., 2001). However, central airway AM on the mucociliary escalator originate from the bronchioles and alveoli (Lehnert, 1992). Thus, 48 hours after experimental particle exposure, loading of central AM and distal AM is identical (Lay et al., 1998). Second, phagocytosed particles are concentrated and aggregated by AM (Bunn et al., 2001), and the areas of carbon identified by image

analysis do not represent the size distribution of inhaled PM. Third, I assessed carbon in a single focal plane, whereas loading *in vivo* is distributed in three dimensions. However, all digital images were obtained with the nucleus in focus, which ensured uniformity of focal plane and maximised the surface area of intracellular carbon. AM particle loading in three dimensions can be measured using confocal microscopy, but would require fluorescent labeling of biomass-PM prior to inhalation: an impractical option.

In Ethiopia only women were recruited as they were exposed to the highest amount of biomass, unlike in Leicester, where men and women from a higher social class were recruited. In future studies, the ideal group for comparison with Ethiopian women would be housewives from lower socioeconomic class. A more detailed questioning on time of cooking, duration of cooking in relation to the timing of AM sampling will help in assessing exposure and also study kinetics of particles in AM. For example, to assess if there is any difference in carbon area in women on the day of cooking as opposed to that on third day.

Notwithstanding the above limitations, is carbon loading of AM a valid way of assessing individual exposure? The ambient PM levels were not measured to validate the data. However, PM_{10} levels have been reported during biomass cooking, with peak levels of 2000$\mu g/m^3$, and mean 24 h levels of 231$\mu g/m^3$(Balakrishnan et al., 2002), i.e. 10 times greater than the annual 24 h mean PM_{10} in Leicester (19$\mu g/m^3$ in 2003): a difference compatible with the 13-fold increase in loading seen in Ethiopian women. Whether AM carbon reflects short-term peaks of exposure (e.g. cooking in the last 3 days), or long-term exposure (e.g. over several months/lifetime), or a combination of both, is unclear. Lay et al. (Lay et al., 1998) instilled a single dose of iron particles into the lower airways of human volunteers, and found particle-containing AM 24 h post-instillation, and a fifth of AM containing particles at 90 days. Thus AM carbon loading is most likely an integral

of short-and long-term exposure. Could I have used a less technologically demanding way of assessing loading (e.g. presence/absence of carbon)? Indeed, after nebulisation of 1μm latex spheres, the proportion of AM with one or more ingested particle increases with increasing dose (Suarez et al., 2001). Does this data provide any practical insights into ways of reducing biomass-PM exposure? It was surprising to find that carbon loading of AM in Ethiopian children was significantly less than their mothers but, on questioning, these children spent very little time near the outside fire. In contrast, infants (the age group most vulnerable to adverse effects of biomass smoke); (Bruce et al., 2000) were strapped to their mothers backs during cooking. Moving infants away from the fire to areas used by older children may therefore attenuate exposure. Sputum induction has been used in developing countries in the diagnosis of pulmonary infections(Zar et al., 2000a;Hartung et al., 2002), and hemosiderin-laden AM have been described in spontaneously produced sputum samples from traffic policemen in India (Roy et al., 2001). The absence of a cyto-centrifuge and ice in Ethiopia meant that the standard sputum processing methodology had to be modified. A similar cyto-centrifuge-free technique has been reported for processing of induced sputum samples (Saraiva-Romanholo et al., 2003). Induced sputum processing may therefore offer a new approach to the study of respiratory disease in the developing world.

Indeed, our data suggests that airway neutrophils are increased in healthy, asymptomatic, women who are chronically exposed to biomass smoke. Since neutrophils are implicated in the pathogenesis of cigarette smoke-associated chronic obstructive pulmonary disease (COPD)(Cosio Piqueras and Cosio, 2001), this may be a factor in the early pathogenesis of non-cigarette smoke associated COPD in women in the developing world (Varkey, 2004). There was neutrophil clumping in some slides, which could possibly be due to up-regulation of adhesion molecules. In summary, I have demonstrated high levels of carbon loading of AM after biomass-smoke exposure in mothers and children. Analysis of AM

in a larger cohort of biomass exposed women may (i) provide insights into the major determinants of exposure, (ii) inform exposure-reduction interventions, and (iii) guide cellular and whole animal models of the association between biomass-smoke and increased vulnerability to infection. For animal studies, the AM carbon loading seen in extreme exposure should be achieved in experimental conditions to mimic the natural individual exposure of lower airways.

5.2 Traffic derived PM exposure and AM carbon

In this study, a group of healthy children living in a single geographical region of the UK were recruited and the relationship between carbon loading in AM and modelled exposure to locally generated PM_{10} at the home address was assessed. Home addresses were exposed to near uniform levels of background PM_{10} that were blown in from distant areas and countries. Thus, in children undergoing induced sputum, variations in their home exposure can be assumed to be a result of variations in locally generated primary PM_{10}. Using a predefined measure of both AM carbon loading, and modelled exposure to primary PM_{10}, a weak association between median carbon area of carbon in AM and modelled exposure over the previous 12 months was found. A stronger negative association was found between median carbon area in AM and lung function. Exploratory analysis did not show that shorter periods of modelled exposure were more closely associated with median area of carbon in AM.

5.2.1 CARBON AREA DIAMETER

Our light microscopic data on carbon area diameter is similar to the data of Dumortier (Dumortier et al 1994), who measured particle size as the "area equivalent diameter". To estimate aerodynamic diameter from the actual diameter (assuming there is no aggregation or disaggregation in phagolysosomes) information on particle density,

determined by composition, and shape, would be required. The aerodynamic diameter of inhaled particles cannot therefore be reliably estimated from our carbon area diameter distribution data.

5.2.2 MODELLED PRIMARY PM

Though there was a weak but positive trend in carbon loading and modelled PM_{10}, the reason why there was no clear association between modelled PM_{10} and median area of carbon in AM is that both variables may have limitations in predicting individual exposure.

Outdoor modelled PM_{10} at the residence and school are not enough to explain personal exposure – Personal exposure includes outdoor and indoor exposure. The limitation of the modelled PM_{10} is restriction of exposure estimations from outdoor sources. The ambient outdoor PM enters inside, till it equilibrates and the coarse component (>2.5 size fraction) settles quickly. Indoor contributions to personal exposure arise mainly from human activities like cooking, dusting, walking on carpets and consist of larger particles. The major indoor pollutant, environmental tobacco smoke (Monn et al., 1997) was excluded, as the children recruited were from non-smoking families and had low salivary cotinine levels. Families who used coal fire for indoor heating were also excluded. The AM particle measurement does not differentiate between outdoor (traffic-related) or indoor sources, though the size distribution is suggestive of $PM_{2.5}$.

Accuracy of modelled data - modelled data is dependent upon inputs e.g. traffic flows, emissions which in themselves have limitations and change with time. The modelled data (ADMS Urban) underestimated the PM_{10} values at the roadside and over predict at the background sites (Leicester Air Quality Report 2000). A further limitation of the AIRVIRO model is that there were insufficient numbers of sites for validation. Future validation studies could use passive sampling of carbon monoxide - a marker of primary

PM_{10} (Ebelt et al., 2001). Indeed, Airviro performs well when predicting the spatial distribution of traffic-associated carbon monoxide (Mukherjee and Viswanathan, 2001), but its resolution is not perfect since PM_{10} is modelled at the 50-m^2 scale and variations for traffic-derived pollutants have been reported at smaller spatial resolution (Monn et al., 1997).

The levels of ambient PM are low – the possibility is that PM levels that children are exposed to are generally too low to detect a significant difference in the particle loading. Higher exposures as seen in women exposed to biomass smoke AM loading was higher compared to low levels of traffic derived PM exposure in adults in the UK(Kulkarni et al., 2005). Similarly rats exposed to higher amounts of wood smoke had more particles in AM (Tesfaigzi et al., 2002).

Size fraction measured – the majority of the particles in the AM were <2.5μm(though not aerodynamic). The correlation might be better with ambient $PM_{2.5}$. A review of panel studies (Ward and Ayres, 2004) has shown that adverse effect greater for $PM_{2.5}$ than for PM_{10}.

Elemental carbon - Elemental carbon (EC) is emitted from combustion sources and chemical transformations of EC are limited, therefore EC is considered as a good indicator of primary anthropogenic air pollutants. The proportion of elemental carbon in a given quantity of PM can vary depending on the source(Ho et al., 2002;Chow et al., 2005). It is possible that the black carbon that is measured in AM, might correlate better with amount of elemental carbon.

Individual variation in PM clearance and kinetics– there will be individual differences in amount cleared by the mucociliary mechanisms and also by any asymptomatic respiratory conditions. The study assumes that same proportions of PM enter the lower respiratory tract in all healthy individuals. Also the particle kinetic studies performed in animals cannot be extrapolated to humans, as there are species differences in distribution

of particles with chronic inhalation. Most animal experiments study kinetics with either acute or sub chronic exposure. In humans acute episodes occur over chronic exposure making it difficult to compare with animal studies.

Duration of exposure measurement – Do particles persist in AM for a long time? Titanium dioxide was seen in the lysosomes of AM 3 years after the workers had stopped working at a dye factory (Maatta and Arstila, 1975). Smoker's inclusions were seen in non-smoker transplanted with smoker's lung for at least 2 years (Marques et al., 1997). All these provide evidence that particles in AM are detected many years after inhalation. As particles in AM may be long lasting, one-year annual average may be inadequate in explaining the loading and may be life time exposure modelling should be considered. Modelling of air quality began in 1997 in Leicester therefore lifetime exposure cannot be assessed for study children.

5.2.3 DISTANCE FROM ROAD

The increased prevalence of respiratory symptoms and an affect on lung function has been found in children living near major roads(Oosterlee et al., 1996;Brunekreef et al., 1997;Brauer et al., 2002;Janssen et al., 2003). Cough, wheeze and doctor diagnosed asthma were significantly more reported in children living 100m from the freeway in Netherlands (van Vliet et al., 1997). In a study in the UK, children living within 150m from the main road had increasing risk of wheeze (odds ratio 1.08) and most risk localised to living in 90m (Venn et al., 2001). There was no association found between, living near a main road and increased asthma admissions or asthma medication use (Livingstone et al., 1996;Wilkinson et al., 1999) in some studies.. The assumption that individuals living within a certain distance from the road have the same exposure is not true, as meteorological conditions alter dispersion and type and volume of traffic can differ on different roads. There was no difference in median particle loading in children

living <150m and >150m road-to-home distance. Distance from main road-to-home alone is insufficient and AIRVIRO probably represents an improvement over the home-main road distance, as it integrates the contribution from all roads and takes into account traffic flows on these roads.

5.2.4 EXERCISE AND DEMOGRAPHIC VARIABLES

I found no demographic or reported activity variable, other than ethnicity, to be associated with AM carbon loading. Similarly, body mass index and indicators of physical activity were not significant confounding variables in the Southern Californian Communities study (Lockwood et al., 2004). The most plausible explanation why non-Caucasian children had higher carbon loading is that, they lived in areas of higher primary PM_{10} pollution. The higher modelled exposures to primary PM_{10} for the home address in non-Caucasian children supports this hypothesis.

5.2.5 LUNG FUNCTION

In this cross-sectional study of healthy children living in an area with relatively low levels of air pollution, I found a consistent inverse association between increased carbon loading of AM and reduced levels of FEV_1, and FEF_{25-75}, and to a lesser extent FVC. These associations were not due to reversible bronchoconstriction. The decrement in FEV_1 and FEF_{25-75} indicate large and small airway effects.

These data showing attenuation in lung function with carbon loading are consistent with epidemiological studies showing reductions in lung function with increased chronic PM_{10} exposure. For example, cross sectional analysis of the Southern California 12 communities cohort (Peters et al., 1999), found that the proportion of young adults with FEV_1 <80% predicted, was 4.9 times higher in communities with higher annual PM < 2.5μm ($PM_{2.5}$) concentrations. Since the growth in lung function over an 8 year period was also attenuated, the cross section findings were interpreted as a reflecting a long-term

effect of $PM_{2.5}$ (Peters et al., 1999). In the present study, I excluded children with a post-bronchodilator FEV_1 of <80%, and it is therefore possible that I have underestimated the strength of the association between carbon loading and lung function. Short term, reversible, changes in lung function with short-term changes in PM_{10} have also been reported. A recent systematic review of 22 panel studies of children estimated that a $50\mu g/m^3$ rise in PM_{10} would result in a 1.95 litres/min decrease in the peak expiratory flow rate (Ward and Ayres, 2004). However, short-term decrements in lung function are unlikely to account for the associations in the present study. First, insoluble environmental particles persist in human AM for at least several months after instillation or inhalation (Marques et al., 1997;Lay et al., 1998), and although the kinetics of carbon loading of human AM has not been fully defined to date, long term exposure of rats to increasing ambient concentrations of PM_{10} results in a dose-dependent increase in AM carbon loading that persists for at least one month after the exposure has ended (Finch et al., 2002). Second, the significant, albeit weak, association between annual modelled exposure of the home to traffic-derived PM_{10} and carbon loading of AM is consistent with a long-term effect. I did not expect a strong association between modelled exposure and loading, since adolescent children are highly mobile, and do not spend all of their time at the home address. Third, decrements in lung function were not reversed by bronchodilator therapy, thus excluding a likely short-term mechanism. To completely exclude short-term effects (<7days) of PM_{10}, longitudinal follow up of the study group would be required.

The composition of the black material seen in AM was not completely analyzed in the present study, and it is therefore possible that some areas classified as carbonaceous were not of vehicular origin. However, our recent bronchoalveolar lavage study of Leicestershire children, found that particles in AM examined by electron microscopy and microanalysis consisted exclusively of aggregates of carbon with a morphology and

chemical composition identical to that of ambient fossil-fuel derived PM_{10} (Bunn et al., 2001). Furthermore, I minimized the possibility of exposure to other significant sources like cigarette smoke and coal fires. However some additional sources, like use of incense sticks and candles was not asked specifically in all children.

The peak at 0.1μm probably represents very small "dots" identified as "separate" by the image analysis programme, but dots are actually attached to larger areas. The majority of individual carbon areas were <2.5μm - a finding that is compatible with the hypothesis that $PM_{2.5}$ may more accurately reflects the component of PM_{10} reaching the distal airways.

5.2.6 INFLAMMATORY MARKERS AND MARCO PERCENT POSITIVITY

AMs have shown to produce inflammatory mediators on stimulation by particulate matter(Becker et al., 2003), (Fujii et al., 2002) and interact through the mediators with epithelial cells to influence the airway inflammatory response(Ishii et al., 2004). The supernatant from human AMs incubated with 100 μg/ml of PM_{10} amplified the proinflammatory mediator expression, including IL-8 in epithelial cell line(Ishii et al., 2004). IL-8 is a low molecular weight proinflammatory chemokine produced by variety of cells including AM and is involved in neutrophil migration. Airway neutrophilia and increased IL-8 have been reported in BAL fluid in healthy humans exposed to diesel exhausts (Salvi et al., 2000;Stenfors et al., 2004). Increase in sputum neutrophil differential, not associated with increase in supernatant IL-8 was found in 10 healthy volunteers exposed to 200μg/m^3 of diesel exhaust (Nightingale et al., 2000) By contrast, other researchers have found no increase in induced sputum IL-8, or airway neutrophils after exposure to $PM_{10,}$ or ambient particulates(Nordenhall et al., 2000), (Gong, Jr. et al., 2003). Compatible with these later studies, I found no association between the induced sputum IL-8, or the neutrophil differential count with carbon in AM. One possible

explanation is that IL-8 is an acute response, whereas carbon in AM represents long-term exposure. The possibility of low levels of ambient exposure being insufficient in eliciting an increase in inflammatory mediators cannot be ruled out. The exposures levels used in chronic animal exposure experiments showing neutrophilia, was high (1000 $\mu g/m^3$) (Kato et al., 2000) and inflammatory markers were not elevated to the same magnitude when animals were exposed to lower levels of PM in urban air for 60 months(Kato and Kagawa, 2003). Salivary contamination is a limitation of induced sputum especially in children and can affect the supernatant chemokine levels (Simpson et al., 2004). I selected sputum plugs and therefore, the squamous cell % (indicative of salivary contamination) was well within the accepted range for children(Gibson et al., 2000).

It has been suggested that eNO may be a useful marker of adverse effects of air pollution(van Amsterdam et al., 2000). Elevated eNO has been reported in healthy children (Steerenberg et al., 2001) and healthy non-smoking adults (van Amsterdam et al., 1999) exposed to increased levels of air pollutants. Diesel exhaust particle exposed mice had two-fold increase in exhaled NO and pre-treatment with Nitric Oxide Synthase Inhibitor prevented the airway hyper responsiveness in mice. In the same study, iNOS (inducible Nitric Oxide Synthase) was localised to AM by immunohistochemical staining (Lim et al., 1998). However I did not find any relation of AM carbon to eNO.

The toxic effects of DEP are exerted possibly through oxidative stress. Healthy individuals exposed to environmentally relevant levels of DEP did not show any airway inflammation, instead showed influx of reduced glutathione into bronchial fluid (Mudway et al., 2004). The anti-oxidant network at the air liquid interface in healthy subjects may prevent oxidative damage. Surfactant also plays a role in preventing damage caused by particles(Gao et al., 2000). Therefore *in vitro* studies lack the same internal environment as the airway and so are difficult to compare with *in vivo* studies.

The percentage of AM positive for MARCO was not associated with median carbon area in AM. The possibility is that level of exposure that children are exposed to does not result in increased MARCO expression. However if the cells are older and the cell membrane is damaged during processing the MARCO positivity may be affected.

5.2.7 ELECTRON MICROSCOPY

Electron microscopic analysis of fixed, embedded pellets of AM, consistently showed nanoparticles embedded in homogenous matrix. These discrete nanoparticles are very likely to be carbonaceous PM, but the origin of the homogenous matrix is unclear. EM cannot easily distinguish carbon from lipid, as both appear black in osmium stained sections. Indeed, one advantage of light microscopy over EM is that black material is usually environmental carbon. Since the homogeneous material seen under EM was consistently in AM phagolysosomes, it probably represents ingested material. The lipoprotein surfactant is present in the alveolar epithelial fluid lining layer and is ingested and recycled by AM (Wright, 1990). I speculate that the homogenous matrix represents surfactant into which carbon nanoparticles have impacted prior to, or during phagocytosis. Our findings contrast with the absence of homogenous matrix in AM sampled from healthy children using BAL (Bunn et al., 2001). Induced sputum selectively samples AM on the mucociliary escalator, whereas BAL samples more distal AM. The morphological difference in phagolysosomes in AM sampled by induced sputum and BAL may therefore be due to sampling of "older" AM by induced sputum.

Light microscopy cannot detect very small carbon aggregates or single nanoparticles. EM will detect all particulates, but quantitation of carbon loading in EM images is difficult, as only a thin cross-section of individual AM is examined. However, attempts have been made to quantify material in AM by EM, by estimating the thickness of each section and extrapolating the AM volume(Hauser R, 2001).

With the limitation of knowing the composition of the dark electron dense material and inability to quantify particles in whole of AM, TEM was not considered as a suitable method. Moreover the number of AM recovered after processing for TEM were inadequate.

5.3 Summary

Biomass Exposure

This study has demonstrated that it is feasible to induce sputum and process it by simplified technique in the developing world. Induced sputum processing may therefore offer a new approach to the study of respiratory disease in the developing world. As the AM morphology is well preserved, this simplified technique is suitable for assessing carbon loading.

The carbon loading is approximately 13 times higher in women exposed to biomass smoke than adults from a UK city. The 24 hour mean PM_{10} levels reported during biomass cooking are 10 times greater than the annual 24 h mean PM_{10} in Leicester: a difference compatible with the 13-fold increase in loading seen in Ethiopian women. The carbon loading of AM in Ethiopian children was significantly less than their mothers but, on questioning, these children spent very little time near the fire. This suggests that moving children (especially infants) away from cooking area attenuates their exposure.

Traffic derived PM Exposure

The most significant finding was the decrement in lung function (FEV_1 and FEF_{25-75} percent predicted). Thus for every $0.1\mu m^2$ increase in median carbon area in AM, there was 1.7% decrement in FEV_1 and a 3.47% decrement in FEF_{25-75} (% predicted). These associations were not affected by bronchodilator treatment, which indicates that the decrement in lung function is not the result of reversible bronchoconstriction. These effects seen are compatible with other epidemiological studies. However what is not clear is whether the carbon in AM is an indicator of exposure to other pollutants or a mediator of damage.

There was a weak but positive association between median carbon area and modelled PM_{10}. The possible explanations are that the modelled PM at home and school are not

enough to estimate personal exposures, the exposures are low to detect a significant difference in AM carbon loading and a 1 year exposure measurement may be inadequate (as opposed to life time measurement). There was no association between distance from road and carbon loading. The assumption that individuals living within certain distance from road have same exposure is not true, as meteorological conditions alter dispersion and type and volume of traffic can differ on different roads. Also the demographic and exercise parameters were not significantly associated with AM carbon indicating, they are not major determinants of carbon loading. EM because of its limitations in quantification was not suitable for the current study.

5.4 Future directions

The AM carbon loading was found to be good marker of individual exposure in biomass group, showing a clear difference between mothers and children. This observation also indicates that the behaviour of children can influence the amount of exposure. Recently a modified stove (reduced smoke exposure) has been introduced in developing countries. The effectiveness of such interventions is normally measured by monitoring the PM in air. However, to date there are no non-invasive measures to assess the amount of carbon reaching the lower respiratory tract. AM carbon loading as a measure of individual exposure can be used to assess the effectiveness of such interventions along with the inflammatory markers. More detailed questioning on the duration of cooking, time of cooking to the sampling are needed to accurately quantify exposure to PM, in absence of personal monitors.

My data provides a point of reference for median area of carbon in AM analysis in other cities and in animal exposure experiments. Future work should include replication in a separate cohort of children, ideally combined with longitudinal assessment of lung function growth. More detailed assessment of exposure, including any other indoor sources, for example use of candles, incense sticks needs to be undertaken. Validation of modelled exposure (AIRVIRO), possibly by passive sampling devices, remains a priority, since dispersion modelling is the more practical method of assessing individual exposure in large numbers of children required for cohort studies. In conclusion, I assessed the association between modelled exposure of the home address to PM_{10} and carbon loading of AM in a group of 64 healthy children. A weak but significant positive association was found between the two variables. However, a stronger significant inverse association was found between median area of carbon in AM and lung function.

Appendices

Appendix 1: Protocol for imaging and analysis

- Adjusting the microscope – see the setting your microscope protocol
- Clean the light source, condenser, objectives, eyepiece with the lens cleaning tissues and 70% IMS (industrial ethylated spirit)
- Clean the slide on both sides with the lens cleaning tissue
- Switch on the camera
- Adjust the view on the microscope – (to see in through the eyepiece and the camera. i.e. computer screen)
- Make sure no filters are used
- Switch on the computer and open the scion image programme
- Click on the "special" icon and select capture image
- Screen with "live" image will appear
- Place the slide with the label on the right hand side
- Adjust the focus at x10 objective magnification and gradually move up the magnification to x40
- Choose the upper most and left corner (as seen in through the eyepiece) area to start imaging
- Move the x40 objective and add a small drop of oil (oil for microscopy Olympus)
- Now focus with x100 (oil immersion) objective
- Adjust the light intensity until the cells are clearly seen on the screen
- Identify a macrophage
    - Include the whole cell
    - Borders should be clearly seen
    - Nucleus and borders should be focused
    - No artefacts should be seen in the cell area
    - Isolated cells to be preferred

- Click file - "save as" – in "Save as type" select TIF and type the ID number and cell number. – E.g. –TPC 14 – 1
- Save the in removable disc/ computer
- Total of 108 images are stored per individual
- Mark the slide with a dot to indicate that slide has been imaged.

Storage of images

- Store images from each individual in separate CD and also in the computer in a separate file.

Imaging the stage micrometer graticule

- Using oil immersion objective (exactly the same setting as for the macrophage images) take images of the graticule. Take several images at different positions of the graticule and store a tiff images.

Image analysis

Storing cut images

- Programme used – Jasc Paint Shop Pro version 7.04
- Open the image
- Using the free hand drawing tool draw around the cell along the cell border
- Copy the selected area (copy command)
- Paste as a new image using "Paste" icon
- Using the freehand tool draw around the nucleus and delete it using cut command

Using PC USB Graphics Tablet (Medion) for cutting images

- Using freehand drawing tool draw around the cell with the pen on the pad
- Use the copy and paste command on the pad
- Cut the nucleus

Save the image as a tiff file with the ID number and cell number (same as original number)
Save all the images of same individual in one file and name it.

Image analysis

Setting the scale

- Open the scion image programme
- Open the calibration image (with the known distance). 1 division = 2 micrometer.
- In analyse
  - Select the options – and select length
  - Select set scale - pixels for measurements (1 pixel = 1 pixel) – so the results for the selected length is displayed in pixels

Using the straight line drawing tool draw a line along the calibration (Figure) marks with the known distance (= 20 microns).

Choose analyse command – select measure - select show results
Results (length) will be displayed in pixels. Repeat the steps of drawing and measuring and the same result that is repeatedly shown is used

(246 pixels = 20 microns in our study)

Cell area analysis

Steps for cell area

1. Open the cut and pasted image
2. Analyse - Options – select area and decimal points to 5
3. Analyse - Set scale –Enter the units as micrometers, Measured distance = 246 pixels, Known distance = 20. Scale appears as 12.3 pixels per micrometer
4. Open – grey scale image
5. Options – density slice –drag the cursor to maximum density for total cell area

6. Analyse particles –(select min particle –1 pixel and max –999999 pixels, label particle and reset measurement counter. Do not select include interior holes, out line particles)
7. Analyse - Show results
8. Edit - Copy measurements
9. Prepare excel sheet - one sheet for each individual with the name of the individual (code number) and cell numbers. Paste in column for that cell number.

Particle area analysis

Steps for particle area

- Follow steps as in cell area until you reach step 3
- Also open colour image in Paint Shop Pro programme to identify particle and differentiate from bacteria etc
- In step 4 - density slice – drag the cursor to include all particles
- As particles may be of different densities and therefore may have to be selected out. Selection may be done by erasing the non- particle areas or by selecting the particle only and measuring the area. Bacteria and some dense cell wall areas can interfere and therefore the colour image and shapes are used for differentiating
- Results are copied in the same column as that of the total cell area.

Macro

- Written using the Pascal- like language and refer file for command names.

For cell area-

```
begin
 SetScale(12.3,'µm');
 SetDensitySlice(1,254);
 AnalyzeParticles;
 SetParticleSize(1,999999);
 LabelParticles(true);
 OutlineParticles(false);
 SetOptions('Area');
 ShowResults;
 CopyResults;

end;
```

For particle area

```
begin
 SetScale(12.3,'µm');

 AnalyzeParticles;
 SetParticleSize(1,999999);
 LabelParticles(true);
```

```
  OutlineParticles(false);
  SetOptions('Area');
  ShowResults;
  CopyResults;

end;
```

Equipment

- Microscope –
  Olympus
  Supplier – Olympus Optical Co. (UK) LTD
  2-8 Honduras Street London
  EC1Y 0TX
  UK
- PC
- Camera – JVC digital camera

- PC USB Graphics Tablet (Medion)
  Medion Electronics
  130 Faraday Park
  Faraday Road
  Dorcan
  Swindon
  SN3 5JL
  UK
  Tel- 0870 7270370
  Fax – 01793 715716

- Compact discs/ Zip discs
- Oil for microscopy
- Lens cleaning tissues
- 70% IMS (industrial methylated spirit)

Softwares needed

- Scion Image –
  Free download from web site - http://www.scioncorp.com/

Contact details

82 Worman's Mill Court
Suite H
Frederick, Maryland 21701
USA

Tel (301) 695-7870

Fax (301) 695-0035

- Jasc Paint Shop Pro (Version 7.04)
  Available at web site - http://www.jasc.com/
  For orders

  Jasc Software, Inc. Attn: Orders
  7905 Fuller Road
  Eden Prairie, MN 55344
  Fax 952-930-9172
  Tel 800-622-2793

- SPSS – 11.5 for windows
- Microsoft Excel

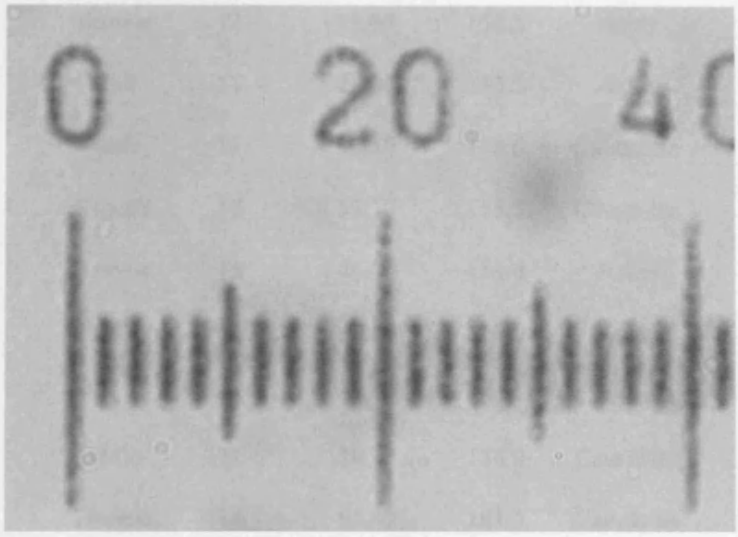

Figure – stage micrometer image, 1 division = 2 micrometers

Appendix 2: Individual data of the children with an adequate induced sputum sample.

ID no	Gender	Age (Years)	Weight (Kgs)	Height (Cms)	Ethnicity	Screened PM_{10} ($\mu g/m^3$)	Salivary cotinine (ng/ml)	Baseline FEV1 (% Predicted)
TPC 02	Male	13	32.35	154.1	Asian	7	0.3	76.4
TPC 04	Male	13	40.00	152.5	Asian	5.26	0.2	90.8
TPC 05	Male	12	34.10	142.0	Asian	5.94	1.6	85.1
TPC 06	Female	12	55.00	159.3	Asian	4.55	0.4	93.1
TPC 08	Male	11	46.20	152.5	Asian	5.23	0.2	108.8
TPC 12	Male	11	36.30	148.5	Caucasian	4.41	0.5	102.7
TPC 13	Female	15	53.10	155.5	Caucasian	0.25	0.2	92.1
TPC 15	Female	15	46.90	151.4	Asian	4.09	0.4	99.2
TPC 16	Male	14	62.60	167.0	Asian	4.75	<0.1	84.6
TPC 17	Male	13	43.70	159.4	Caucasian	0.43	0.5	101.6
TPC 20	Male	11	39.30	156.0	Caucasian	1.64	0.2	103.2
TPC 21	Female	14	53.80	161.5	Caucasian	1.09	0.3	92
TPC 22	Male	15	67.90	179.4	Caucasian	4.66	0.5	98
TPC 27	Male	15	49.70	161.9	Asian	4.51	0.2	96.2
TPC 28	Male	15	87.80	187.2	Caucasian	2.02	<0.1	118.4
TPC 29	Female	12	53.50	151.3	Caucasian	2.23	0.5	105.8
TPC 31	Female	14	47.30	157.0	Asian	5.24	<0.1	104.2
TPC 35	Female	12	49.70	150.2	Caucasian	4.33	0.5	123.1
TPC 37	Female	11	34.40	143.7	Asian	4.19	<0.1	111.2
TPC 38	Female	14	53.90	156.7	Asian	4.19	0.7	98.8
TPC 39*	Male	14	62.60	158.4	Asian	4.07	0.3	93.7
TPC 40*	Female	10	44.03	143.0	Asian	4.07	0.2	83.7
TPC 41	Male	15	59.90	170.8	Caucasian	4.59	1.2	97.4
TPC 45	Male	13	56.70	166.0	Caucasian	1.75	0.3	81.7

Appendix 2 continued

TPC 47	Male	9	46.30	140.3	Caucasian	5.78	<0.1	98.3
TPC 48	Male	15	59.30	173.0	Caucasian	4.17	<0.1	90.7
TPC 49	Female	13	55.40	161.4	Caucasian	4.26	<0.1	118.1
TPC 50	Male	13	62.90	161.6	Asian	5.56	0.4	82.2
TPC 51	Male	14	64.20	158.9	Caucasian	2.28	0.2	115.9
TPC 54	Male	12	44.10	154.0	Caucasian	0.15	0.4	104.4
TPC 55	Female	14	56.40	149.6	Caucasian	0.15	0.8	115.3
TPC 56	Male	9	34.90	137.5	Asian	5.06	0.4	90.6
TPC 57	Female	8	30.60	137.5	Others	4.77	0.8	81.6
TPC 58	Female	10	39.30	145.4	Others	4.77	0.7	87.7
TPC 60	Male	11	57.30	155.4	Caucasian	0.41	0.2	95
TPC 63	Male	8	39.30	138.4	Caucasian	1.91	0.2	102.7
TPC 64	Female	8	25.90	130.0	Caucasian	0.23	1.9	91
TPC 66	Male	8	26.70	132.0	Asian	5	0.6	112.1
TPC 69	Male	9	19.40	137.	Asian	4.09	<0.1	90.5
TPC 71	Male	12	35.70	153.3	Asian	4.36	0.7	95.8
TPC 72	Female	9	41.50	133.0	Asian	4.36	<0.1	122.3
TPC 75	Female	8	30.60	133.0	Caucasian	1.45	0.3	109
TPC 77	Female	14	68.00	154.1	Asian	4.1	0.2	89.2
TPC 78	Male	9	41.00	134.0	Asian	1.91	0.2	106.6
TPC 80	Female	9	59.8	140.0	Caucasian	0.44	0.3	107.2
TPC 82	Female	9	31.30	142.0	Caucasian	1.72	0.3	106.4
TPC 83	Female	9	29.70	143.2	Caucasian	1.72	0.3	100.9
TPC 84	Female	14	54.5	157.0	Caucasian	0.2	0.3	112
TPC 85	Male	12	49.10	147.0	Caucasian	0.2	0.3	95.3
TPC 87	Male	12	45.00	154.0	Caucasian	1.78	0.2	101
TPC 88	Male	9	28.60	131.4	Caucasian	1.62	0.2	102.2
TPC 89	Male	11	42.30	152.9	Caucasian	1.62	0.2	106.5

Appendix 2 continued

TPC 93	Male	9	29.2	131.0	Caucasian	0.17	<0.1	96
TPC 94	Female	10	41.50	134.5	Caucasian	0.44	0.2	104.7
TPC 97	Female	10	61.20	149.6	Asian	4.27	0.2	117.8
TPC 98	Male	9	28.1	129.2	Caucasian	4.02	<0.1	98.9
TPC 99	Male	15	70.5	169.4	Caucasian	4.02	0.5	99.1
TPC 100	Female	13	50.9	162.1	Caucasian	4.02	0.3	99
TPC 104	Male	12	37.90	147.0	Caucasian	1.06	0.3	123.1
TPC 105	Female	11	48.00	155.0	Caucasian	4.46	0.7	82.3
TPC 106	Female	10	44.20	142.0	Caucasian	5.4	0.3	98.2
TPC 108	Male	8	25.80	132.0	Caucasian	1.79	0.4	91
TPC 109	Female	9	36.40	137.5	Caucasian	0.29	<0.1	106.2
TPC 112	Female	8	27.00	124.0	Caucasian	0.37	0.5	108.8
TPC 114	Female	13	54.80	161.6	Asian	1.46	0.7	83.6
TPC 115	Male	9	35.70	139.5	Asian	1.46	0.3	104

Appendix 3: Individual data on carbon area parameters

ID no	Carbon Area		Carbon Area Number		% AM with carbon
	Median	Mean	Mean	Median	
TPC 02	0.958	1.447	14.200	12.0	94.0
TPC 04	0.294	0.513	4.910	2.0	77.0
TPC 05	0.899	1.758	7.207	6.0	90.2
TPC 06	0.529	1.282	10.160	5.0	79.0
TPC 08	0.509	0.940	10.560	9.0	93.0
TPC 12	0.370	0.528	6.010	4.0	88.0
TPC 13	0.631	1.148	6.670	4.0	92.0
TPC 15	0.446	0.991	7.060	4.0	87.0
TPC 16	0.602	1.155	9.040	6.0	82.0
TPC 17	0.175	0.365	2.140	1.0	70.0
TPC 20	0.327	1.037	5.290	3.5	89.0
TPC 21	0.899	1.617	6.930	4.0	89.0
TPC 22	0.430	0.777	5.350	3.0	87.0
TPC 27	0.559	0.809	5.080	4.0	88.0
TPC 28	0.307	0.523	3.750	2.0	77.0
TPC 29	0.357	0.561	4.490	3.0	85.0
TPC 31	0.360	0.574	3.680	3.0	90.0
TPC 35	0.436	0.766	4.470	3.0	90.0
TPC 37	0.711	1.198	5.760	4.0	95.0
TPC 38	0.403	0.690	5.870	4.0	80.0
TPC 41	0.377	0.688	5.100	3.0	84.0
TPC 45	0.311	0.543	3.790	2.0	77.0
TPC 47	0.159	0.335	2.070	1.0	66.0
TPC 48	0.254	0.424	4.100	2.0	80.0
TPC 49	0.235	0.517	2.350	1.0	81.0
TPC 50	1.144	2.072	9.400	7.0	95.0
TPC 51	0.426	0.714	4.980	3.0	83.0
TPC 54	0.410	0.720	5.460	3.0	84.0
TPC 55	0.231	0.659	3.040	2.0	76.0
TPC 56	0.446	0.858	6.490	3.0	86.0
TPC 57	0.793	1.614	5.410	4.0	99.0
TPC 58	0.215	0.402	3.870	2.0	80.0
TPC 60	0.344	0.591	4.180	2.5	90.0
TPC 63	0.651	1.481	6.040	4.0	96.0
TPC 64	0.274	0.600	4.440	2.0	87.0
TPC 66	0.347	0.814	5.660	2.0	85.0
TPC 69	0.714	1.523	9.050	4.5	96.0
TPC 71	0.364	1.064	5.450	2.0	88.0
TPC 72	0.516	0.875	5.845	3.0	96.4
TPC 75	0.430	0.802	5.280	3.0	87.0
TPC 77	0.664	1.255	8.130	4.5	97.0
TPC 78	0.297	0.598	2.930	2.0	81.0
TPC 80	0.175	0.320	1.760	1.0	71.0
TPC 82	0.423	1.006	5.910	3.0	85.0
TPC 83	0.347	0.799	6.100	3.0	79.0
TPC 84	0.357	0.650	3.480	2.0	80.0
TPC 85	0.535	0.892	5.800	4.0	95.0
TPC 87	0.026	0.281	2.070	0.5	50.0
TPC 88	0.869	1.875	11.570	6.0	95.0
TPC 89	0.423	0.740	4.990	3.0	91.0
TPC 93	0.089	0.256	2.130	1.0	57.0
TPC 94	0.096	0.187	1.190	1.0	61.0
TPC 97	0.588	0.905	5.210	4.0	96.0

Appendix 3 continued					
TPC 98	0.509	1.012	4.070	2.0	81.0
TPC 99	0.377	0.565	2.810	2.0	74.0
TPC 100	0.400	0.727	4.220	2.0	80.0
TPC 104	0.215	0.485	3.210	2.0	81.0
TPC 105	0.449	0.916	6.660	4.0	95.0
TPC 106	0.423	0.702	4.600	2.0	82.5
TPC 108	0.370	0.508	3.250	3.0	86.0
TPC 109	0.165	0.250	1.260	1.0	61.0
TPC 112	0.291	0.535	3.300	2.0	86.0
TPC 114	0.585	1.007	7.530	5.0	95.0
TPC 115	1.008	1.456	9.880	7.5	98.0

Appendix 4: Individual data on distance from road, modelled PM and secondary PM

		Modelled Primary PM (μg/m³)									Secondary Monitored PM (μg/m³)		
		Residence			School			Total (Home + School)					
ID no	Distance from road (metres)	Annual	One Month	One week	Annual	One Month	One week	Annual	One Month	One week	Annual	One Month	One week
TPC 02	79.27	2.714	3.503	3.010	1.152	1.214	0.613	2.325	2.870	2.449	3.627	2.849	3.357
TPC 04	26.17	2.038	2.619	2.540	1.431	1.794	2.462	1.914	2.454	2.353	3.661	2.676	2.735
TPC 05	341.50	2.189	2.395	1.944	1.158	1.086	1.282	1.921	1.975	1.618	3.802	5.218	8.763
TPC 06	533.88	1.469	1.307	1.676	1.152	1.075	0.905	1.399	1.285	1.656	3.763	5.060	2.962
TPC 08	444.07	1.750	1.654	1.364	1.152	1.237	1.017	1.588	1.563	1.136	3.730	4.242	3.290
TPC 12	483.15	1.434	1.359	0.936	1.130	1.301	0.962	1.371	1.335	0.822	3.735	3.781	2.998
TPC 13	3000.65	0.145	0.119	0.001	0.321	0.282	0.217	0.208	0.156	0.072	3.732	2.965	2.132
TPC 15	286.39	1.310	1.365	1.489	1.101	1.100	0.769	1.266	1.336	1.434	3.724	2.821	1.932
TPC 16	439.77	1.580	1.808	2.206	1.079	1.207	1.704	1.470	1.666	2.132	3.764	3.115	8.790
TPC 17	391.88	0.171	0.192	0.104	0.755	0.916	0.663	0.326	0.423	0.272	3.932	5.173	11.046
TPC 20	1419.98	0.467	0.392	0.219	0.576	0.613	0.398	0.550	0.508	0.304	3.975	5.646	10.668
TPC 21	198.03	0.422	0.510	0.556	0.350	0.504	0.672	0.418	0.517	0.585	3.995	5.886	10.232
TPC 22	205.13	1.787	1.581	1.491	0.751	0.657	0.639	1.482	1.178	1.164	4.121	6.884	9.179
TPC 27	374.55	1.535	1.510	2.158	1.082	1.121	1.284	1.445	1.413	2.080	4.249	7.018	13.408
TPC 28	36.48	0.662	0.698	0.835	0.737	0.666	0.623	0.720	0.756	0.906	4.404	9.011	15.876
TPC 29	388.22	1.016	1.298	2.223	0.737	0.666	0.623	0.995	1.245	2.095	4.404	9.011	15.876
TPC 31	377.83	1.804	1.855	1.556	1.101	1.036	0.733	1.641	1.697	1.456	4.348	8.781	5.652
TPC 35	222.47	1.439	1.435	1.055	1.092	0.980	0.754	1.369	1.377	0.964	4.343	9.733	8.832
TPC 37	295.05	1.406	1.111	0.543	1.597	1.100	0.674	1.490	1.180	0.590	4.509	9.616	12.891
TPC 38	295.05	1.406	1.111	0.543	1.077	0.798	0.484	1.348	1.080	0.527	4.509	9.616	12.891
TPC 41	163.90	1.546	1.032	1.100	1.082	0.537	0.544	1.442	0.923	0.987	4.504	2.746	2.753
TPC 45	343.99	0.469	0.391	0.570	0.560	0.385	0.378	0.526	0.445	0.623	4.567	3.422	5.571
TPC 47	51.21	2.142	1.401	1.170	0.968	0.482	0.346	1.795	1.206	0.993	4.623	4.936	4.520
TPC 48	710.84	1.342	0.864	0.703	1.081	0.413	0.243	1.323	0.824	0.672	4.629	5.005	4.337
TPC 49	570.50	1.368	1.165	0.730	1.070	0.410	0.245	1.349	1.202	0.760	4.668	5.681	4.840
TPC 50	138.74	2.017	1.250	1.209	1.075	0.264	0.211	1.756	1.086	1.031	4.718	4.985	5.088
TPC 51	586.94	0.903	0.494	0.403	0.722	0.229	0.263	0.903	0.519	0.420	4.730	4.717	4.103
TPC 54	138.11	0.185	0.126	0.125	1.000	0.408	0.606	0.412	0.214	0.146	4.839	4.803	6.936
TPC 55	138.11	0.185	0.126	0.125	1.000	0.408	0.606	0.412	0.214	0.146	4.839	4.803	6.936
TPC 56	29.13	2.013	1.313	1.143	1.287	0.426	*	1.793	1.202	1.143	4.866	5.010	5.300
TPC 57	197.96	1.749	1.150	1.211	1.287	0.433	*	1.620	1.093	1.211	4.867	5.002	4.584

Appendix 4 continued

TPC 58	197.96	1.749	1.150	1.211	1.287	0.433	*	1.620	1.093	1.211	4.867	5.002	4.584
TPC 60	99.52	0.357	0.238	0.169	1.000	0.446	*	0.552	0.309	0.169	4.867	5.002	4.584
TPC 63	36.63	0.737	0.431	0.136	0.564	0.190	*	0.735	0.408	0.136	4.867	4.933	4.371
TPC 64	1466.39	0.141	0.055	0.053	*	*	*	*	*	*	4.867	4.933	4.371
TPC 66	301.58	2.003	1.262	1.549	1.448	0.688	*	1.833	1.243	1.549	4.835	5.119	6.827
TPC 69	842.79	1.062	0.813	0.640	0.618	*	*	1.037	0.813	0.640	5.003	6.761	14.164
TPC 71	227.63	1.427	1.167	1.505	1.077	*	*	1.358	1.167	1.505	4.990	5.783	3.515
TPC 72	227.63	1.427	1.167	1.505	2.100	*	*	1.639	1.167	1.505	4.990	5.783	3.515
TPC 75	1516.81	0.468	0.668	0.259	0.399	0.619	0.272	0.473	0.652	0.256	4.906	3.185	4.433
TPC 77	152.93	1.339	1.605	0.923	1.046	1.572	1.161	1.281	1.545	0.923	4.904	3.062	3.160
TPC 78	437.81	0.600	0.869	0.120	1.164	1.767	0.363	0.819	1.263	0.211	4.904	3.062	3.160
TPC 80	567.61	1.676	2.176	2.352	0.416	0.678	0.826	1.352	1.560	1.712	4.896	2.963	2.636
TPC 82	1034.59	0.634	0.779	0.744	1.134	1.795	1.311	0.795	1.100	0.958	4.902	3.059	2.728
TPC 83	1034.59	0.634	0.779	0.744	1.134	1.795	1.311	0.795	1.100	0.958	4.902	3.059	2.728
TPC 84	455.40	1.733	2.319	2.553	1.492	2.238	1.778	1.736	2.319	2.415	4.902	3.059	2.728
TPC 85	455.40	1.733	2.319	2.553	1.166	1.745	1.380	1.646	2.155	2.283	4.902	3.059	2.728
TPC 87	83.56	0.541	0.731	0.460	0.453	0.797	1.057	0.546	0.765	0.541	4.905	3.103	2.571
TPC 88	347.06	0.689	0.980	0.648	0.351	0.584	0.693	0.669	0.936	0.592	4.905	3.103	2.571
TPC 89	347.06	0.689	0.980	0.648	*	*	*	*	*	*	4.905	3.103	2.571
TPC 93	365.94	0.585	0.857	0.947	0.148	0.253	0.143	0.513	0.692	0.847	4.882	2.764	3.273
TPC 94	582.99	0.237	0.346	0.270	*	*	*	*	*	*	4.966	3.616	6.792
TPC 97	286.22	1.414	2.072	1.810	1.619	2.455	1.907	1.504	2.225	1.972	4.969	3.393	5.533
TPC 98	634.37	1.124	1.869	0.984	*	*	*	*	*	*	4.969	3.393	5.533
TPC 99	634.37	1.124	1.869	0.984	0.460	0.642	0.205	1.066	1.605	0.927	4.969	3.393	5.533
TPC 100	634.37	1.124	1.869	0.984	0.451	0.642	0.186	1.064	1.605	0.920	4.969	3.393	5.533
TPC 104	128.54	0.396	0.387	0.427	*	*	*	*	*	*	4.926	3.094	2.134
TPC 105	31.50	1.558	2.414	2.583	0.848	1.263	1.534	1.346	2.078	2.156	4.926	3.183	2.380
TPC 106	113.24	2.060	2.541	2.681	2.189	2.834	3.885	2.147	2.722	2.855	4.926	3.183	2.380
TPC 108	1324.90	0.664	1.140	1.856	0.406	0.622	0.893	0.629	1.036	1.699	4.933	3.448	3.243
TPC 109	402.12	0.215	0.302	0.181	0.154	0.239	0.139	0.217	0.301	0.187	4.981	4.050	4.661
TPC 112	339.52	0.102	0.169	0.420	0.317	0.633	0.424	0.174	0.328	0.360	4.952	3.527	5.593
TPC 114	1316.72	0.498	0.961	1.097	0.616	1.083	1.283	0.547	1.007	1.218	4.901	3.298	3.907
TPC 115	1316.72	0.498	0.961	1.097	0.611	1.384	1.389	0.546	1.107	1.253	4.901	3.298	3.907

Appendix 5: Individual lung function data of 64 children

ID no	Baseline FEV1% predicted	z scores FEV1	Best FVC %	Z scores for FVC	% Pred FEV1/FVC	Z scores FEV1/FVC%	% Pred FEF 25-75	Z scores FEF 25 -75	Post salbutamol FEV1%	Z scores PS FEV1
TPC 02	76.4	-1.66	85.3	-1.76	89.5	-0.15	57	-1.75	80	-1.41
TPC 04	90.8	-0.51	90.9	-0.69	91.3	0.06	67.5	-1.04	95.8	-0.10
TPC 05	85.1	-1.16	97.7	-1.02	87	-0.64	67.5	-1.35	87.5	-0.97
TPC 06	93.1	-1.72	119.4	-0.62	86.4	-2.19	48	-2.46	107.2	-0.87
TPC 08	108.8	-0.01	114.2	-0.52	97.7	0.87	106.5	0.31	109.6	0.05
TPC 12	102.7	0.31	110.2	0.60	92	-0.52	92	-0.77	105.5	0.55
TPC 13	92.1	-0.58	93.2	-0.68	97.5	-0.09	84.1	-1.21	93.9	-0.44
TPC 15	99.2	0.30	98	-0.30	113	0.86	105.2	0.23	105.7	0.82
TPC 16	84.6	-1.89	88.1	-2.46	96.1	0.79	86.4	-1.14	85.5	-1.83
TPC 17	101.6	0.95	104	0.96	95.6	-0.05	89.2	-0.58	99.6	0.78
TPC 20	103.2	0.41	99.1	-0.25	103.2	0.81	102.4	-0.39	106.5	0.68
TPC 21	92	-0.03	90	-0.82	*	*	97	-0.69	92	0.02
TPC 22	98	-0.36	95.3	-0.92	103.3	0.79	102.1	-0.45	95.7	-0.52
TPC 27	96.2	1.54	95	0.48	101.2	1.35	127.8	1.79	96.2	1.54
TPC 28	118.4	1.22	128.1	1.59	95.2	-0.01	103	-0.34	120.2	1.35
TPC 29	105.8	0.73	117.2	1.41	89.8	-1.28	78.6	-1.13	111.5	1.15
TPC 31	104.2	-0.47	104.5	-0.93	110.9	0.69	107.8	-0.39	104.4	-0.44
TPC 35	123.1	2.07	123	1.86	99.9	-0.01	133	1.00	118.5	1.71
TPC 37	111.2	0.10	112.2	-0.28	109.6	0.36	97.3	-0.12	114.9	0.36
TPC 38	98.8	-0.78	99.9	-1.19	96.2	-1.06	68.9	-1.74	*	*
TPC 41	97.4	-0.37	*	*	*	*	*	*	102.3	0.02
TPC 45	81.7	-1.78	*	*	*	*	*	*	82.4	-1.74
TPC 47	98.3	-0.02	110.6	0.69	87.3	-1.16	72.4	-1.47	98.5	0.02
TPC 48	90.7	-0.88	96.5	-0.75	93.7	-0.22	75	-1.47	93.8	-0.64
TPC 49	118.1	0.95	110.8	0.31	107.4	0.85	135.8	0.37	113.2	0.60
TPC 50	82.2	-1.13	89.1	-1.47	86.5	-0.40	59.1	-1.62	83.9	-0.99
TPC 51	115.9	2.42	110.9	1.86	102.4	0.71	130.5	1.23	118.1	2.62
TPC 54	104.4	0.79	100.8	0.34	100.7	0.52	113.6	0.21	97.6	0.23
TPC 55	115.3	2.06	111.6	1.52	101.8	0.41	130.4	1.38	116.3	2.16
TPC 56	90.6	-1.91	109.7	-1.46	80	-1.63	46.5	-2.27	101.2	-1.23
TPC 57	81.6	-2.20	82.4	-2.00	95.7	-0.72	66.2	-1.83	86.7	-1.87

Appendix 5 continued

TPC 58	87.7	-0.03	97.5	-0.17	105.8	-0.07	99.5	-0.06	87.6	-0.06
TPC 60	95	0.51	100.8	0.01	94.2	0.57	95.3	-0.13	92.3	0.26
TPC 63	102.7	0.31	106.5	0.37	94.8	-0.23	89.2	-0.85	101.4	0.23
TPC 64	91	-0.50	94.3	-0.17	93.2	-0.95	78.6	-1.25	97.8	-0.03
TPC 66	112.1	-1.33	115.7	-1.89	96.9	0.61	89.2	-0.53	115	-1.20
TPC 69	90.5	-2.34	83.5	-3.24	106.2	1.40	100.1	-1.18	91.8	-2.26
TPC 71	95.8	-0.50	101.6	-0.95	94.7	0.50	74.3	-1.02	89.6	-0.97
TPC 72	122.3	0.37	127.6	0.30	105.5	-0.27	113.1	0.42	118.4	0.10
TPC 75	109	0.81	103	0.49	102.2	0.13	119.3	0.17	95.3	-0.20
TPC 77	89.2	-1.40	96.9	-1.39	102.4	-0.35	76.4	-1.55	88.3	-1.49
TPC 78	106.6	-0.76	107.9	-1.45	98.8	0.87	116.5	0.61	111.7	-0.42
TPC 80	107.2	1.51	115.8	1.11	108.7	0.20	111.2	0.42	104.9	1.32
TPC 82	106.4	0.62	106.5	0.82	96	-0.66	99.8	-0.72	107.5	0.69
TPC 83	100.9	0.20	98.7	0.22	98.3	-0.39	102.1	-0.68	103.3	0.35
TPC 84	112	0.73	111.6	0.49	106.7	0.94	134.3	0.43	113.3	0.81
TPC 85	95.3	0.29	105.8	0.23	91.5	0.13	101.9	0.13	102.4	0.90
TPC 87	101	0.51	114.1	1.49	86.7	-1.11	73.9	-1.32	105.6	0.88
TPC 88	102.2	0.27	109.6	0.63	91.6	-0.69	82.7	-1.08	107.6	0.71
TPC 89	106.5	0.67	*		*	*	*	*	112.9	1.17
TPC 93	96	-0.17	90.3	-0.88	102.4	0.65	100.8	-0.36	97	-0.08
TPC 94	104.7	0.57	99.5	0.34	100.1	0.01	108.8	-0.23	112.5	1.17
TPC 97	117.8	0.01	118.9	-0.37	101.3	-0.54	84.6	-0.66	120.5	0.18
TPC 98	98.9	0.07	109.1	0.63	91.1	-0.77	78.1	-1.23	102.8	0.35
TPC 99	99.1	1.42	98.5	1.10	99.8	0.43	94.9	-0.04	102.6	1.73
TPC 100	99	-0.46	96.7	-0.70	103.6	0.38	90.6	-1.14	99.5	0.47
TPC 104	123.1	1.86	115.7	1.25	103.4	0.85	144.9	1.16	126.4	2.10
TPC 105	82.3	-1.87	82.1	-1.95	100.7	-0.06	91.1	-1.42	86.1	-1.62
TPC 106	98.2	0.02	91.5	-0.30	102.5	0.23	134.2	0.46	97.9	-0.02
TPC 108	91	-0.53	85.9	-1.24	103.9	0.95	105.2	-0.21	89.5	-0.67
TPC 109	106.2	0.70	105.5	0.81	96.6	-0.55	102.7	-0.52	102.9	0.42
TPC 112	108.8	0.81	107.9	0.76	97.7	-0.14	97.3	-0.39	119.1	1.61
TPC 114	83.6	-2.05	86.9	-2.19	100.9	-0.43	57.6	-2.07	88.6	-1.75
TPC 115	104	-1.11	110.5	-1.46	94.1	0.30	80.2	-0.87	105.3	-0.99

Appendix 6: Individual data of sputum differential count and inflammatory markers

ID no	Neutrophil (%)	Eosinophil (%)	Macrophage (%)	Lymphocyte (%)	Epithelial cell (%)	IL- 8 (ng/ml)	ENO (ppb)
TPC 02	17.25	0.50	81.25	0.50	0.50	15.41	*
TPC 04	68.25	10.25	21.00	0.00	0.25	1.24	*
TPC 05	18.12	0.00	81.00	0.50	0.00	0.51	*
TPC 06	11.25	35.00	53.25	0.25	0.25	11.21	*
TPC 08	1.75	0.00	93.25	0.25	4.75	0.93	*
TPC 12	56.00	6.50	37.50	0.00	0.00	8.63	*
TPC 13	9.50	2.00	88.00	0.25	0.25	1.3	*
TPC 15	7.50	0.00	91.75	0.75	0.00	1.34	*
TPC 16	7.00	0.00	90.50	0.50	2.00	0.69	*
TPC 17	3.25	0.00	96.25	0.75	0.75	0.64	*
TPC 20	3.25	0.00	96.50	0.00	0.25	0.91	*
TPC 21	75.50	0.00	24.25	0.00	0.25	102.35	*
TPC 22	5.50	0.00	93.25	0.25	1.00	0.79	34.9
TPC 27	34.50	0.75	64.50	0.25	0.00	1.55	39.3
TPC 28	8.50	0.25	90.75	0.25	0.25	13.35	*
TPC 29	18.25	0.00	81.75	0.00	0.00	5.55	*
TPC 31	20.25	0.00	79.50	0.25	0.00	1.66	6.7
TPC 35	0.00	0.00	99.25	0.25	0.50	0.14	*
TPC 37	6.16	0.00	93.80	0.00	0.00	0.64	13.5
TPC 38	87.25	0.25	12.50	0.00	0.00	107.93	13.3
TPC 41	50.00	6.00	44.00	0.00	0.00	10.8	46.4
TPC 45	25.50	0.25	74.25	0.00	0.00	68.65	*
TPC 47	16.83	0.24	81.95	0.24	0.73	7.13	4.3
TPC 48	44.42	0.74	54.84	0.00	0.00	0.52	27.96
TPC 49	3.00	0.25	96.75	0.00	0.00	1.17	*
TPC 50	27.75	0.25	72.00	0.00	0.00	14.91	19.06
TPC 51	5.25	0.25	94.25	0.25	0.00	0.96	9.4
TPC 54	85.25	0.50	14.25	0.00	0.00	1.11	*
TPC 55	4.50	0.25	95.00	0.25	0.00	1.2	*
TPC 56	58.75	17.75	23.50	0.00	0.00	9.08	*
TPC 57	77.50	0.25	22.00	0.00	0.25	7.6	15.13
TPC 58	63.75	0.75	35.00	0.00	0.50	6.26	17.3
TPC 60	2.68	0.00	96.10	0.49	0.73	1.25	14.56
TPC 63	10.25	0.50	88.75	0.25	0.25	13.05	11.8
TPC 64	21.00	0.00	78.50	0.50	0.00	1.67	18.26
TPC 66	56.00	3.00	41.00	0.00	0.00	14.71	*
TPC 69	2.51	0.25	96.49	0.50	0.25	10.32	*
TPC 71	9.73	0.75	87.78	0.00	1.75	0.3	*
TPC 72	0.00	0.00	99.51	0.00	0.49	0.28	*
TPC 75	21.00	0.25	78.75	0.00	0.00	*	*
TPC 77	2.25	0.00	96.50	0.00	1.25	0.45	*
TPC 78	56.50	0.75	42.50	0.25	0.00	8.17	*
TPC 80	47.25	0.00	52.25	0.25	0.25	49.78	8.2
TPC 82	23.50	0.25	75.75	0.00	0.50	4.98	*
TPC 83	13.75	0.25	85.00	0.00	1.00	6.72	*
TPC 84	0.00	0.25	99.25	0.00	0.50	1.55	7.2
TPC 85	1.00	1.25	96.75	0.00	1.00	1.15	14.36

Appendix 6 continued							
TPC 87	91.50	0.75	7.75	0.00	0.00	104.65	*
TPC 88	19.25	0.50	80.00	0.00	0.25	6.28	5.9
TPC 89	84.75	1.00	14.00	0.00	0.25	47.53	8.9
TPC 93	25.75	0.25	73.50	0.25	0.25	11.79	*
TPC 94	48.50	0.25	51.25	0.00	0.00	9.75	8.06
TPC 97	2.75	0.00	97.25	0.00	0.00	0.84	7.5
TPC 98	49.00	1.00	46.25	0.50	3.25	57.45	11.23
TPC 99	72.25	3.25	24.50	0.00	0.00	17.29	83.6
TPC 100	50.75	3.00	45.00	0.25	1.00	7.67	8.5
TPC 104	46.25	1.50	51.75	0.00	0.50	3.85	*
TPC 105	3.03	0.00	96.97	0.00	0.00	0.29	3.6
TPC 106	8.22	1.37	90.41	0.00	0.00	0.5	*
TPC 108	71.25	0.00	28.75	0.00	0.00	12.16	*
TPC 109	90.75	0.00	9.00	0.00	0.25	107.09	*
TPC 112	72.00	0.75	27.25	0.00	0.00	8.93	*
TPC 114	76.25	0.25	23.00	0.25	0.25	12.06	*
TPC 115	37.50	0.00	62.00	0.50	0.00	8.38	*

References

A.C.Davison, D. V. Hinkley R. Gill B. D. Ripley S. Ross B. Silverman M. Stein. Bootstrap Methods and Their Application (Cambridge Series in Statistical and Probabilistic Mathematics) . 2003. Press Syndicate of University of Cambridge.

Aaron DJ, Kriska AM, Dearwater SR, Anderson RL, Olsen TL, Cauley JA, Laporte RE. The epidemiology of leisure physical activity in an adolescent population. Med Sci Sports Exerc 1993; 25: 847-853.

Albalak R, Frisancho AR, Keeler GJ. Domestic biomass fuel combustion and chronic bronchitis in two rural Bolivian villages. Thorax 1999; 54: 1004-1008.

Alexis NE, Hu SC, Zeman K, Alter T, Bennett WD. Induced sputum derives from the central airways: confirmation using a radiolabeled aerosol bolus delivery technique. Am J Respir Crit Care Med 2001; 164: 1964-1970.

American Thoracic Society. Health effects of outdoor air pollution. Committee of the Environmental and Occupational Health Assembly of the American Thoracic Society. Am J Respir Crit Care Med 1996; 153: 3-50.

American Thoracic Society. Recommendations for Standardized Procedures for the Online and Offline Measurement of Exhaled Lower Respiratory Nitric Oxide and Nasal Nitric Oxide in Adults and Children---1999. Am J Respir Crit Care Med 1999; 160: 2104-2117.

Andrea M.Kriska and Carl J.Caspersen. Introduction to a Collection of Physical Activity Questionnaires. A Collection of Physical Activity Questionnaires for Health-Related Research. Medicine & Science in Sports & Exercise. 29(6) Supplement: 5-9. 1997.

Balakrishnan K, Sankar S, Parikh J, Padmavathi R, Srividya K, Venugopal V, Prasad S, Pandey VL. Daily average exposures to respirable particulate matter from combustion of biomass fuels in rural households of southern India. Environ Health Perspect 2002; 110: 1069-1075.

Becker S, Soukup JM. Exposure to urban air particulates alters the macrophage-mediated inflammatory response to respiratory viral infection. J Toxicol Environ Health A 1999; 57: 445-457.

Becker S, Soukup JM, Sioutas C, Cassee FR. Response of human alveolar macrophages to ultrafine, fine, and coarse urban air pollution particles. Exp Lung Res 2003; 29: 29-44.

Belda J, Leigh R, Parameswaran K, O'Byrne PM, Sears MR, Hargreave FE. Induced sputum cell counts in healthy adults. Am J Respir Crit Care Med 2000; 161: 475-478.

Blood smear technique. Blood smear technique. Biomedical Laboratory Animations, IU school of Medicine. 11-5-2004.

Bobak M. Outdoor air pollution, low birth weight, and prematurity. Environ Health Perspect 2000; 108: 173-176.

Brauer M, Hoek G, van Vliet P, Meliefste K, Fischer PH, Wijga A, Koopman LP, Neijens HJ, Gerritsen J, Kerkhof M, Heinrich J, Bellander T, Brunekreef B. Air pollution from traffic and the development of respiratory infections and asthmatic and allergic symptoms in children. Am J Respir Crit Care Med 2002; 166: 1092-1098.

Brightling CE, Monteiro W, Ward R, Parker D, Morgan MD, Wardlaw AJ, Pavord ID. Sputum eosinophilia and short-term response to prednisolone in chronic obstructive pulmonary disease: a randomised controlled trial. Lancet 2000a; 356: 1480-1485.

Brightling CE, Ward R, Woltmann G, Bradding P, Sheller JR, Dworski R, Pavord ID. Induced sputum inflammatory mediator concentrations in eosinophilic bronchitis and asthma. Am J Respir Crit Care Med 2000b; 162: 878-882.

Bruce N, Perez-Padilla R, Albalak R. Indoor air pollution in developing countries: a major environmental and public health challenge. Bull World Health Organ 2000; 78: 1078-1092.

Brunekreef B, Hoek G. The relationship between low-level air pollution exposure and short-term changes in lung function in Dutch children. J Expo Anal Environ Epidemiol 1993; 3 Suppl 1: 117-128.

Brunekreef B, Janssen NA, de Hartog J, Harssema H, Knape M, van Vliet P. Air pollution from truck traffic and lung function in children living near motorways. Epidemiology 1997; 8: 298-303.

Bunn HJ, Dinsdale D, Smith T, Grigg J. Ultrafine particles in alveolar macrophages from normal children. Thorax 2001; 56: 932-934.

Bunn HJ, Woltmann G, Grigg J. Applicability of laser scanning cytometry to study paediatric alveolar macrophages. Eur Respir J 2002; 20: 1437-1443.

Calderon-Garciduenas L, Mora-Tiscareno A, Fordham LA, Chung CJ, Garcia R, Osnaya N, Hernandez J, Acuna H, Gambling TM, Villarreal-Calderon A, Carson J, Koren HS, Devlin RB. Canines as sentinel species for assessing chronic exposures to air pollutants: part 1. Respiratory pathology. Toxicol Sci 2001; 61: 342-355.

Cataldo D, Foidart JM, Lau L, Bartsch P, Djukanovic R, Louis R. Induced sputum: comparison between isotonic and hypertonic saline solution inhalation in patients with asthma. Chest 2001; 120: 1815-1821.

Chow JC, Watson JG, Louie PKK, Chen L-WA, Sin D. Comparison of PM2.5 carbon measurement methods in Hong Kong, China. Environmental Pollution 2005; 137: 334-344.

Cosio Piqueras MG, Cosio MG. Disease of the airways in chronic obstructive pulmonary disease. Eur Respir J Suppl 2001; 34: 41s-49s.

Dockery DW, Pope CA, Xu X, Spengler JD, Ware JH, Fay ME, Ferris BG, Speizer FE. An Association between Air Pollution and Mortality in Six U.S. Cities. N Engl J Med 1993; 329: 1753-1759.

Ebelt S, Brauer M, Cyrys J, Tuch T, Kreyling WG, Wichmann HE, Heinrich J. Air quality in postunification Erfurt, East Germany: associating changes in pollutant concentrations with changes in emissions. Environ Health Perspect 2001; 109: 325-333.

Ezzati M, Kammen D. Indoor air pollution from biomass combustion and acute respiratory infections in Kenya: an exposure-response study. Lancet 2001a; 358: 619-624.

Ezzati M, Kammen DM. Quantifying the effects of exposure to indoor air pollution from biomass combustion on acute respiratory infections in developing countries. Environ Health Perspect 2001b; 109: 481-488.

Feyerabend C, Russell MA. A rapid gas-liquid chromatographic method for the determination of cotinine and nicotine in biological fluids. J Pharm Pharmacol 1990; 42: 450-452.

Finch GL, Hobbs CH, Blair LF, Barr EB, Hahn FF, Jaramillo RJ, Kubatko JE, March TH, White RK, Krone JR, Menache MG, Nikula KJ, Mauderly JL, Van Gerpen J, Merceica MD, Zielinska B, Stankowski L, Burling K, Howell S. Effects of subchronic inhalation exposure of rats to emissions from a diesel engine burning soybean oil-derived biodiesel fuel. Inhal Toxicol 2002; 14: 1017-1048.

Fireman E, Greif J, Schwarz Y, Man A, Ganor E, Ribak Y, Lerman Y. Assessment of hazardous dust exposure by BAL and induced sputum. Chest 1999; 115: 1720-1728.

Fujii T, Hayashi S, Hogg JC, Mukae H, Suwa T, Goto Y, Vincent R, van Eeden SF. Interaction of Alveolar Macrophages and Airway Epithelial Cells Following Exposure to Particulate Matter Produces Mediators that Stimulate the Bone Marrow. Am J Respir Cell Mol Biol 2002; 27: 34-41.

Gao N, Keane MJ, Ong T, Wallace WE. Effects of simulated pulmonary surfactant on the cytotoxicity and DNA-damaging activity of respirable quartz and kaolin. J Toxicol Environ Health A 2000; 60: 153-167.

Gauderman WJ, Avol E, Gilliland F, Vora H, Thomas D, Berhane K, McConnell R, Kuenzli N, Lurmann F, Rappaport E, Margolis H, Bates D, Peters J. The effect of air pollution on lung development from 10 to 18 years of age. N Engl J Med 2004; 351: 1057-1067.

Gibson PG, Grootendor DC, Henry RL, Pin I, Rytila PH, Wark P, Wilson N, Djukanovic R. Sputum induction in children. Eur Respir J Suppl 2002; 37: 44s-46s.

Gibson PG, Henry RL, Thomas P. Noninvasive assessment of airway inflammation in children: induced sputum, exhaled nitric oxide, and breath condensate. Eur Respir J 2000; 16: 1008-1015.

Giovagnoli MR, Alderisio M, Cenci M, Nofroni I, Vecchione A. Carbon and hemosiderin-laden macrophages in sputum of traffic policeman exposed to air pollution. Arch Environ Health 1999; 54: 284-290.

Gong H, Jr., Sioutas C, Linn WS. Controlled exposures of healthy and asthmatic volunteers to concentrated ambient particles in metropolitan Los Angeles. Res Rep Health Eff Inst 2003; 1-36.

Harrison RM, Yin J. Particulate matter in the atmosphere: which particle properties are important for its effects on health? Sci Total Environ 2000; 249: 85-101.

Harrison RM, Jones M. The chemical composition of airborne particles in the UK atmosphere. Science of The Total Environment 1995; 168: 195-214.

Hartung TK, Maulu A, Nash J, Fredlund VG. Suspected pulmonary tuberculosis in rural South Africa--sputum induction as a simple diagnostic tool? S Afr Med J 2002; 92: 455-458.

Hauser R, Godleski JJ Hatch V Christiani DC. Ultrafine particles in human lung macrophages. Arch Environ Health 56(2), 150-156. 2001.

Ho KF, Lee SC, Yu JC, Zou SC, Fung K. Carbonaceous characteristics of atmospheric particulate matter in Hong Kong. The Science of The Total Environment 2002; 300: 59-67.

Horak F, Jr., Studnicka M, Gartner C, Spengler JD, Tauber E, Urbanek R, Veiter A, Frischer T. Particulate matter and lung function growth in children: a 3-yr follow-up study in Austrian schoolchildren. Eur Respir J 2002; 19: 838-845.

Ishii H, Fujii T, Hogg JC, Hayashi S, Mukae H, Vincent R, van Eeden SF. Contribution of IL-1 beta and TNF-alpha to the initiation of the peripheral lung response to atmospheric particulates (PM10). Am J Physiol Lung Cell Mol Physiol 2004; 287: L176-L183.

Janssen NA, Brunekreef B, van Vliet P, Aarts F, Meliefste K, Harssema H, Fischer P. The relationship between air pollution from heavy traffic and allergic sensitization, bronchial hyperresponsiveness, and respiratory symptoms in Dutch schoolchildren. Environ Health Perspect 2003; 111: 1512-1518.

Jarvis MJ, Strachan DP, Feyerabend C. Determinants of passive smoking in children in Edinburgh, Scotland. Am J Public Health 1992; 82: 1225-1229.

Jedrychowski W, Flak E, Mroz E. The adverse effect of low levels of ambient air pollutants on lung function growth in preadolescent children. Environ Health Perspect 1999; 107: 669-674.

Jones PD, Hankin R, Simpson J, Gibson PG, Henry RL. The tolerability, safety, and success of sputum induction and combined hypertonic saline challenge in children. Am J Respir Crit Care Med 2001; 164: 1146-1149.

Kato A, Kagawa J. Morphological effects in rat lungs exposed to urban roadside air. Inhal Toxicol 2003; 15: 799-818.

Kato A, Nagai A, Kagawa J. Morphological changes in rat lung after long-term exposure to diesel emissions. Inhal Toxicol 2000; 12: 469-490.

Kiraz K, Kart L, Demir R, Oymak S, Gulmez I, Unalacak M, Ozesmi M. Chronic pulmonary disease in rural women exposed to biomass fumes. Clin Invest Med 2003; 26: 243-248.

Kleinman MT, Sioutas C, Chang MC, Boere AJ, Cassee FR. Ambient fine and coarse particle suppression of alveolar macrophage functions. Toxicol Lett 2003; 137: 151-158.

Kulkarni NS, Prudon B, Panditi SL, Abebe Y, Grigg J. Carbon loading of alveolar macrophages in adults and children exposed to biomass smoke particles. Sci Total Environ 2005; 345: 23-30.

Lay JC, Bennett WD, Kim CS, Devlin RB, Bromberg PA. Retention and intracellular distribution of instilled iron oxide particles in human alveolar macrophages. Am J Respir Cell Mol Biol 1998; 18: 687-695.

Lehnert BE. Pulmonary and thoracic macrophage subpopulations and clearance of particles from the lung. Environ Health Perspect 1992; 97: 17-46.

Leicester Air Quality Report Review and Assessment. Leicester City Council, Pollution Control Group. Final Report. December 2000. Accessed on 28/07/2005 at http://www.leicester.gov.uk/your-council--services/regeneration--culture/environmental-health-and-licensing/pollution-control/air-quality/review. 2000.

Leicester City Council. Air Quality Reviews and Assessments 2003. Draft Report September 2003. Accessed on 28/07/2005 at http://www.leicester.gov.uk/your-

council--services/regeneration--culture/environmental-health-and-licensing/pollution-control/air-quality/review. 2003.

Lim HB, Ichinose T, Miyabara Y, Takano H, Kumagai Y, Shimojyo N, Devalia JL, Sagai M. Involvement of superoxide and nitric oxide on airway inflammation and hyperresponsiveness induced by diesel exhaust particles in mice. Free Radical Biology and Medicine 1998; 25: 635-644.

Livingstone AE, Shaddick G, Grundy C, Elliott P. Do people living near inner city main roads have more asthma needing treatment? Case-control study. BMJ 1996; 312: 676-677.

Lockwood AH, Merkus PJFM, Tetrault GA, Gauderman WJ, Avol E, Gilliland F. Air Pollution and Lung Function. N Engl J Med 2004; 351: 2652-2653.

Maatta K, Arstila AU. Pulmonary deposits of titanium dioxide in cytologic and lung biopsy specimens. Light and electron microscopic x-ray analysis. Lab Invest 1975; 33: 342-346.

Marques LJ, Teschler H, Guzman J, Costabel U. Smoker's lung transplanted to a nonsmoker. Long-term detection of smoker's macrophages. Am J Respir Crit Care Med 1997; 156: 1700-1702.

McNeill AD, Jarvis MJ, West R, Russell MA, Bryant A. Saliva cotinine as an indicator of cigarette smoking in adolescents. Br J Addict 1987; 82: 1355-1360.

Monn C, Fendt R, Koller T. Ambient PM(10) extracts inhibit phagocytosis of defined inert model particles by alveolar macrophages. Inhal Toxicol 2002; 14: 369-385.

Monn C, Fuchs A, Hogger D, Junker M, Kogelschatz D, Roth N, Wanner H-U. Particulate matter less than 10 [mu]m (PM10) and fine particles less than 2.5 [mu]m (PM2.5): relationships between indoor, outdoor and personal concentrations. Science of The Total Environment 1997; 208: 15-21.

Moschandreas DJ, Watson J, D'Abreton P, Scire J, Zhu T, Klein W, Saksena S. Chapter three: methodology of exposure modeling. Chemosphere 2002; 49: 923-946.

Mudway IS, Stenfors N, Duggan ST, Roxborough H, Zielinski H, Marklund SL, Blomberg A, Frew AJ, Sandstrom T, Kelly FJ. An in vitro and in vivo investigation of the effects of diesel exhaust on human airway lining fluid antioxidants. Archives of Biochemistry and Biophysics 2004; 423: 200-212.

Mukherjee P, Viswanathan S. Carbon monoxide modeling from transportation sources. Chemosphere 2001; 45: 1071-1083.

Nerriere E, Zmirou-Navier D, Blanchard O, Momas I, Ladner J, Le Moullec Y, Personnaz MB, Lameloise P, Delmas V, Target A, Desqueyroux H. Can we use fixed ambient air monitors to estimate population long-term exposure to air pollutants? The case of spatial variability in the Genotox ER study. Environ Res 2005; 97: 32-42.

Nightingale JA, Maggs R, Cullinan P, Donnelly LE, Rogers DF, Kinnersley R, Chung KF, Barnes PJ, Ashmore M, Newman-Taylor A. Airway inflammation after controlled exposure to diesel exhaust particulates. Am J Respir Crit Care Med 2000; 162: 161-166.

Nordenhall C, Pourazar J, Blomberg A, Levin JO, Sandstrom T, Adelroth E. Airway inflammation following exposure to diesel exhaust: a study of time kinetics using induced sputum. Eur Respir J 2000; 15: 1046-1051.

Oosterlee A, Drijver M, Lebret E, Brunekreef B. Chronic respiratory symptoms in children and adults living along streets with high traffic density. Occup Environ Med 1996; 53: 241-247.

Pabst M, Hofer F. Deposits of different origin in the lungs of the 5,300-year-old Tyrolean Iceman. Am J Phys Anthropol 1998; 107: 1-12.

Palecanda A, Paulauskis J, Al Mutairi E, Imrich A, Qin G, Suzuki H, Kodama T, Tryggvason K, Koziel H, Kobzik L. Role of the scavenger receptor MARCO in alveolar macrophage binding of unopsonized environmental particles. J Exp Med 1999; 189: 1497-1506.

Peiser L, Mukhopadhyay S, Gordon S. Scavenger receptors in innate immunity. Curr Opin Immunol 2002; 14: 123-128.

Peters A. Particulate matter and heart disease: Evidence from epidemiological studies. Toxicology and Applied Pharmacology 2005; 207: 477-482.

Peters JM, Avol E, Gauderman WJ, Linn WS, Navidi W, London SJ, Margolis H, Rappaport E, Vora H, Gong H, Jr., Thomas DC. A study of twelve Southern California communities with differing levels and types of air pollution. II. Effects on pulmonary function. Am J Respir Crit Care Med 1999; 159: 768-775.

Rainey LC, Bolsaitis P, Dirsa B, Vander Sande JB. Characterization by scanning transmission electron microscopy of silica particles from alveolar macrophages of coal miners. Environ Health Perspect 1994; 102: 862-868.

Renwick LC, Donaldson K, Clouter A. Impairment of alveolar macrophage phagocytosis by ultrafine particles. Toxicol Appl Pharmacol 2001; 172: 119-127.

Rosenthal M, Bain SH, Cramer D, Helms P, Denison D, Bush A, Warner JO. Lung function in white children aged 4 to 19 years: I--Spirometry. Thorax 1993; 48: 794-802.

Roy S, Ray MR, Basu C, Lahiri P, Lahiri T. Abundance of siderophages in sputum: indicator of an adverse lung reaction to air pollution. Acta Cytol 2001; 45: 958-964.

Salvi SS, Nordenhall C, Blomberg A, Rudell B, Pourazar J, Kelly FJ, Wilson S, Sandstrom T, Holgate ST, Frew AJ. Acute exposure to diesel exhaust increases IL-8 and GRO-alpha production in healthy human airways. Am J Respir Crit Care Med 2000; 161: 550-557.

Saraiva-Romanholo BM, Barnabe V, Carvalho AL, Martins MA, Saldiva PHN, Nunes MdP. Comparison of Three Methods for Differential Cell Count in Induced Sputum. Chest 2003; 124: 1060-1066.

Schwartz J. Air pollution and children's health. Pediatrics 2004; 113: 1037-1043.

Simpson JL, Timmins NL, Fakes K, Talbot PI, Gibson PG. Effect of saliva contamination on induced sputum cell counts, IL-8 and eosinophil cationic protein levels. Eur Respir J 2004; 23: 759-762.

Smith KR, Samet JM, Romieu I, Bruce N. Indoor air pollution in developing countries and acute lower respiratory infections in children. Thorax 2000; 55: 518-532.

Spanevello A, Confalonieri M, Sulotto F, Romano F, Balzano G, Migliori GB, Bianchi A, Michetti G. Induced sputum cellularity. Reference values and distribution in normal volunteers. Am J Respir Crit Care Med 2000; 162: 1172-1174.

Steerenberg PA, Nierkens S, Fischer PH, van Loveren H, Opperhuizen A, Vos JG, van Amsterdam JG. Traffic-related air pollution affects peak expiratory flow, exhaled nitric oxide, and inflammatory nasal markers. Arch Environ Health 2001; 56: 167-174.

Stenfors N, Nordenhall C, Salvi SS, Mudway I, Soderberg M, Blomberg A, Helleday R, Levin JO, Holgate ST, Kelly FJ, Frew AJ, Sandstrom T. Different

airway inflammatory responses in asthmatic and healthy humans exposed to diesel. Eur Respir J 2004; 23: 82-86.

Suarez S, Kazantseva M, Bhat M, Costa D, Hickey AJ. The influence of suspension nebulization or instillation on particle uptake by guinea pig alveolar macrophages. Inhal Toxicol 2001; 13: 773-788.

Tesfaigzi Y, Singh SP, Foster JE, Kubatko J, Barr EB, Fine PM, McDonald JD, Hahn FF, Mauderly JL. Health Effects of Subchronic Exposure to Low Levels of Wood Smoke in Rats. Toxicol Sci 2002; 65: 115-125.

van Amsterdam JG, Nierkens S, Vos SG, Opperhuizen A, van Loveren H, Steerenberg PA. Exhaled nitric oxide: a novel biomarker of adverse respiratory health effects in epidemiological studies. Arch Environ Health 2000; 55: 418-423.

van Amsterdam JG, Verlaan BP, van Loveren H, Elzakker BG, Vos SG, Opperhuizen A, Steerenberg PA. Air pollution is associated with increased level of exhaled nitric oxide in nonsmoking healthy subjects. Arch Environ Health 1999; 54: 331-335.

van Eeden SF, Tan WC, Suwa T, Mukae H, Terashima T, Fujii T, Qui D, Vincent R, Hogg JC. Cytokines involved in the systemic inflammatory response induced by exposure to particulate matter air pollutants (PM(10)). Am J Respir Crit Care Med 2001; 164: 826-830.

van Vliet P, Knape M, de Hartog J, Janssen N, Harssema H, Brunekreef B. Motor Vehicle Exhaust and Chronic Respiratory Symptoms in Children Living near Freeways. Environmental Research 1997; 74: 122-132.

Varkey AB. Chronic obstructive pulmonary disease in women: exploring gender differences. Curr Opin Pulm Med 2004; 10: 98-103.

Venn AJ, Lewis SA, Cooper M, Hubbard R, Britton J. Living Near a Main Road and the Risk of Wheezing Illness in Children. Am J Respir Crit Care Med 2001; 164: 2177-2180.

Ward DJ, Ayres JG. Particulate air pollution and panel studies in children: a systematic review. Occup Environ Med 2004; 61: e13.

Wilkinson P, Elliott P, Grundy C, Shaddick G, Thakrar B, Walls P, Falconer S. Case-control study of hospital admission with asthma in children aged 5-14 years: relation with road traffic in north west London. Thorax 1999; 54: 1070-1074.

Wilson NM, Bridge P, Spanevello A, Silverman M. Induced sputum in children: feasibility, repeatability, and relation of findings to asthma severity. Thorax 2000; 55: 768-774.

Wright JR. Clearance and recycling of pulmonary surfactant. Am J Physiol Lung Cell Mol Physiol 1990; 259: L1-12.

Xu X, Ding H, Wang X. Acute effects of total suspended particles and sulfur dioxides on preterm delivery: a community-based cohort study. Arch Environ Health 1995; 50: 407-415.

Zar HJ, Dechaboon A, Hanslo D, Apolles P, Magnus KG, Hussey G. Pneumocystis carinii pneumonia in South African children infected with human immunodeficiency virus. Pediatr Infect Dis J 2000a; 19: 603-607.

Zar HJ, Tannenbaum E, Apolles P, Roux P, Hanslo D, Hussey G. Sputum induction for the diagnosis of pulmonary tuberculosis in infants and young children in an urban setting in South Africa. Arch Dis Child 2000b; 82: 305-308.

Publication from Thesis

Kulkarni NS, Prudon B, Panditi SL, Abebe Y, Grigg J. Carbon loading of alveolar macrophages in adults and children exposed to biomass smoke particles. Sci Total Environ 2005; 345: 23-30.

Neeta S Kulkarni, Nevil Pierce, Lesley Rushton, and Jonathan M Grigg. Carbon in airway macrophages and lung function in children. New England Journal of Medicine (in press).

Presentations/abstracts

Neeta S Kulkarni, Nevil Pierce, Lesley Rushton, and Jonathan M Grigg. Association of alveolar macrophage carbon loading and annual modelled PM_{10} at residence in healthy children. Thorax Supplement II, Vol 60, p ii18, Dec 2005. Oral presentation at the British Thoracic Society Winter Meeting 2005.

Neeta S Kulkarni, Nevil Pierce, Lesley Rushton, and Jonathan M Grigg. Association between sputum inflammatory markers and carbon loading of alveolar macrophages in healthy children. European Respiratory Journal. Poster Presentation At ERS congress Copenhagen 2005.

N.S. Kulkarni, N. Pierce, L. Rushton and J Grigg. Association between lung function and carbon loading of alveolar macrophages in healthy children. Proceedings of the American Thoracic Society Conference. 2005 page A523. Oral Presentation at the American Thoracic Society Conference San Diego 2005.

N S Kulkarni, A Rutman, C O'Callaghan, J Grigg. Environmental particulates in induced sputum alveolar macrophages from healthy children - electron microscopic appearance. European Respiratory Journal, Volume 24, supplement 48, September 2004 Page 606s. Poster presentation at the ERS Congress Glasgow 2004.

N S Kulkarni, B Prudon, S Panditi, Y Abebe, G Wedldessellassie, J Grigg; Alveolar macrophage particle loading from exposure to biomass smoke-comparison of adults and children from Ethiopia. American Journal of Respiratory and Critical Care Medicine Vol 169, (7) Supplement, April 2004, page A640. Poster Presentation at the American Thoacic Society Conference, Orlando 2004.

N S Kulkarni, D Kempkens, J Grigg. A simplified method for induced sputum processing that can be applied to developing countries. Paediatric Research Society Scientific Abstracts, Current Paediatrics Vol 13(5) Oct 2003 page 403

N S Kulkarni, D Kempkens, J Grigg; Simplified processing of induced sputum applicable to the developing world: comparison with standard methodology. European Respiratory Journal, Volume 22, supplement 45, September 2003 Page 38s. Poster Presentation at the ERS Congress Vienna, 2003.

E-Letter- Response to an article published in Chest.

Neeta S Kulkarni, Jonathan Grigg Simplified method of sputum processing. (24 September 2003).

Comparison of Three Methods for Differential Cell Count in Induced Sputum. Beatriz M. Saraiva-Romanholo, Viviani Barnabé, Ana Lúcia I. Carvalho, Milton A. Martins, Paulo H. N. Saldiva, and Maria do Patrocínio T. Nunes Chest 2003; 124: 1060-1066.